

8-9-2008

Human lumbar nuclear intervertebral disc prosthesis: an experimental study

Wuraola F. Larinde

Follow this and additional works at: <https://scholarsjunction.msstate.edu/td>

Recommended Citation

Larinde, Wuraola F., "Human lumbar nuclear intervertebral disc prosthesis: an experimental study" (2008).
Theses and Dissertations. 2514.
<https://scholarsjunction.msstate.edu/td/2514>

This Graduate Thesis - Open Access is brought to you for free and open access by the Theses and Dissertations at Scholars Junction. It has been accepted for inclusion in Theses and Dissertations by an authorized administrator of Scholars Junction. For more information, please contact scholcomm@msstate.libanswers.com.

HUMAN LUMBAR NUCLEAR INTERVERTEBRAL DISC PROSTHESIS: AN
EXPERIMENTAL STUDY

By

Wuraola F. Larinde

A Thesis
Submitted to the Faculty of
Mississippi State University
in Partial Fulfillment of the Requirements
for the Degree of Master of Science
in Biological Engineering
in the Department of Biological Engineering

Mississippi State, Mississippi

August 2008

HUMAN LUMBAR NUCLEAR INTERVERTEBRAL DISC PROSTHESIS: AN
EXPERIMENTAL STUDY

By

Wuraola F. Larinde

Approved:

Steven H. Elder
Assistant Professor of Biomedical
Engineering and Graduate Coordinator
(Director of Thesis)

Jun Liao
Assistant Professor of Biomedical
Engineering
(Committee Member)

S.D. Filip To
Associate Professor of Instrumentation
and Undergraduate Coordinator
(Committee Member)

Walter Eckman
Spinal Surgeon
(Committee Member)

Sarah A. Rajala
Dean of the Bagley College of Engineering

Name: Wuraola F. Larinde

Date of Degree: August 9, 2008

Institution: Mississippi State University

Major Field: Biomedical Engineering

Major Professor: Dr. Steven Elder

Title of Study: HUMAN LUMBAR NUCLEAR INTERVERTEBRAL DISC
PROSTHESIS: AN EXPERIMENTAL STUDY

Pages in Study: 136

Candidate for Degree of Master of Science

Low back pain is also a vast socioeconomic issue which costing American taxpayers more than \$50 billion yearly. Estimates state that up to 75% of low back pain is caused by lumbar degenerative disc disease. The nucleus seems plays a critical role in pain related to disc degeneration; it is the starting point of the degenerative cascade. All of these factors make it the focus of novel treatment options.

The goal of this study is to create idealized models to determine the shape of nuclear implant best suited to resist the standard shear and torsional stresses that are generated in the lumbar spine. Thus, five nuclear intervertebral disc prosthetics (Implant designs 1-5) were designed.

Shear testing was conducted using an Instron, and torsion testing was conducted using the LabVIEW in conjunction with a torsional pneumatic cylinder. Implant design 4 was determined to be the implant design best suited to resist shear stresses. Implant design 3 was determined to be the implant design best suited to allow normal torsion of

the spine. Therefore, it was determined that a combination of implant design 3 and implant design 4 might be optimal in terms of shear, torsion, wear, and stability.

ACKNOWLEDGEMENTS

I would like to express my sincere gratitude and appreciation to the individuals without whom, I could not have completed this endeavor. First and foremost, I would like to thank God for making this opportunity possible for me and giving me the strength to complete it. I also owe my family a great debt of gratitude for their support of me and my work over the years. Express gratitude is also due to my committee head Dr. Steven Elder for overseeing my project, always pointing me in the right direction, and patiently answering an unending flood of questions. Sincere thanks are also due to my other committee members for their invaluable help, namely Doctors Walter Eckman, Filip To, and Jun Liao. I also like to thank Yuan Yuan, for his swift and greatly appreciated assistance. Lastly, I would like to thank the following people Samuel Griffin, Laura Ford, Charles McRae, Donald Green. Thank you all for making this possible.

TABLE OF CONTENTS

ACKNOWLEDGEMENTS	ii
LIST OF TABLES	v
LIST OF FIGURES	vi
1. INTRODUCTION	1
2. BACKGROUND	5
2.1 Spinal Anatomy	5
2.2 Intervertebral Disc Structure and Function.....	6
2.3 Intervertebral Disc Mechanical Behavior	9
2.3.1 Compressive and Tensile Characteristics	9
2.3.2 Bending, Torsion, and Shear Characteristics.....	10
2.3.3 Viscoelastic Characteristics	11
2.4 Intervertebral Disc Degeneration and Disease.....	12
2.5 Treatments for Degenerative Disc Disease.....	14
2.5.1 Conservative Treatments for Disc Degeneration and Disease.....	14
2.5.2 Invasive Surgical Treatments for Disc Degeneration and Disease...15	
2.5.2.1 Discectomy	15
2.5.2.2 Spinal Fusion	16
2.5.2.3 Artificial Disc Technology	17
2.5.2.4 Artificial Nucleus Prosthesis.....	20
3. NUCLEAR PROSTHESIS DESIGN	45
4. SHEAR TESTING.....	53
4.1 Machinery and Setup	53
4.2 Methods and Materials.....	54
4.3 Results and Analysis	57
5. TORSIONAL TESTING	98
5.1 Machinery and Setup	98

5.2 Methods and Materials.....	100
5.3 Results and Analysis.....	102
6. CONCLUSION	126
REFERENCES CITED.....	131

LIST OF TABLES

2.1. Table depicting various forms of Nucleus Prosthesis Design ⁵⁷	44
4.1. Example of preliminary result table for testing in shear.....	79
4.2. Results table for testing in shear	82
4.3. Result table for testing in shear under heavy load	82
4.4. Statistical ranking of the various implant designs	83
5.1. Table of voltage entered in LabVIEW and resulting torque.....	114
5.2. Voltage entered in LabVIEW and the resulting torque and degrees of rotation.....	116
5.3. A statistical ranking of the various implant designs	125

LIST OF FIGURES

2.1.	Diagram of the Human Spinal Column ⁵³	25
2.2.	Diagram of a vertebral body ⁵²	26
2.3.	Diagram of spinal ligaments ⁵²	27
2.4.	Diagram of an Intervertebral Disc ⁴⁹	28
2.5.	Diagram of an Intervertebral Disc ⁵³	29
2.6.	Diagram of a Functional Spinal Unit ²⁴	30
2.7.	Diagram of a typical load deformation curve for a disc in compression ⁵⁰	31
2.8.	Diagram of the Stresses on an Intact Intervertebral Disc in Compression ⁵⁰	32
2.9.	Diagram of an Intact Intervertebral Disc in Compression ⁵⁰	33
2.10.	Diagram of the Stresses on an Intact Intervertebral Disc in Flexion and Extension ⁵⁰	34
2.11.	Radiographs showing advanced degeneration of an intervertebral disc. Notice the almost complete loss of disc height and the formation of vertebral osteophytes. Top: anterior-posterior radiograph. Bottom: lateral radiograph ⁶¹	35
2.12.	A–D Photographs of the different cage designs and lateral plain radiographs from a typical specimen after insertion of two parallel interbody cages. A Left and B : Brantigan cage – a rectangular, porous carbon-fiber implant. A Centre and C : Ray cage – a cylindrical, threaded, porous titanium implant. A Right and D : Stratec cage – a porous titanium implant designed to fit on the endplate Contours ¹⁶	36
2.13.	Diagram of the LINK” SB Charité artificial disc ¹²	37
2.14.	Diagram of the LINK” SB Charité artificial disc ⁶⁰	38

2.15.	Diagram of the Acroflex® implant ¹³	39
2.16.	Diagram of the ProDisc implant ⁶⁹	40
2.17.	Diagram of the Maverick implant ⁶⁹	41
2.18.	Diagram of the FlexiCore implant ⁷⁰	42
2.19.	Diagram of a prosthetic disc nucleus ²¹	43
3.1.	Implant Design 1 for the Nuclear Intervertebral Disc Implants	48
3.2.	Implant Design 2 for the Nuclear Intervertebral Disc Implants	49
3.3.	Implant Design 3 for the Nuclear Intervertebral Disc Implants	50
3.4.	Implant Design 4 for the Nuclear Intervertebral Disc Implants	51
3.5.	Implant Design 5 for the Nuclear Intervertebral Disc Implants	52
4.1.	Picture of bottom fixation device used in setup for testing in shear	71
4.2.	Picture of top fixation device used in setup for testing in shear	72
4.3.	Drawing of setup for testing in shear	73
4.4.	Picture of setup for testing in shear	74
4.5.	Picture of setup for testing in shear	75
4.6.	Picture of setup for testing in shear	76
4.7.	Picture of heavy plate used for testing in shear	77
4.8.	Picture of setup for testing in heavy shear	78
4.9.	Sample diagram of force-distance graph.	80
4.10.	Trapezoidal Integration Equation ⁷²	81
4.11.	Graph of comparison of average failure forces in implant designs in bonded and unbonded testing	84

4.12.	Graph of comparison of average failure forces in implant designs in testing on an incline and on a decline.....	85
4.13.	Graph of comparison of average failure distance in implant designs in bonded and unbonded testing.....	86
4.14.	Graph of comparison of average failure distance in implant designs in testing on an incline and on a decline	87
4.15.	Graph of comparison of average initial shear stiffness in implant designs in bonded and unbonded testing.....	88
4.16.	Graph of comparison of average initial shear stiffness in implant designs in testing on an incline and on a decline	89
4.17.	Graph of comparison of average shear stiffness before dislocation in implant designs in bonded and unbonded testing	90
4.18.	Graph of comparison of average shear stiffness before dislocation in implant designs in testing on an incline and on a decline	91
4.19.	Graph of comparison of average work needed for dislocation for implant designs in bonded and unbonded testing	92
4.20.	Graph of comparison of average work needed for dislocation in implant designs in testing on an incline and on a decline	93
4.21.	Graph of comparison of average failure forces in implant designs in testing under heavy compression.....	94
4.22.	Graph of comparison of average failure distance in implant designs in testing under heavy compression	95
4.23.	Graph of comparison of average work required for shear in implant designs under heavy compression.....	96
4.24.	Graph of comparison of average initial shear stiffness and shear stiffness before dislocation on implant designs in testing under heavy compression	97
5.1.	A torsional pneumatic cylinder attached to an adjustable platform.....	107
5.2.	Side view of the implant fixation devices for torsional testing	108
5.3.	Front view of the implant fixation devices for torsional testing.....	109

5.4.	Setup for torsional pneumatic torsional testing	110
5.5.	Modified bottom fixation device for torsional testing with a load cell.....	111
5.6.	Picture of Implant after dislocation in torsional testing.....	112
5.7.	A) Side view of an illustration of an implant that is centered B) Side view of an illustration of an implant that if off centered	113
5.8.	Graph of the voltage entered in LabVIEW and the resulting torque	115
5.9.	Graph of minimum torque required for movement when the implant is centered.....	117
5.10.	Graph of minimum torque required for movement when the implant is at a 3mm offset	118
5.11.	Graph of minimum torque required for movement when the implant is at a 6mm offset	119
5.12.	Graph of minimum torque required for movement when the implant is at a 9mm offset	120
5.13.	Graph of maximum torque required for implant dislocation when the implant is centered	121
5.14.	Graph of maximum torque required for dislocation when the implant is at a 3mm offset	122
5.15.	Graph of maximum torque required for dislocation when the implant is at a 6mm offset	123
5.16.	Graph of maximum torque required for dislocation when the implant is at a 9mm offset	124

CHAPTER I

INTRODUCTION

After the common cold, nonspecific low back pain is the most common complaint reported to primary care physicians in the US; it is the cause of more than 15 million outpatient physician visits yearly. Between 65% and 80% of individuals will suffer from low back pain within their lifetimes; for 28% of those, the pain will be disabling^{2,3,46,47}. Low back pain is also a vast socioeconomic issue which costs American workers compensation systems more than \$50 billion and results in roughly 149 million lost work days per year. It is the leading cause of work related disability in individuals under the age of 45^{4,5,46}. Between 80 and 90% of people who suffer from low back pain recover within a three month period, however, the 10 % who do not recover incur up to 85% of expenses caused by low back pain sufferers⁴. The causes of low back pain are extremely difficult to diagnose; however, estimates state that up to 75% of low back pain is caused by lumbar degenerative disc disease²⁵.

Degeneration is a progressive and irreversible process that takes place in intervertebral discs as well as all other connective tissue. Degenerative disc disease is defined as the pain or irritation caused by the loss of structural integrity of a disc⁴⁸. Intervertebral discs are located between vertebrae; they consist of the annulus fibrosus which surrounds the nucleus pulposus. The annulus is made of fibrocartilage and it helps

to distribute pressure evenly across the disc. The nucleus is made primarily of proteoglycans and acts as a structural support²³. At around the age of 30, there is a change in the chemical composition of the intervertebral disc. The nucleus of the disc dehydrates and shrinks because of a loss of overall water content and a change in the types of proteoglycans that the disc contains. This causes a simultaneous decrease in the load on the nucleus and increase in the load on the annulus. This in turn causes the annulus to crack and tear; if the tears do not heal, the nucleus can migrate from the center of the disc through the tear and this is called a herniation¹². Herniation happens often and in several directions. When a disc herniates radially, it is almost always in the posterior direction for anatomical reasons. Often when these posterior herniations occur, the spinal nerves or nerve roots compressed, often causing pain and discomfort³⁰.

Currently there are many different treatments used to combat degenerative disc disease; some are conservative and noninvasive and some require major surgery. Conservative treatment is usually the first course of action; the treatments include rest, physical therapy, and non steroidal anti inflammatory medication^{1,33}. Surgical treatments include foraminotomy (where pain caused by the intervertebral foramen is relieved by the removal of offending bone and tissue), laminotomy (where the lamina is removed to increase the amount of space that neural tissue can occupy), and facet thermal ablation (where a laser is used to clean the facet joint and deaden the nerve that is causing the painful symptoms). However, the most common surgical treatments are discectomy and spinal fusion. Discectomy is used in cases of herniation when the nucleus is impinging on a nerve root. The impinging portion of the disc is removed to relieve pressure on the nerve root. In the case of severe annular degeneration spinal fusion is used, the damaged

disc is removed and bone growth is encouraged between adjacent vertebrae. The problem with these treatments is that they neither help restore the biomechanical function of the spine nor preserve the range of motion between vertebrae; they may even generate additional stresses causing further disc degeneration^{12,13,25,32}.

The nucleus seems to play a critical role in pain related to disc degeneration. It is the core of spinal motion segments, it assists the annulus in bearing the weight placed on individual intervertebral discs, and it is the starting point of the degenerative cascade. All of these factors make it the focus of novel treatment options¹⁴. The eventual goal of this research endeavor is to produce a novel nuclear replacement which restores disc biomechanics, allows the annulus fibrosus to maintain disc height, and performs normal disc function while preserving range of motion. When placed in patients with disc degeneration who still have substantially preserved annulus fibrosus and endplates, these implants would also reduce the risk of extrusion as compared to previously designed nuclear replacements and could be implanted utilizing minimally invasive surgical techniques. The goal of this study is to create idealized models to determine the shape of nuclear implant best suited to resist the standard shear and torsional stresses that are generated in the lumbar spine. Since this is a laboratory study focused mainly on mechanical properties, almost all of the emphasis is placed on the shape of the inner surfaces of the implants and not on the means of fixation for the outer surface of the implant. Thus, based on the recommendations and patents of spinal surgeon Dr. Walter Eckman, five nuclear intervertebral disc prosthetics (Implant designs 1-5) with identical exteriors and a variety of potential contours for the interior articulating surfaces were designed (refer to chapter 3 for designs). After consideration, based on the poor fidelity

with which implant design 2 was reproduced during the prototyping process, it was excluded from testing. Implant designs 1, 3, 4, and 5, were tested in shear and tested in torsion. Specifically, this project was designed to select which one of these four remaining rigid two part nuclear implants would serve best as a substitute for a degenerated nucleus pulposus in intervertebral discs. After intensive testing and careful consideration, it was determined that implant design number 4 would be the implant design best suited to serve as a substitute for degenerate nucleus pulposus, and it is the best candidate for further study.

CHAPTER II

BACKGROUND

2.1 Spinal Anatomy

The human spinal column can be thought of as a modified elastic rod that plays a major role in the upright posture and stability of the body. Its major functions are to protect the delicate nerves of the spinal cord from injury and trauma, transfer loads from the head and neck to the pelvis, and allow flexibility and bending of the neck and trunk^{52,53}. The spine is an articulating and segmented structure which consists of seven cervical vertebrae, twelve thoracic vertebrae, five lumbar vertebrae, five fused sacral vertebrae, and four fused coccygeal segments as shown in Figure 2.1^{50,51}. Each of the 24 cervical, thoracic, and lumbar vertebra articulate with the adjacent vertebra to permit motion in three planes^{49,50,51,52}. There are four normal curves in the lateral or sagittal plane; starting from the top of the spine cervical lordosis curves about 9° (concave backwards), thoracic kyphosis curves about 39° (concave forwards), and lumbar lordosis curves an average of 57° (concave backwards). The thoracic and sacral curves are structural and due to the fact that the vertical heights of the anterior vertebral borders are less than the vertical heights of the posterior vertebral borders. These curves have a mechanical function; they increase the flexibility and shock absorbing capacity of the spine while maintaining stability at the intervertebral joint level^{50,53}.

A vertebra consists of a vertebral body and a posterior bony ring called the neural arch which contains the articular, transverse, and spinous processes and is connected to the body by two pedicles as seen in Figure 2.2. The pedicles, the vertebral body, and the neural arch form a triangular space which contains the spinal cord. Projecting from each pedicle towards the midline is a small plate of bone called the lamina; the laminae from each side meet and fuse with each other in the midline. A vertebral body consists of less than 1mm of cortical bone surrounding a trabecular center; its superior and inferior surfaces are called vertebral endplates and they are slightly concave. The basic design of the vertebra is the same throughout the articulating region of the spine (C3 to L5). The size of the vertebra increase from the top of the neck to the base of the spine; this is to accommodate the increased compressive force that the vertebrae are subject to further down the spine because the vertebral body is the primary weight bearing area. Adjacent vertebral bodies are separated by intervertebral discs, which are discs of cartilage that lie between the hard bones of the vertebra and act as structural supports^{50,51,52,53}.

The muscles and ligaments of the spine are composed of fibrous tissues and keep the vertebra and joints in alignment by providing support and stability as shown in Figure 2.3; the muscles provide extrinsic support while the ligaments and intervertebral discs provide intrinsic support⁵³.

2.2 Intervertebral Disc Structure and Function

Intervertebral discs account for approximately one third of the spinal column; their main purpose is to separate vertebral bodies. The space that the discs provide

between the vertebra allow for flexion, extension, and torsion of the spine without bone on bone interaction between adjacent vertebral bodies^{49,58}. Intervertebral discs, along with facet joints carry all compressive loads from the trunk, transfer that load along vertebra without collapsing, and deform to allow bending and torsion of individual vertebra⁵⁰.

The three main components of the intervertebral disc are the nucleus pulposus, the annulus fibrosus, and vertebral endplates. The nucleus pulposus occupies between 50 to 60 percent of the area of the disc, the annulus fibrosus surrounds the nucleus pulposus, and the vertebral endplates separate the disc from the vertebra above and below it (Figure 2.4)^{7,44,49}. The nucleus pulposus is a semi fluid mass made up of chondrocyte like cells that are dispersed in an intercellular matrix made up of mucoprotein gels that contain various mucopolysaccharides. The nucleus is mostly composed of proteoglycans which can be as much as 65 percent of the dry weight of the nucleus. Because of its polar hydroxyl groups, the polysaccharides, chondroitin, and sulfates that compose proteoglycans gives the nucleus the ability to bind large amounts of water; the nucleus is between 70 and 90 percent water. Proteoglycans also contain large negatively charged sulfate groups and this prevents them from diffusing out of the nucleus. All of these components come together to form a three-dimensional lattice gel system. Proteoglycan (and thus fluid) concentrations are highest in the nucleus and lowest in the annulus; also concentrations are smaller in the lower lumbar than in the upper lumbar.

The annulus fibrosus gradually becomes differentiated from the outer margins of the nucleus and forms the outer boundary of the intervertebral disc. The fibers of the innermost layers blend in with the intercellular matrix of the nucleus so there is no clear differentiation between the nucleus and the annulus. The annulus is made of collagen

fibers that are arranged in 10 to 20 sheets of concentric laminated rings that surround the nucleus; these sheets are called lamellae and are strongly bound to one another (Figure 2.5). The orientation of the fibers of the lamella alternate between consecutive bands but their orientation with respect to a transaxial plane is always the same (about 65°). So, viewing a disc frontally, the fibers in one lamella would be oriented 65° to the right and the fibers of the next lamella would be oriented 65° to the left.

Within each lamella, collagen fibers are oriented in a parallel fashion and run from the upper vertebra to the lower vertebra; the attachment is much stronger at the periphery of the annulus than it is close to the nucleus. The anterior and lateral areas of the annulus are twice as thick as the posterior portions, because one of the main purposes of the annulus is to resist the deformation of the nucleus thus maintaining disc height^{6,7,25,38,44,49,50}.

Cartilage endplates also play a critical role in the function of the spinal column. They facilitate the anchoring of the disk as well as serve as a barrier between the nucleus pulposus and adjacent vertebral bodies⁶. Cartilage endplates are composed of hyaline cartilage towards the vertebral body and fibrocartilage towards the nucleus pulposus. The endplates are approximately 0.6-1mm thick and they cover the entire nucleus pulposus and most of the annulus. The collagen fibers of the innermost lamella of the annulus grow into the endplate which ensures that the nucleus is encapsulated by the endplates. The subchondral bone of the vertebral body is deficient over about 10% of the area of the vertebral endplates and this causes pockets of the marrow cavity to lie alongside the surface of the endplates; this is important because these pockets allow blood vessels in the bone marrow to provide nourishment to the intervertebral discs and endplates^{49,50}.

2.3 Intervertebral Disc Mechanical Behavior

2.3.1 Compressive and Tensile Characteristics

The spinal column and intervertebral discs are subject to traumatic loads, which is why compression tests have been the most popular mechanical tests. The mechanical role of the nucleus pulposus is to resist the compressive force by providing internal fluid pressurization or hydrostatic pressure in response to the force.^{34,35,39,50} Experiments to test compressive forces are usually done on a motion segment (as seen in Figure 2.6) using some universal testing apparatus like an INSTRON machine or an MTS machine. A motion segment usually consists of two vertebra, an intervertebral disc, and the ligaments between them; it is the smallest section of the spine possible that still exhibits biomechanical testing characteristics that are comparable to that of an entire spinal column. The load deformation curve made by an intervertebral disc under compression (Figure 2.7) is useful in depicting the behavior of the disc under compression. The curve is typically sigmoid; being concave towards the load axis during initial loading and convex towards the load axis as the failure point approaches. At small loads, the disc provides little resistance (with stiffness values of 475 to 8,250 pounds per inch) but as the load increases the disc becomes much stiffer (with stiffness values of 12,000 to 20,000 pounds per inch); the stiffening behavior of the disc becomes more apparent with increasing load. The collagen fibers of the annulus are mainly responsible for this behavior because they become increasingly stiff when they are subjected to tensile strain due to the transverse bulge of the disc (Figure 2.8 and Figure 2.9). This effect causes the

disc to resist horizontal displacement so the disc provides flexibility at low loads and stability at high loads^{23,50,54}. At high loads and central compression, there is an inward bulge of the vertebral endplates and a radial bulge of the annulus. This illustrates the propensity of the disc to herniate laterally (more specifically, posterolaterally) as seen in clinical situations^{42,50}.

The entire intervertebral disc is rarely subject to pure tensile stresses under normal physiological conditions; the annulus however is subject to tensile stresses during flexion and extension of the spine (Figure 2.10). Both strength of disc material at various locations on the disc and mechanical tensile properties of intact discs have been tested. Strength of disc material is generally tested by cutting a motion segment into axially oriented rectangular sections and stretching them to failure in a testing machine. With the exception of the nucleus, the lateral portion of the annulus is least able to resist tensile stresses. In tension, resistance is only provided by the stretching of the annulus and longitudinal ligaments, and axial tensile stiffness was found to be between 1.5 and 3.0 times less than axial compressive stiffness (approximately 2,300 newtons for axial tension as compared to about 7,000 newtons for axial compression)^{17,23,50}.

2.3.2 Bending, Torsion, and Shear Characteristics

Unlike pure compression, which was found not to be damaging to intervertebral discs, bending and torsion have deleterious effects. Even though the discs mechanical resistance to bending and torsion increases as deformation increases, bending in vertical planes was found to generally result in disc failure when the bending was greater than 15° and there was damage to the posterior element of the disc or when rotation was greater

than 20°. The nucleus pulposus demonstrates significant viscoelastic properties in torsional shear. Shear stiffness of an intact disc in the horizontal plane is approximately 260 N/mm; this shows the large resistance that intact discs have to abnormal horizontal displacement. This value is so large that it is safely assumed that it is rare for the annulus to fail because of pure shear force; clinical evidence shows that most annular disruption is caused by a combination of torsion, tension, and bending^{17,34,50}.

2.3.3 Viscoelastic Characteristics

Viscoelastic characteristics measure the physical properties of a structure that document its behavior over time. Like a number of other biological tissues, intervertebral discs exhibit creep, relaxation, and hysteresis characteristics (creep and relaxation techniques are generally used to measure viscoelastic behavior). An experiment was performed which studied creep testing under three different loads on spinal lumbar segments, and it was found that higher loads cause greater deformation and faster rates of creep. Creep behavior was also found to be closely related to disc degeneration, the deformation of the structure over time correlated with the degree of degeneration of the disc. Nondegenerated discs have smaller deformation and it is reached over a much longer period of time than degenerated discs, this shows that as a disc becomes progressively degenerate it also loses its ability to attenuate shocks and evenly distribute loads^{25,50}.

All viscoelastic structures exhibit hysteresis; it is a protective measure which causes a loss of energy when a structure is subjected to repetitive cycles of loading and unloading. Hysteresis varies with the magnitude of applied load, the age of the

intervertebral disc, and at what level of the spine the disc is situated. Hysteresis was found to be directly proportional to applied load, increasing as the load increased. It was also found to be largest in very young individuals and smallest in middle aged individuals. Lastly it was found that lower lumbar discs exhibited much greater hysteresis than lower thoracic and upper lumbar discs. Hysteresis was observed to decrease when discs were subject to repetitive loading, this suggests that repetitive axial vibrations may lead to the increase of disc herniation^{25,50}.

2.4 Intervertebral Disc Degeneration and Disease

Aging has deleterious effects on biological tissues. Disc degeneration is the alteration of disc biochemistry and age related deterioration of the disc that leads to decreased mechanical functioning, loss of ability to maintain optimal disc height, loss of ability to aid in painless normal spinal function, and loss of ability to absorb and distribute loads(Figure 2.11). There is a decrease in nutrition supplied to the discs due to the occlusion of blood vessels over time; endplate calcification may also inhibit nutrient transport. The impaired nutritional delivery is suspected to be an underlying cause for biochemical changes in the discs. Over time the nucleus also becomes more fibrotic, going from a mostly aqueous state to a more solid state. It contains more granular material (thought to be betaproteoglycanlipid complex) that may be a byproduct of degenerate cells; it also contains more chondrones^{9,26,62}.

Proteoglycans can hold up to 200 times their weight in water. Their synthesis decreases with age and the chemical composition of the proteoglycans that are still synthesized is altered. Water content of the annulus fibrosus and nucleus pulposus are

80% and 90% respectively at birth; but the water content of the entire disc can decrease by up to 63% over the years^{19,25,36,61}. As water content decreases many changes occur. The nucleus loses its ability to transmit weight to the annulus impairing the load distribution pattern that a healthy disc would have. The nucleus is also less capable of maintaining hydrostatic pressure and disc height decreases leading to an outward bulging of the annulus during compression. Under this continual strain, the annular lamella can eventually shear, crack, or fissure, allowing the nucleus to migrate from the center of the disc through the annulus (herniation). The migrated nucleus can compress the nerve root and cause excruciating pain as well as nerve root damage. Also, the herniated material which would now be on the outside of the annulus would initiate an inflammatory response attracting macrophages and lymphocytes and producing chemical pain mediators which is another cause of back pain. Overall collagen content as well as collagen strength decreases with age, making intervertebral discs more susceptible to injuries associated with everyday stresses. Lastly, there is an overall decrease in bone density and strength; this causes the vertebral endplate to continuously bear increased load. The endplates may fracture over time allowing the nucleus to migrate into the vertebral body causing pain and decreased function. It is estimated that by age 50, 97% of lumbar discs are degenerated to some degree^{6,9,44,26,61,62,63}.

2.5 Treatments for Degenerative Disc Disease

2.5.1 Conservative Treatments for Disc Degeneration and Disease

Low back pain generally refers to spinal and paraspinal symptoms in the lumbosacral region of the spine. Although back pain is the most common reason for primary care physician visits, many back pain sufferers never seek medical assistance. In a medical survey of North Carolina residents with back pain, it was determined that only 39% of them sought medical assistance. This is because episodes of pain are typically brief, persisting for one month or less in 75% to 90% of patients^{64,65}. Low back pain may be managed by many different types of health care providers such as internists, family practitioners, general practitioners, neurologists, emergency physicians, rheumatologists, neurological surgeons, osteopathic physicians, chiropractors, physical therapists, acupuncturists, and massage therapists. In many cases, an exact pathoanatomic cause for pain can not be determined by physical examination or diagnostic means because of the weak associations among symptoms, anatomic problems, and physical examination findings. Since many individuals have nonspecific mechanical causes for their pain, the goal of examination is to exclude potentially serious causes of pain and identify patient who may be at risk of delayed improvement due to physical abnormality^{15,64,65}.

Many therapeutic options are recommended to patients with low back pain; the most widely used are bed rest, medication, activity modification, and physical therapy. Bed rest has been so widely recommended for years because disc pressure is minimized in the supine position. However, recent clinical trials show that continuation of usual

activity without any formal recommendations for bed rest produce a better outcome; so limiting bed rest to periods of severe pain seems to be the most reasonable option.

Nonsteroidal anti-inflammatory drugs (NSAIDs) and acetaminophen are the most commonly prescribed medications for the treatment of low back pain. Muscle relaxants and opioids have also been prescribed but have not been proven to be more effective in clinical studies, though muscle relaxants that cause sedation can be particularly useful for night time discomfort. Activity modification is designed to avoid continued activity which would further aggravate the affected area. The most common situations to avoid are prolonged sitting or standing; patients are generally instructed to get up at short regular intervals (30 minutes to an hour) and do low stress aerobic activities such as walking and light back stretches. Physical Therapy includes therapeutic exercise, manual therapy, and spinal manipulation. Patient satisfaction from physical treatment is often higher than that of patients who only receive physician directed care, so physicians often refer back pain patients to physical therapists⁶⁵.

2.5.2 Invasive Surgical Treatments for Disc Degeneration and Disease

2.5.2.1 Discectomy

Discectomy is performed when a spinal disc becomes damaged and the nucleus migrates through the annulus and presses against spinal nerves causing pain. These protruding or prolapsed discs can be seen by CT, MRI, or Myelogram. Ideal candidates for this procedure have symptoms of unilateral sciatica with mechanical signs of nerve root involvement when they stand erect, exhibit positive tension signs, and improve with

supine positions. A small opening is made between adjacent lamina and the portion of the disc that is pressing on the spinal nerve is removed. The surgery takes an average of an hour and fifteen minutes and the average hospital stay after the surgery is 2 days. Success rates for lumbar discectomy are between 46 and 96%^{10,66}.

2.5.2.2 Spinal Fusion

The traditional response to disc degeneration is spinal fusion, it has become the standard for many different spinal conditions over the past 60-70 years, having been performed for over 100 years. Spinal fusion involves inducing bone growth between two adjacent vertebrae above and below a damaged disc. Posterior lateral lumbar fusion came into use in the mid 40's; the process is meant to restore mechanical stability to the affected area of the spine. Later, interbody devices became available to help provide structural support within the disc space itself (Figure 2.12). Clinical studies showed that fusion and decompression of the lumbar spine were the superior form of surgical management for lumbar disc degeneration in older adults. Despite all of the theoretical advantages of spinal fusion, which has increased in incidence over the past twenty years and has begun to be performed on younger patients, concerns regarding the disadvantages of the fusion have become increasingly critical. In spite of interbody fusion, studies have reported that postoperative disc height can fall below preoperative disc heights. Failure of the bone graft is also a marked possibility because of nonunion or failure to heal; it has resulted in the return of pain in many cases. To help allay these concerns, interbody implants have been made in many different designs and from various materials but this has not resolved physicians major concern. A major concern being that the lack of motion

in the fused area may lead to the degeneration of the discs above and below the fused vertebra, ultimately causing more degeneration and possibly other fusions^{16,25,59,60}.

2.5.2.3 Artificial Disc Technology

Research into the development of artificial discs started in the 1950's because researchers believed that replacing a damaged disc with an artificial disc would provide significant functional improvement over spinal fusion^{37,45,67}. Spinal surgery is extremely dangerous because of the risk of injury to the spinal cord and other important nerves, so because of these risks, disc prosthesis should last for the life of the recipient. Since the average age of spinal fusion patients is between 35 and 50, artificial disc prosthesis will optimally last over 40 years. A conservative estimate of the number of loading cycles made during that 40 year period is about 85 million cycles (assuming one million gait cycles per year and 125,000 significant bends), so the material to be used for the implant should be tested to at least 100 million cycles. Materials are another main concern when designing intervertebral disc prosthesis. Materials used must be resistant to wear because as parts of the implant articulate against each other, wear particulate can cause inflammation and irritation at the site of implantation. The implant must also be biocompatible. The implant should also be able to fit within the space that an intervertebral disc normally occupies, the size of the implant would depend on the location of the implant. It is of the utmost importance for the implant to restore normal disc height in order to preserve spinal biomechanics because proper load transmission depends on the similarity of the dynamic response of the prosthetic disc to the dynamic response of normal disc. That being said, a well designed prosthetic disc will duplicate an

intact discs stiffness in all three planes of rotation and in axial compression. If an implant is not capable of transmitting loads properly to the bones and tissues adjacent to it, bone resorption may take place in an area where the bone is under stressed or bone deposit can take place in an area where the bone is overstress leading to structural complications. This is a major reason that complete disc replacement is often thought to be more favorable than spinal fusion, which is shown to demonstrate dynamic stiffness that is significantly greater than that of the natural spine^{27,37}.

Another critical standard that a prosthetic disc must meet is adequate freedom of movement. A typical L4-L5 joint can comfortably undergo 13° of flexion, 3° of extension, 3° of right lateral bending, and 0-1° of axial rotation⁶⁸. A good disc prosthesis should allow for at least this much movement while at the same time constraining movement so that it will not be much greater than this; thus allowing normal range of motion while preventing excess movement which may cause damage to nerve structures in the region of the implant³⁷.

Fixation is also another important factor concerning implant success, immediate and continuing fixation of the implant to the bone is required for successful prosthetic function. Screws only hold securely for six weeks, press fit implants (like spikes and pegs) can shift under tensile loading and also only hold for a short period of time, and porously coated material meant to encourage bone ingrowth requires long periods of low or no amplitude movement in order for fixation to occur properly.

Lastly, the implant device should be designed in such a way that failure of one of its components will not cause catastrophic failure of the whole device, or excessive

damage to the nerves and tissues surrounding it. The prosthesis should also maintain integrity in the event of accident or mechanical shock to the spine³⁷.

Although research into artificial discs started in 1956, it wasn't until 1973 that Urbaniak et al. reported the first prosthetic disk which was prototyped and implanted into chimpanzees. Many artificial disc designs have been proposed since then but only 3 have undergone extensive testing procedures and been used clinically. The Charité artificial disc was the first available and is the most clinically tested artificial disc prosthetic in the world. The Charité disc was first developed in the mid 80's by Professor Karin Büttner-Janz and Professor Kurt Schellnack at the Charité hospital in Berlin. The design was further refined with the help of the staff at Waldemar Link GmbH, a leading European based medical device manufacturer^{11,67}. The Charité disc is a three piece articulating prosthesis which consists of a sliding core that is sandwiched between two metal endplates (Figure 2.13 and Figure 2.14); the mobile biconcave polyethylene core allows for rotation in all three directions and translation and it articulates against two Cobalt Chromium baseplates. The plates have teeth that eliminate the need for cement during vertebral body fixation. Many refinements have been made to this prosthesis over time including the increase of the device footprint to ensure more even loading, modification of the location of the teeth to encourage tighter bonding to vertebral bodies, and the addition of plasma spray coating also to encourage better fixation. Due to the lack of elasticity of materials used, this device does not completely replicate the normal compressive stiffness of a natural intervertebral disc^{11,12,13,60,67}.

Other notable intervertebral disc prosthesis are as follows: the Acroflex was designed in 1988 by Dr. Art Steffee. The Acroflex is a polymeric one-piece disc was

composed of an elastomeric core bonded to titanium alloy baseplates (Figure 2.15). The ProDisc was produced in 1989 by Dr. Thierry Marnay. The ProDisc is a semi constrained disc in the popular 3 piece design with a polyethylene core with Cobalt Chrome baseplates (Figure 2.16). The Maverick was designed in 1993 by Dr. Kenneth Pettine and Dr. Richard Salib. The maverick is a two piece metal on metal articulating prosthetic (Figure 2.17) that incorporates a posterior center of rotation. The FlexiCore was designed in 2001 by Dr. Thomas Errico. It is a two piece metal on metal articulating design with superior and inferior components which are linked by a capture ball and socket joint (Figure 2.18), this prosthetic is inserted as a single unit. There are currently more than 20 other total disc replacement prosthesis designs that are currently in various stages of development¹³.

2.5.2.4 Artificial Nucleus Prosthesis

Nachemson first put forth the concept of nucleus replacement as a treatment option to combat low back pain in 1962 and the idea has been developing since then. The main motivation for this concept is the limited success of current treatments (spinal fusion and total disc replacement). Since the nucleus is more than half of the components that make up the intervertebral disc and it is directly related to the pathological changes associated with disc degeneration, it is only logical to consider the replacement of the nucleus as a solution for low back pain in individuals who are suffering from the effects of disc degeneration but still have a well preserved annulus. Some of the advantages of only replacing the nucleus as opposed to replacing the entire disc are as follows: replacing only the nucleus allows the surgeon to leave the rest of the disc (the annulus

and endplates) intact; this is advantageous because no known synthetic material maintains disc biomechanics as well as the original disc components. A nucleus implant would be much smaller than a conventional total disc replacement prosthetic, making it easier to implant and more amenable to minimally invasive surgery. Because surgery would be less invasive, the chances of excessive blood loss, surgical complications, and prolonged recovery times would be reduced. Lastly, product design and fabrication would be more straightforward for this smaller prosthetic. Since the nucleus supports a considerable portion of the load placed on an intervertebral disc, the main objective of a prosthetic nucleus would be to help preserve the annulus and maintain disc height thus restoring disc function and biomechanical stability^{14,20,57}.

In one study by P. Eysel et al., a prosthetic disc nucleus consisting of a polymeric hydrogel incased in a high-tenacity polyethylene jacket was developed (Figure 2.19). The polyethylene jacket in this device allowed it to absorb fluid and thus exert a swelling pressure which was hoped to be similar to the excised nucleus. In this experiment, 11 lumbar segment (L2/L3) were taken from cadavers with a mean age of 62 (47±84 years old) a mean of 12 hours (9±16 hours) after death; discs showing complete annular rupture were excluded from the study. The segments were then fixed onto a testing device and measurements were performed in all directions on the intact discs. Subsequently, 5 to 6 grams of nucleus material was removed by standard nucleotomy (the insertion of a tube into an intervertebral disc to aspirate the contents of the disc) and measurements were taken again. Then two prosthetic nuclear devices were introduced into the disc in the same way that the nucleus was extracted and measurements were taken yet again. Results showed that after nucleotomy with the removal of 5 to 6 grams of nucleus material, spinal

segment mobility increased between 38 and 100%; however, after the insertion of the prosthetic nuclear implants, segment mobility was restored for movement in all directions with no statistical differences between pre nucleotomy measurements and the measurements obtained with the prosthetic nuclear device. This experiment showed that a nucleus pulposus prosthetic can return disc stability, but this has only been proven in in-vitro situations. In in-vivo situations anatomical reactions of the endplates would be a factor as well as sclerotic reactions and the possibility of implant dislocation, however this experiment helped to show the potential that nucleus replacements can have²¹.

In another experiment by Bao and Higham in 1990, hydrogel materials were used. Hydrogels are gel like materials formed from colloidal solutions; they are composed of polymer chains that are water-insoluble and are super absorbent. Because of their beneficial properties, hydrogels have been frequently used for other medical applications since being discovered by Wichterle and Lim in 1960. It was thought that by using these materials, physiological properties of the disc could be reproduced in addition to mechanical properties. Taking into consideration the physiological properties of an intact disc, Bao and Higham realized that replacing the nucleus with silicon, polyurethane, or any elastomer without substantial water content would hinder the supply of nutrients to the rest of the disc leading to further annular degeneration over time, thus the decision to use a hydrogel. Bao and Higham made a nucleus implant containing approximately 70% water content under physiological loading conditions after considering many different hydrogel materials. Since the gel has the ability to absorb and extrude water similar to a natural nucleus, biomechanical studies were able to confirm the restoration of disc function with these hydrogel nucleuses in in-vitro testing. This pair was the first to

demonstrate the ability of hydrogel nucleus implants under cyclic loading conditions. A study using baboon models has thus far shown no adverse local or systemic tissue reactions and this implant is expected to reach clinical trial stages in the near future^{11,12}.

Many other types of nucleus prosthesis have also been proposed and studied. Another very common design concept is the injection of an in situ curable polymer into the disc space; the polymer then cures in situ to form working nucleus prosthesis. Silicone and Polyurethane are the two most widely used medical elastomers and thus the two most popular choices for this method. This method, as all methods, has benefits and disadvantages. The benefits are as follows: since the elastomer cures in situ, it can be injected through a very small annular incision which greatly reduces the risk of implant extrusion. The stability and load distribution of this type of implant is also very good because since the implant is injected, it has very high cavity conformity. The disadvantages of this type of implant are as follows: an in situ cured polymer may not have the mechanical strength to withstand load over the required fatigue life of the implant due to the effect that the curing conditions may have on polymer mechanical properties. Polymerization must also be able to take place within a reasonable amount of time; the longer the polymerization process, the longer the surgical time and the higher the likelihood of incomplete polymerization. Also, since the polymer is very fluid upon initial injection, great care must be taken that it does not extrude from the annular incision or other annular defects. Lastly, polymers cured in situ must also be biocompatible and most monomers are toxic. Therefore it is critical that polymerization be completed with minimal leaching.

There are many current designs on the market for nucleus prosthesis, some of which can be seen in Table 2.1. There are no FDA approved nucleus arthroplasty devices currently available; however as of April 2007 four companies are in the process of conducting clinical trials using nucleus prosthesis designs ^{13,57}.

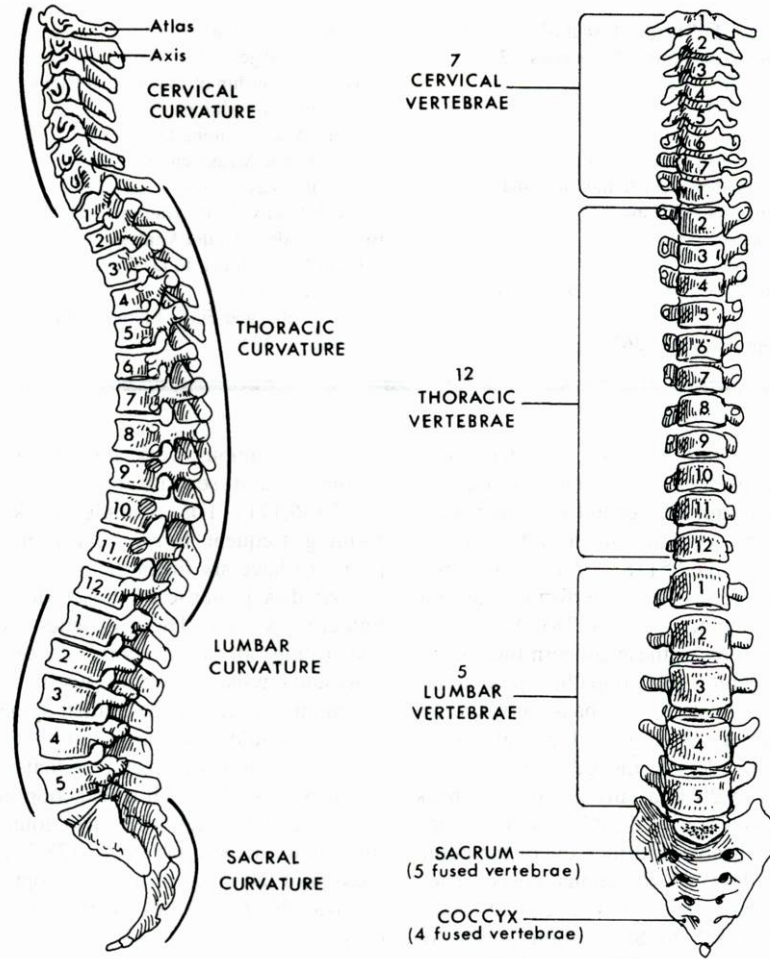


Figure 2.1. Diagram of the Human Spinal Column⁵³

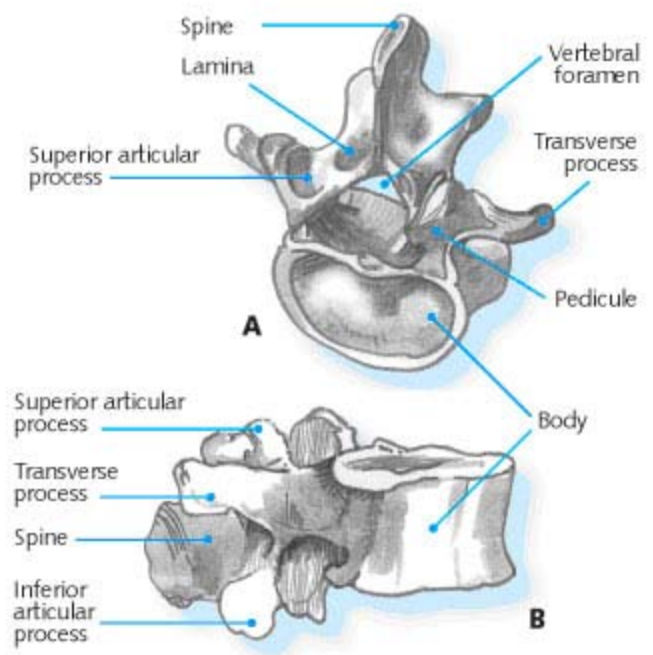


Figure 2.2. Diagram of a vertebral body⁵²

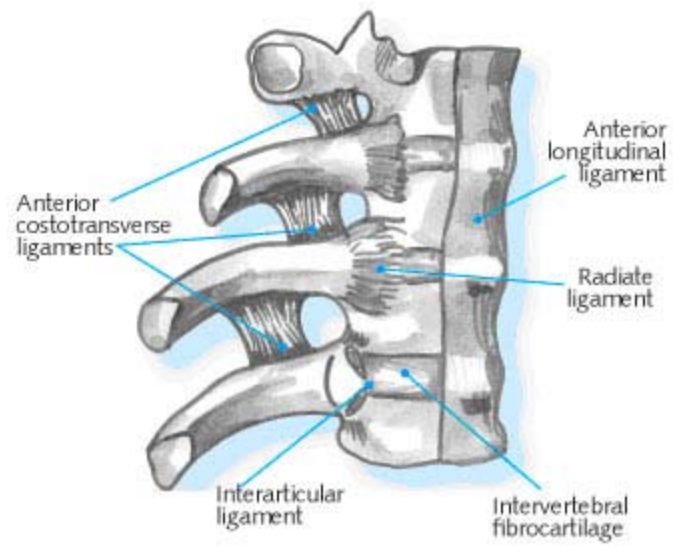
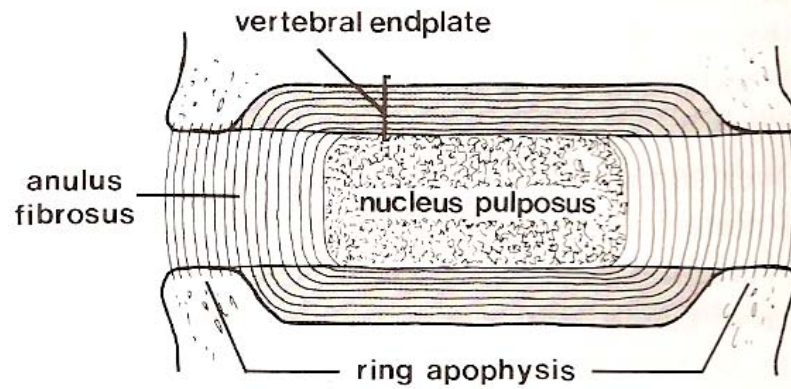


Figure 2.3. Diagram of spinal ligaments⁵².



Detailed structure of the vertebral end-plate.
 The collagen fibres of the inner two-thirds of the anulus fibrosus sweep around into the vertebral end-plate, forming its fibrocartilaginous component. The peripheral fibres of the anulus are anchored into the bone of the ring apophysis.

Figure 2.4. Diagram of an Intervertebral Disc⁴⁹.

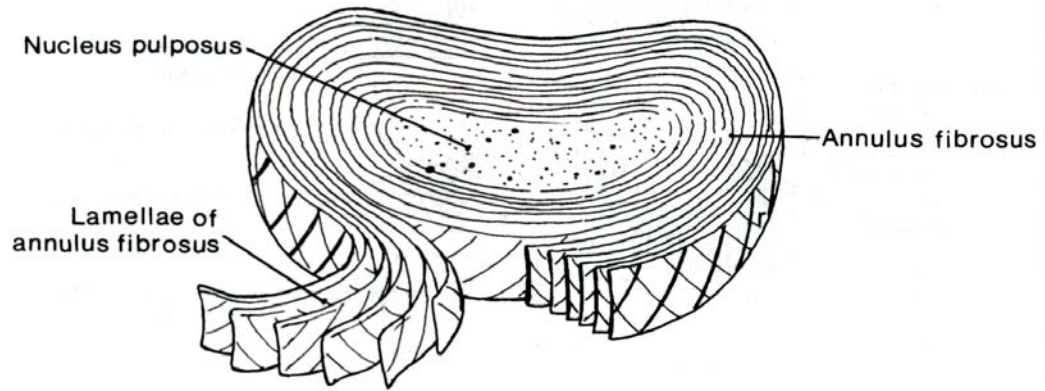


Figure 2.5. Diagram of an Intervertebral Disc⁵³.

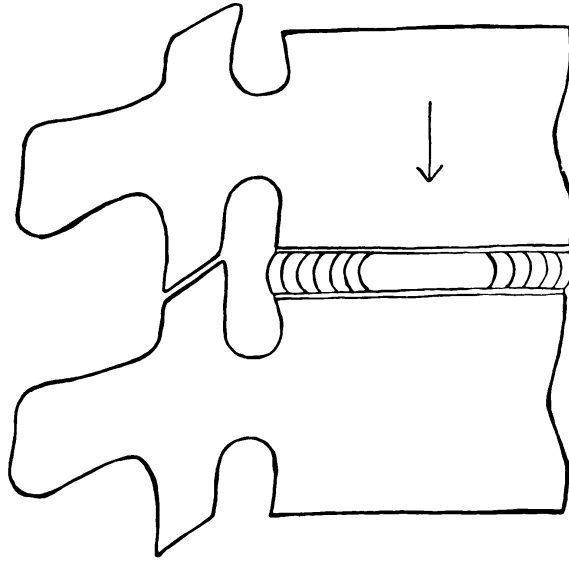


Figure 2.6. Diagram of a Functional Spinal Unit²⁴.

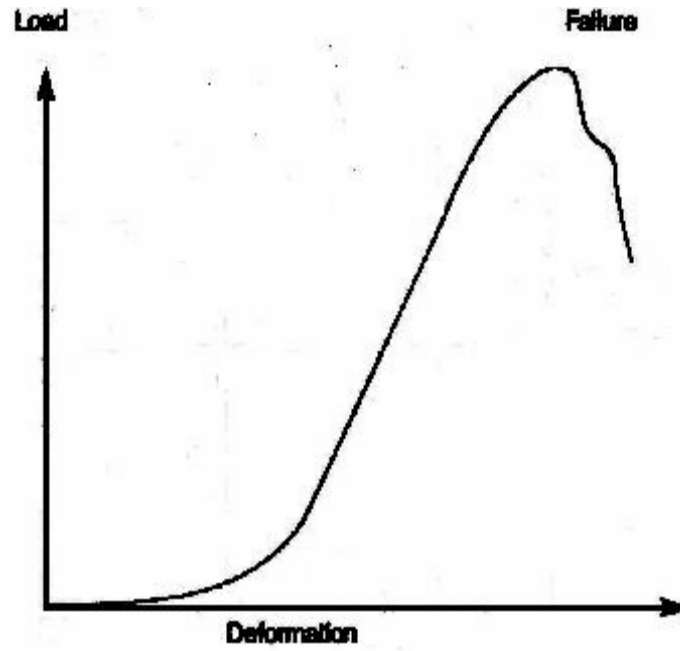


Figure 2.7. Diagram of a typical load deformation curve for a disc in compression⁵⁰.

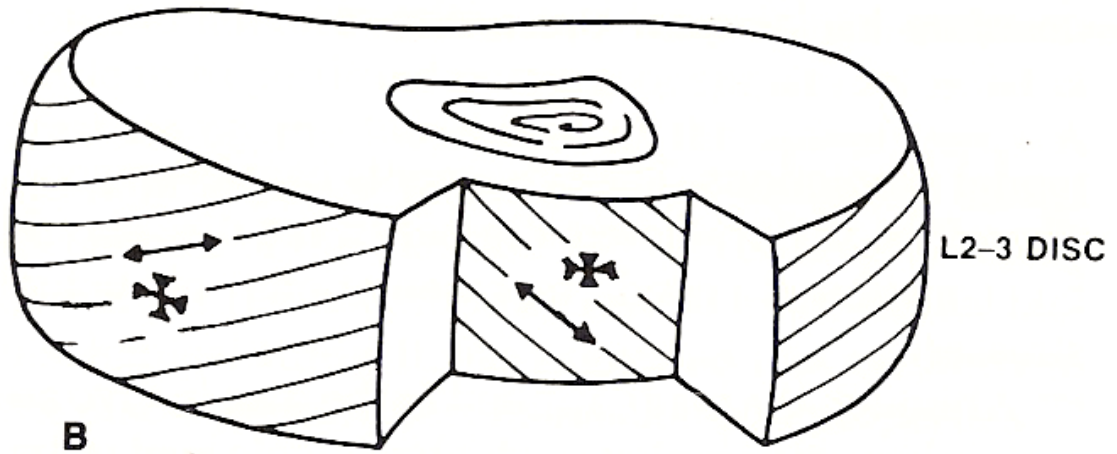


Figure 2.8. Diagram of the Stresses on an Intact Intervertebral Disc in Compression⁵⁰.

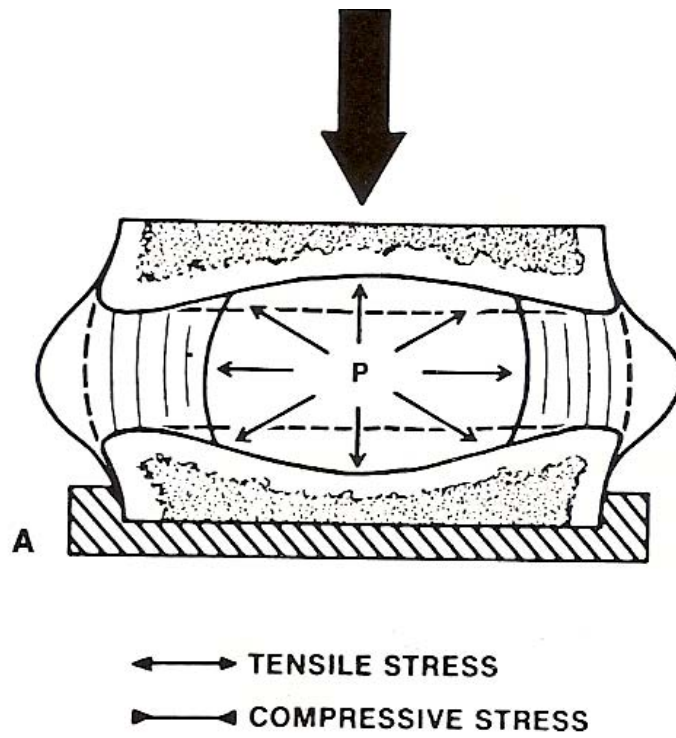


Figure 2.9. Diagram of an Intact Intervertebral Disc in Compression⁵⁰.

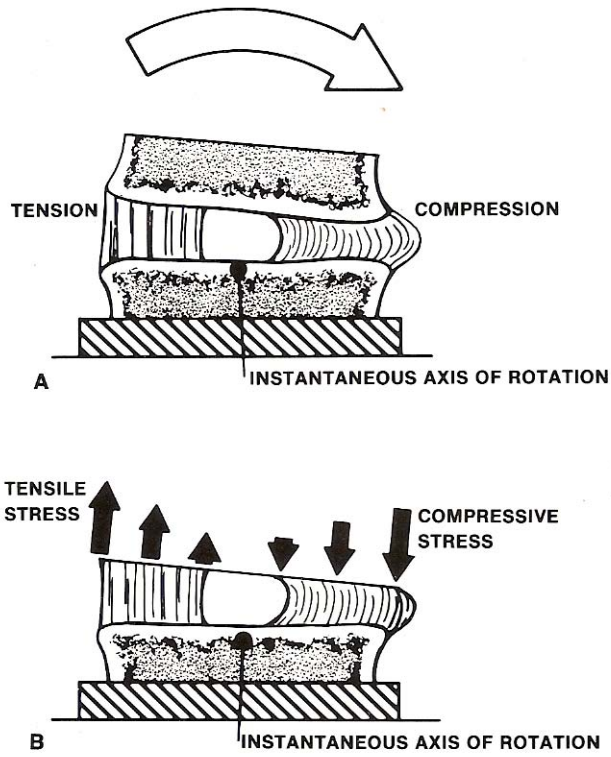


Figure 2.10. Diagram of the Stresses on an Intact Intervertebral Disc in Flexion and Extension⁵⁰



Figure 2.11. Radiographs showing advanced degeneration of an intervertebral disc. Notice the almost complete loss of disc height and the formation of vertebral osteophytes. Top: anterior-posterior radiograph. Bottom: lateral radiograph⁶¹.

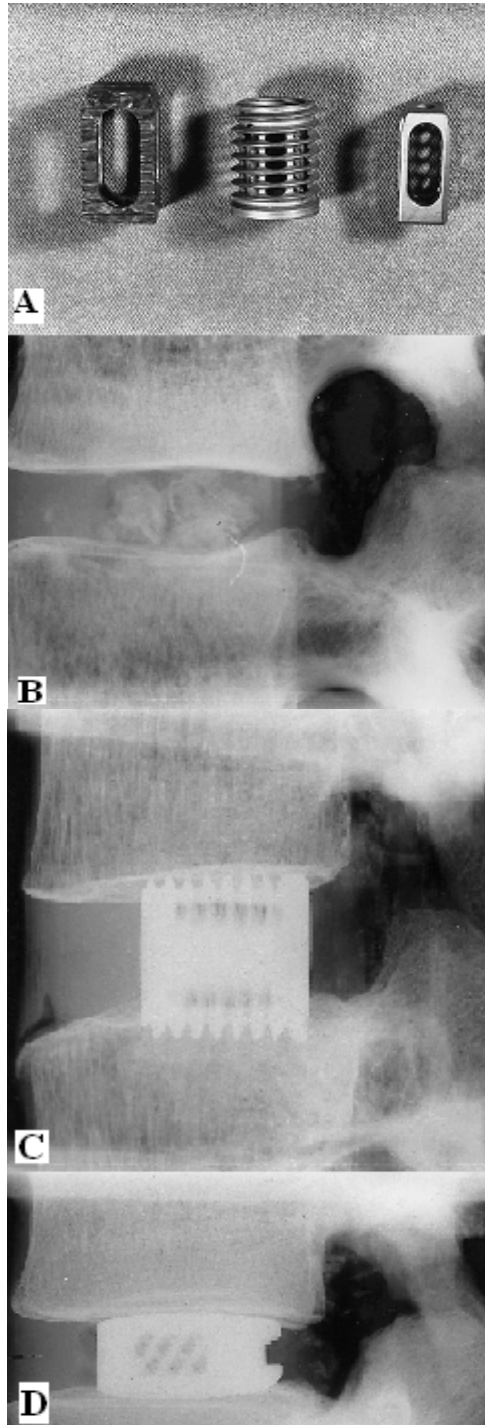


Figure 2.12. **A–D** Photographs of the different cage designs and lateral plain radiographs from a typical specimen after insertion of two parallel interbody cages. **A Left** and **B**: Brantigan cage – a rectangular, porous carbon-fiber implant. **A Centre** and **C**: Ray cage – a cylindrical, threaded, porous titanium implant. **A Right** and **D**: Stratec cage – a porous titanium implant designed to fit on the endplate Contours¹⁶.

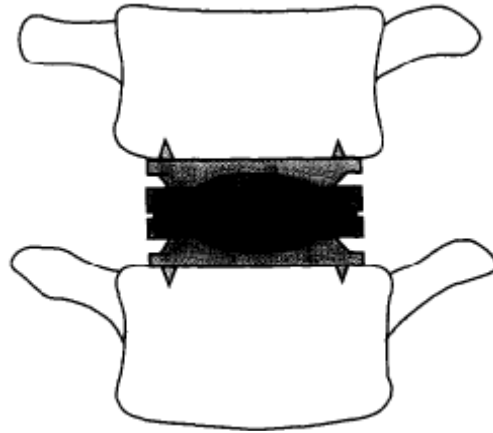


Figure 2.13. Diagram of the LINK[®] SB Charité artificial disc¹²

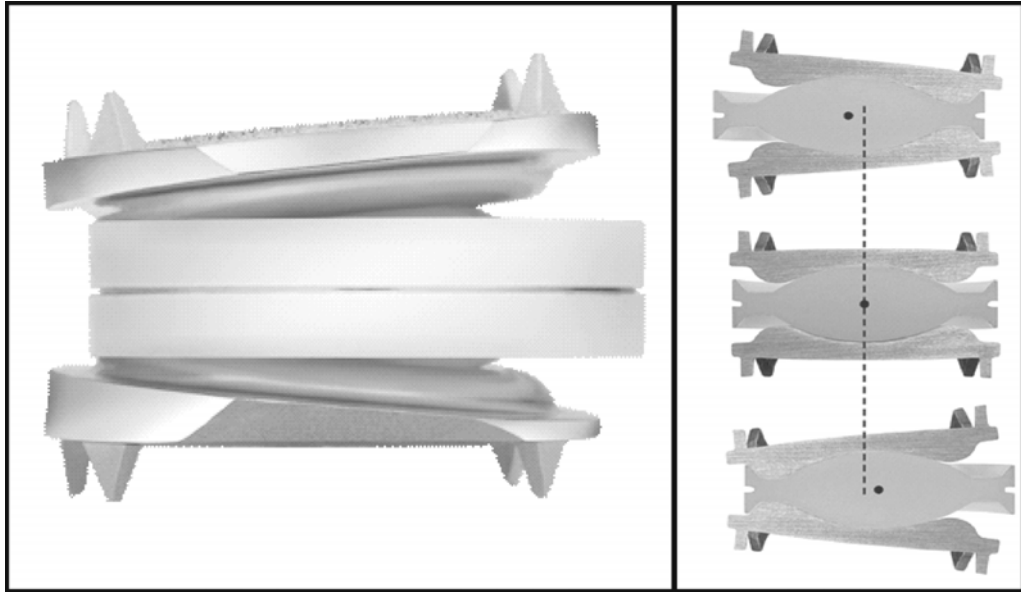


Figure 2.14. Diagram of the LINK SB Charité artificial disc⁶⁰



Figure 2.15. Diagram of the Acroflex® implant¹³



Figure 2.16. Diagram of the ProDisc implant⁶⁹

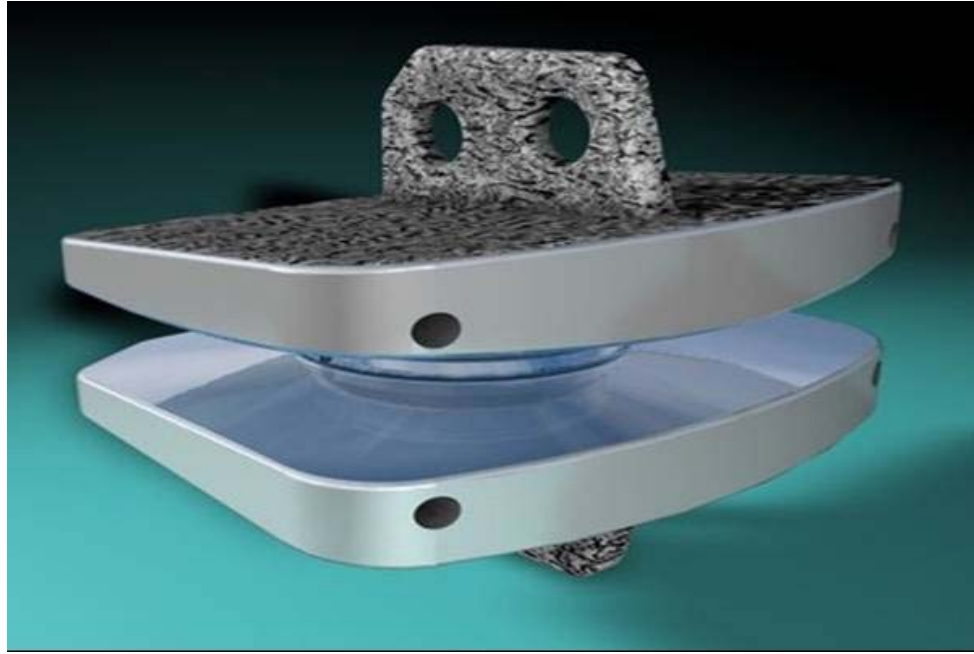


Figure 2.17. Diagram of the Maverick implant⁶⁹



Figure 2.18. Diagram of the FlexiCore implant⁷⁰

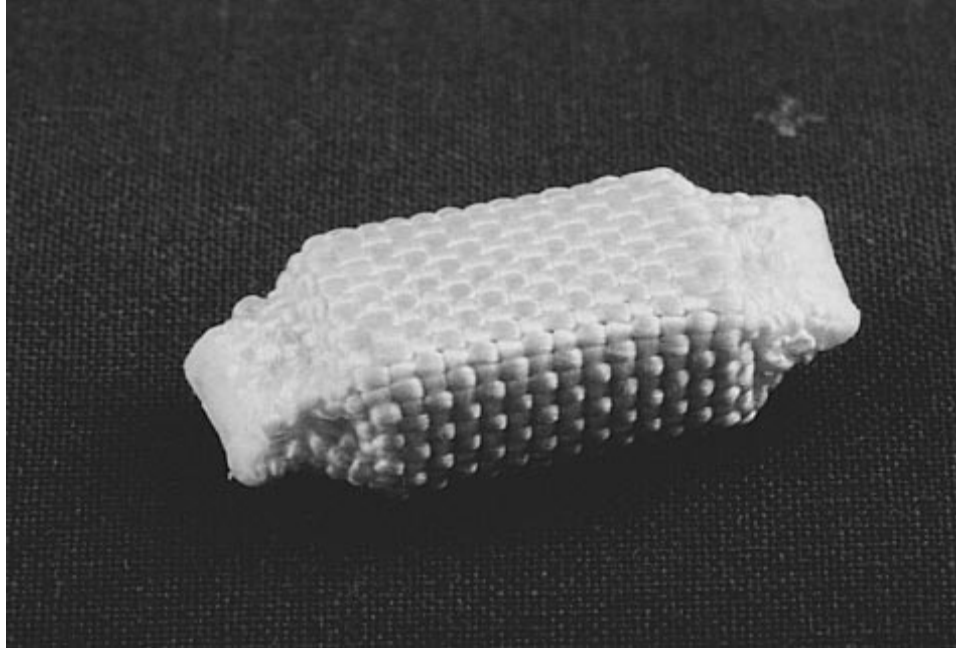


Figure 2.19. Diagram of a prosthetic disc nucleus²¹

Table 2.1 Table depicting various forms of Nucleus Prosthesis Design⁵⁷.

Device	Manufacturer	Material	Design
Prosthetic Disc Nucleus (PDN)	RayMedica, Bloomington, MN	Polyacrylonitrile-polyacrylamide (HYPAN) hydrogel core enveloped by polyethylene (PE) jacket	A pair of pillow-shaped implants with preformed and dehydrated hydrogel pellet encased in flexible but inelastic PE jacket. Implants get hydrated in the disc
Aquarelle	Stryker/Howmedica, Rutherford, NJ	Polyvinyl alcohol (PVA) hydrogel	Preformed bullet-shaped implant injected in semidehydrated state into disc space with an injection device. Implant adjusts its water content based on the intradiscal pressure
Prosthetic Intervertebral Nucleus (PIN)	Disc Dynamics, Minnetonka, MN	Polyurethane elastomer	<i>In situ</i> curable polyurethane is injected into a polyurethane balloon via a catheter and sets in the disc in minutes. The catheter is then removed
Newcleus	Sulze/Spine-Tech, Edina, MN	Polyurethane elastomer	A preformed, curled, spiral-shaped implant is straightened and inserted into disc space with an applicator device. The device is curled back to a spiral coil in the disc
BioDisc	Cryolife, Kennesaw, GA	Protein hydrogel, similar to BioGlue	An <i>in situ</i> curable protein hydrogel is injected into disc space and sets in the disc in minutes

CHAPTER III

NUCLEAR PROSTHESIS DESIGN

Disc nucleus replacements have been constructed of many different materials over the past ten years including plastics, polymers, ceramics, and hydrogels. Over twenty different nucleus arthroplasty devices are currently in the developmental stages^{13,57}.

The goal of this study is to create idealized models to determine the shape of nuclear implant best suited to resist the standard shear and torsional stresses that are generated in the lumbar spine. Based on discussions had with spinal surgeon Dr. Walter Eckman along with patented ideas that he put forth, 5 potential rigid two part nuclear intervertebral disc prosthesis designs were generated. It is hoped that these nuclear replacements will allow the annulus fibrosus to maintain disc height and perform normal function while preserving range of motion. Because the implants are incompressible and because of their ultimate shape, they should also have a reduced risk of extrusion as compared to hydrogel nuclear replacements while still being able to utilize minimally invasive surgical techniques when placed in patients with disc degeneration who still have substantially preserved annulus fibrosus and endplates.

Since this is a laboratory study mainly focused on determining the shape of nuclear implant best suited to resist standard shear and torsional stresses, the focus was placed on the shape of the inner surfaces of the implant rather the means of fixation for

the outer surface of the implant. Dr. Eckman's patent includes a variety of potential shapes for the interior articulating surfaces of the implant designs. The main criteria for all of the implant designs was stated as follows, "The intervertebral disc prosthesis includes a first part, and the first part has a top, a bottom having an opening, an outer surface, an inner surface, and a socket extending into an interior of the first part from the opening and defined by the inner surface. The outer surface proximate the top contacts a concave portion of a first vertebra. The disc prosthesis further includes a second part including a top, a bottom, and an outer surface. The outer surface on the bottom of the second part contacts a concave portion of a second vertebra, and the inner surface on the top of the second part cooperatively engages the inner surface of the first part thereby allowing at least two degrees of freedom of movement."⁷². Preliminary designs for the interior surfaces of the implants were drawn by hand. Based off of those drawings, the designs were then replicated using an AutoCAD program. Lastly, based off of the AutoCAD drawings, the designs were drawn using the SolidWorks 3D mechanical CAD program (the implant designs can be seen in Figures 3.1- 3.5). For mechanical testing purposes, the implants were made out of Acrylonitrile Butadiene Styrene (ABS) thermoplastic through a process called FDM. FDM is a solid-based rapid prototyping method that extrudes material layer-by-layer, to build a model. Based on the poor fidelity with which implant design 2 (Figure 3.2) was reproduced in the prototyping process, the decision was made to exclude it from all testing. Implant designs 1, 3, 4, and 5 were tested as planned. The implants were designed to be circular with a total width of 15mm so that they would easily fit within the boundaries of the annulus. They were also designed so that at maximum bending, they only tilt a maximum of 10° because a typical

L4-L5 joint can comfortably undergo 13° of flexion and 3° of extension⁶⁸. For these purposes of this experiment, the exterior of all implants were smooth and flat (as seen in Figures 3.1- 3.5). With the aid of an Instron Universal Testing Instrument, each of the remaining 4 implant designs were tested in shear to ascertain their mechanical properties; the details of this experiment are presented in Chapter 4. Following the shear testing, with the aid of an electropneumatic torsional device, each of the 4 remaining implant designs were also tested in torsion to further ascertain their mechanical properties; the details of this experiment can be found in Chapter 5.

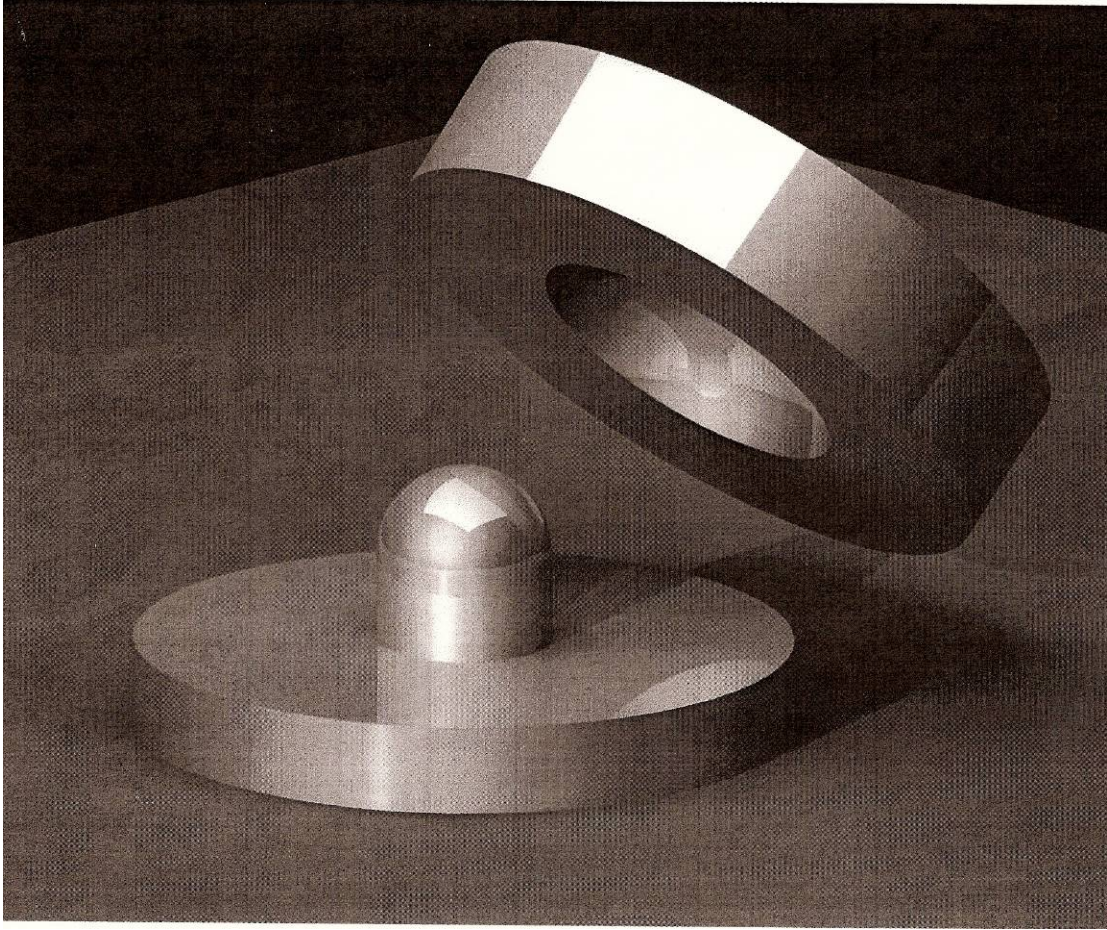


Figure 3.1. Implant Design 1 for the Nuclear Intervertebral Disc Implants.

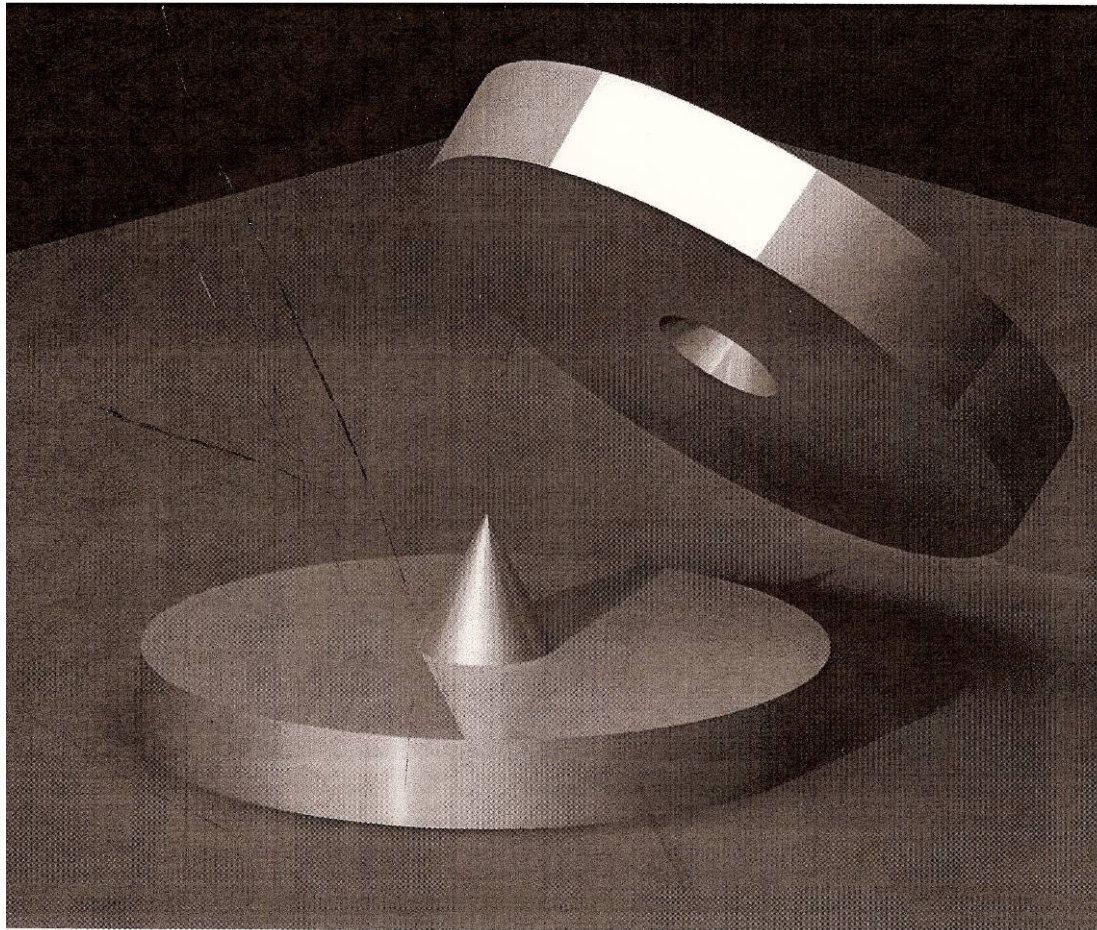


Figure 3.2. Implant Design 2 for the Nuclear Intervertebral Disc Implants.

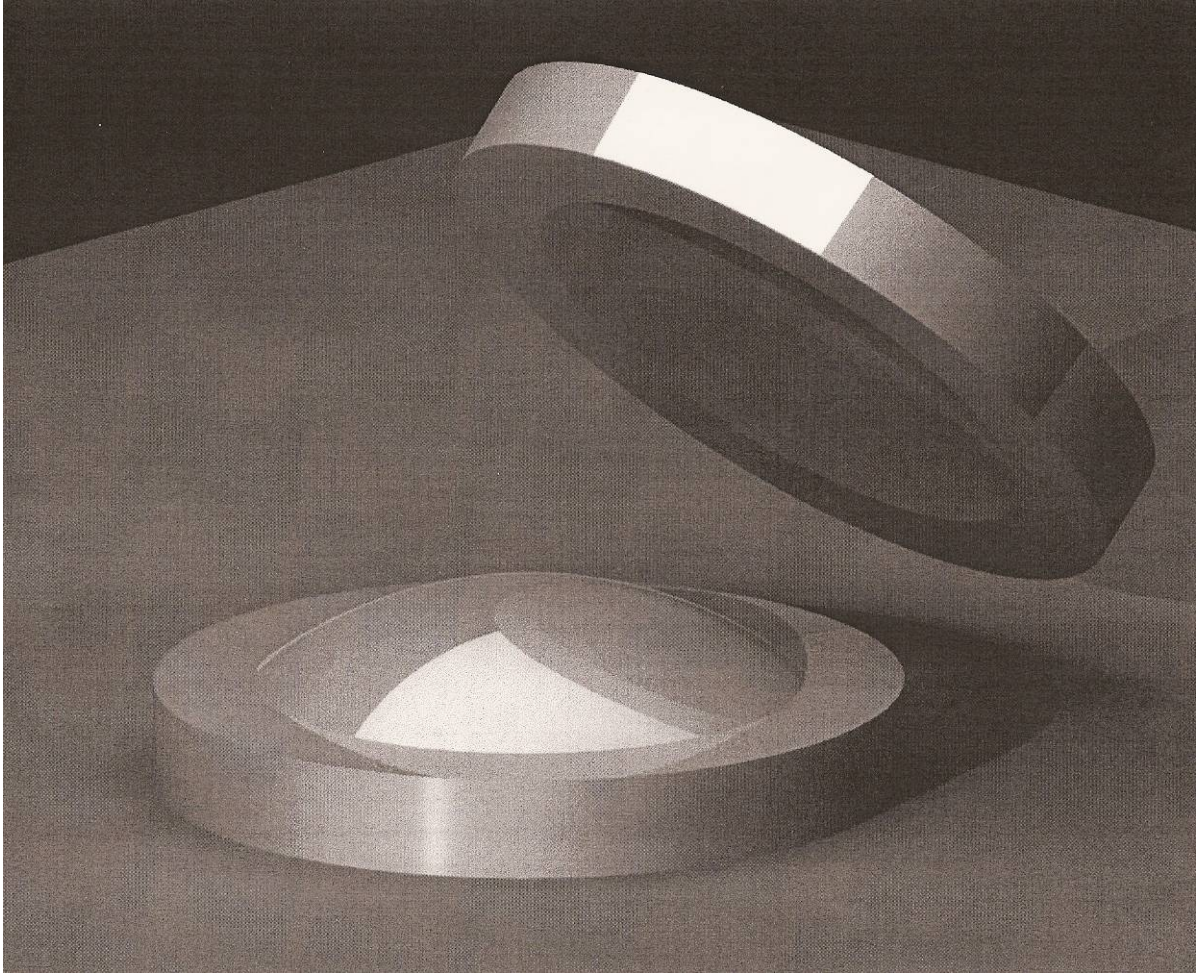


Figure 3.3. Implant Design 3 for the Nuclear Intervertebral Disc Implants.

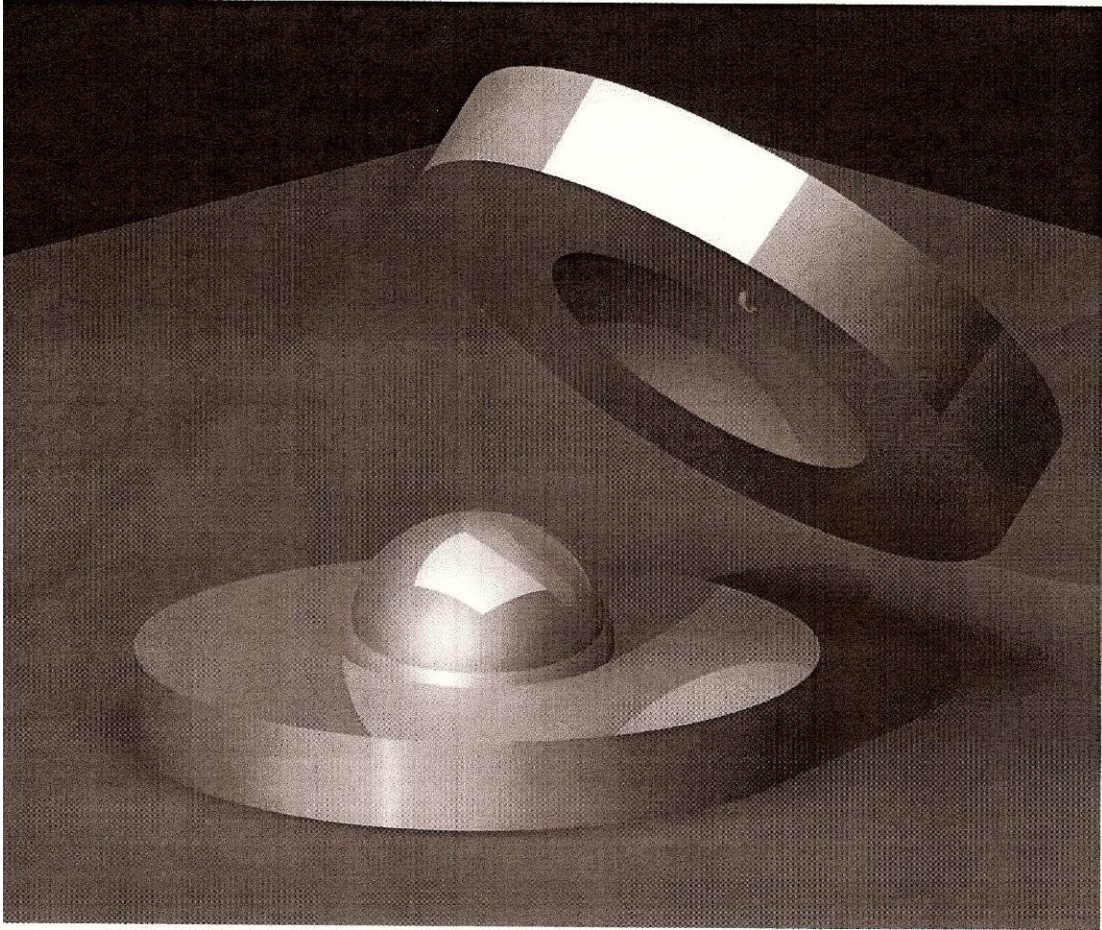


Figure 3.4. Implant Design 4 for the Nuclear Intervertebral Disc Implants

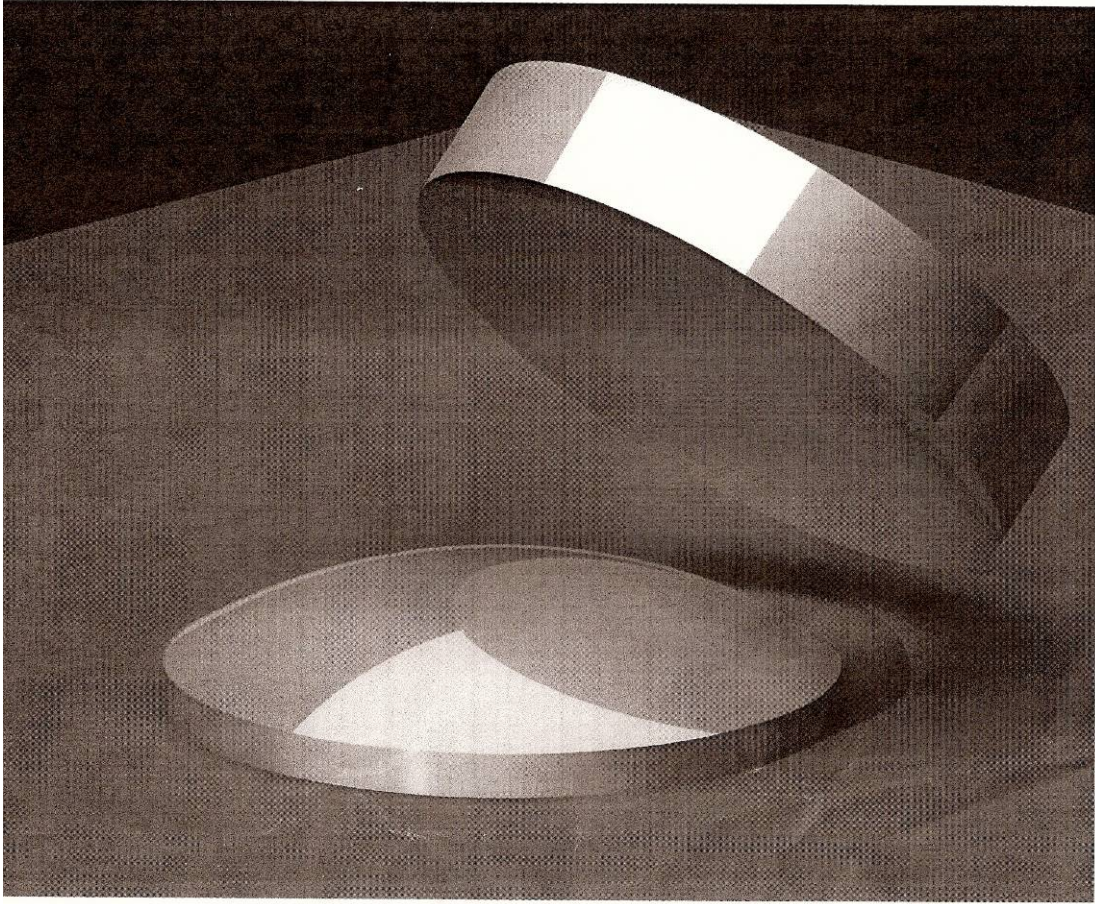


Figure 3.5. Implant Design 5 for the Nuclear Intervertebral Disc Implants

CHAPTER IV

SHEAR TESTING

4.1 Machinery and Setup

Shear testing was conducted using an Instron Universal Testing Instrument Model 1011 machine. An adjustable platform was placed on a table in front of an Instron machine and a circular (156g, 3.94in diameter, .14 in thick) fixation device (Figure 4.1) designed to secure the bottom half of an implant was secured to the platform with industrial strength double sided tape. All of the implants fit into the same fixation devices because they were designed with the same outer dimensions. Another square (533g, 4in x 4in, .75in thick) fixation device (Figure 4.2) designed to secure the top half of the implant was placed on top of the bottom fixation device. The top fixation device is fitted with (.25in steel) ball bearings on its upper side and a hook on its front; these features allow this device (and thus the implants) to be pulled in shear. On top of the ball bearings sit a (600g, 1ft x 1ft, .25in thick) Plexiglas plate with a 500g weight on top of it. The Plexiglas plate and the weight place some compressive force on the implant when it is set in the fixation device. A square (8in x 8in, 3in thick) metal piece on top of the Instron platform and a (1.18in diameter) pulley sits on top of the metal piece. The main purpose of the block and pulley are to provide a way to pull the fixation devices without having to place the heavy and complicated implant fixation setup on the Instron machine itself. A thin

braided steel wire is connected to the Instron; it wraps around the pulley and is attached to the top fixation device. When the Instron pulls, it causes the top fixation device to move horizontally and eventually dislocate the two halves of the implant currently in the device. This multi-component setup can be seen in Figures 4.3-4.6. For various reasons, the weight used for testing was only 500g. Using a lighter load allowed the two halves of the implant design to more easily disarticulate thus allowing us to measure their relative mechanical properties as compared to one another. Since the implant prototypes were made of ABS, testing under a lighter load prevented the severe deformation of the ABS material which would have resulted in skewed data. Lastly, the ABS material used in the prototyping process was not hard enough to be repeatedly tested under normal physiological loads without disintegrating during repeated testing.

4.2 Methods and Materials

During examination of the implants before testing, it was decided that because of the poor fidelity with which implant design 2 (as seen in Figure 3.2) was reproduced during prototyping, it was not feasible for the intended purposes of this project; therefore it was excluded from all testing procedures. The remaining four implants were tested as planned. For all of the types of tests performed, each type of test was performed a minimum of four times on each implant shape in order to insure the accuracy of collected data and to afford the opportunity to exclude tests portraying irregular results. Since the interior surfaces of the top and bottom of all of these implant designs are corresponding/complementary shapes that fit snugly together under compression, when one half of an implant was shifted to a point where it would not go back into proper

position when the force is removed, the two halves were considered to have dislocated and the test was ended.

For the first round of tests, each of the four remaining implant designs were simply placed both top and bottom into the top and bottom fixation devices, then the Instron Series IX Automated Materials Tester program was turned on and calibrated. The pulley system was pre loaded to 2kN so there was slight tension through the wire, the Instron was set to pull at a rate of 10 mm/sec and the sampling rate was set at 10 Hz. The tests were then started and were stopped when the implants dislocated. The Instron Automated Materials Tester program recorded the forces in tension that each implant was subjected to as it was pulled and the distance that it traveled before dislocation; this data was collected for each test.

The second round of tests were performed identically to the first round of tests with the exception the sides of the implant adjacent to the fixation pieces with industrial grade adhesive. This was done to observe whether or not the bonding of the implant impacted its mechanical properties.

The third and fourth rounds of testing were performed identically to the first with the exception that a wedge was placed under the bottom of each implant that set the implant at a 30° incline for the third round of testing and a 30° decline for the fourth round of testing, the implants were also bonded to the fixation devices during these tests. This was done because subsidence of intervertebral implant prosthesis into adjacent endplates is a common cause of failure of spinal prosthesis. Density of vertebra is highest at the periphery near the cortical bone and lowest/weakest in the middle of the vertebra (where the implant will be placed)⁷¹. Another common phenomenon is the accidental angular

misalignment or tilted insertion of spinal implants during placement. The goal of the third and fourth tests was to determine the mechanical properties of the implants even in the cases of subsidence or irregular insertion.

The fifth round of tests were performed identically to the second round of tests with the exception that they were performed under the much heavier load of 60lbs. In the second round of tests, the Plexiglas plate placed on top of the fixation devices only weighed 600g and the weight placed on top of that was only 500g. This round of tests was designed to place the implants under a load closer to the loads that it would face in an in vivo situation. The plate used (Figure 4.7) was a much heavier (1ft x 1ft, .5in thick) 7lb metal plate with various weights placed on it equaling 60lbs the modified setup can be seen in Figure 4.8. For this round of tests, the tests were only run once each because the structural integrity of the implant pieces (since for these purposes they were made of ABS) was compromised after just one test run under a 60lb load. The first test of this round was run with no implant in place at all, but with ball bearings above and below the top fixation device which was pulled by the Instron as normal. This was done to get a virtually “frictionless” reading of the mechanical stresses based on exclusively the 60lb load with no resistance from the various implant designs. The last portion of this test can be seen in the video labeled “Baseline Reading Under Heavy Load” which is located on this CD. The bottom fixation device was replaced in the setup and each implant was tested in turn under the 60lb load. The test for Implant Design 4 under the 60lb load can be seen in the video labeled “Implant 4 Under Heavy Shear” which is located on this CD. The Instron Series IX Automated Materials Tester collected a separate set of data for each test which was saved for later manipulation.

4.3 Results and Analysis

A separate set of raw data was collected for each test, the Instron measured displacement and force which was recorded in mm and kN. The Instron recorded these parameters 10 times per second resulting in a list of increasing force and distance values for each set of data. After collecting the data gathered by the Instron, the distance between each two data points was measured and recorded as mm and the kN measurements were converted to N and recorded as well; a preliminary table was made of mm and kN for each data set. A sample of one of these tables can be seen in Table 4.1. This data was then graphed and a preliminary force- distance graph was made for each data set. A sample graph can be seen in Figure 4.9. The individual area between each two points was also found by using basic Trapezoidal Integration (area under a curve is the sum of all its trapezoids), the exact equation used can be seen in Figure 4.10. After all the individual areas were found, they were summed up to find the cumulative area under each curve; since work = force*distance ($w=f*d$), the area under the curve is essentially the work done to horizontally pull the implant to the point of dislocation. Primary and secondary slope were also calculated for each set of data. The graph made for each data set was visually assessed; the primary slope was taken when the graph initially started to slope, and the secondary slope was taken at another straight area of the graph close to (but before) the implant dislocated. An example of the relative location on each graph where these slopes were calculated can be seen in Figure 4.9. These slopes are important because they illustrate the shear stiffness of the implant at different times during testing. So the five criteria taken/calculated for each data set were failure force, failure distance,

initial shear stiffness of the implant (primary slope), shear stiffness before dislocation (secondary slope), and work. High values for failure force and failure distance are favorable because the more force it takes to dislocate an implant design and the further it can travel before dislocation, the better it is likely to perform. High values for shear stiffness are critical because, without trauma it is not physiologically normal or safe for vertebra to move strictly in shear in relation to one another. Their ability to resist this type of movement is critical to the safety of the spinal cord and other nerves in close proximity to the spinal column. Shear stiffness before dislocation was deemed more important than initial shear stiffness; because initially, when shear forces are just beginning to be generated between two vertebrae, primary stability comes from the annulus fibrosus. Very small shear forces can be resisted by the annulus; but the larger the shear force on the vertebra, the more the implant needs to provide stability and the stiffer the implant needs to be in shear. High values for work required to dislocate the two halves of the implant from one another are favorable because the harder it is for the implant to dislocate, the better. Since there were at least 4 tests performed for each implant design under each of the various conditions, an average of all of those data sets was composed and displayed in graph form (there were twenty-one sets in all and their averages can be seen in Tables 4.2 and 4.3 and Figures 4.11- 4.24). A statistical ranking of the various implant designs can be seen in Table 4.4. The Figures 4.11-4.24 and Table 4.4 are especially helpful when trying to analyze the following results. After the averages of all of the respective sets of data were measured, standard deviation was measured for each set of data and is displayed as Y Error Bars on each graph. Since the standard

deviations for each set of data was low and many tests were run, the conclusion is that the obtained data is accurate.

First the implants were tested in shear without bonding or tilt. Analysis of variance (ANOVA) tests were done on the data obtained, and the data provided sufficient evidence to statistically prove that at least one implant design was significantly different than the other implant designs in terms of failure force, failure distance, shear stiffness before dislocation, and work done. Then a post hoc analysis was done using Least Significant Difference (LSD) tests to determine what exactly those differences were. There was no statistical difference between the implant designs in terms of initial shear stiffness. In terms of failure force, implant designs 1 and 4 were proven to be significantly better than implant designs 3 and 5. Even though implant design 4 had the highest failure force at 16.125, it was not statistically significantly better than implant design 1. Implant design 4 was better than implant designs 3 and 5 by 63% and 64% respectively. In terms of failure distance, implant design 1 was significantly better than implant designs 4 and 5; they were all significantly better than implant design 3. Implant design 1 was better than the next best implant designs (designs 4 and 5) by 22% and 27% respectively. In terms of initial shear stiffness, there was no statistical difference between the initial shear stiffness of all of the implant designs. In terms of shear stiffness before dislocation, implant designs 1, 4, and 5 were all significantly better than implant design 3. Implant design 4 had the highest shear stiffness before dislocation, but it is not significantly better than designs 1 and 5. In terms of work done to dislocate the implant design, implant design 1 (requiring 115.33 N.m) was proven to be significantly better than implant design 4 (requiring 73.84 N.m), and they were both proven to be

significantly better than implant designs 5 (requiring 43.43 N.m) and 3 (requiring 24.10 N.m).

Secondly, the implants were tested in shear while bonded. ANOVA and LSD tests were done on the data obtained, and the data provided sufficient evidence to statistically prove that at least one implant design was significantly different than the other implant designs in terms of failure force, failure distance, shear stiffness before dislocation, and work done. There was no statistical difference between the implant designs in terms of initial shear stiffness. In terms of failure force, implant designs 4 and 1 were not statistically different but were proven to be significantly better than implant designs 3 and 5 which were also not statistically different. Implant design 4 had the highest failure force at 16.125N, but it was not found to be statistically significantly better than implant design 1 (which had a failure force of 15.400N). Implant design 4 was 59% better than the next best implant (implant design 3). In terms of failure distance, implant design 1 was significantly better than implant designs 4 and 5, which were significantly better than implant design 3. Implant design 1 had the longest failure distance (11.254mm), it was significantly larger than the next best failure distance of implant design 4 (8.739mm) by 22%. In terms of initial shear stiffness, there was no statistical difference between the initial shear stiffness of all of the implant designs. In terms of shear stiffness before dislocation, implant designs 4, 1, and 5 were significantly better than implant design 3. Implant design 4 had the highest shear stiffness before dislocation, but it is not significantly better than implant designs 1 or 5. In terms of work done to dislocate the implant, implant design 1 was proven to be significantly better than implant design 4,

which was proven to be significantly better than implant designs 5 and 3. Implant design 1 was better than the next best implant (implant design 4) by 34%.

Thirdly, all of the implants were tested in shear while bonded and positioned on a 30° incline. ANOVA and LSD tests were done on the data obtained, and the data provided sufficient evidence to statistically prove that at least one implant design was significantly different than the other implant designs in terms of failure force, failure distance, shear stiffness before dislocation, and work done. There was no statistical difference between the implant designs in terms of initial shear stiffness. In terms of failure force, implant design 1 was proven to be significantly better than implant design 4, which was proven to be significantly better than implant design 5, which was proven to be significantly better than implant design 3. Implant design 1 had the highest failure force at 23.06N. It was statistically significantly better than implant designs 4, 5, and 3 by 18%, 72%, and 80% respectively. In terms of failure distance, implant designs 5 and 1 were significantly better than implant design 3, which was significantly better than implant design and 4. Implant design 5 had the longest failure distance (9.758mm), but it was not significantly larger than the failure distance than implant design 1 (9.526). Implant design 1 was better than the next best implant (implant design 3) by 5%. In terms of initial shear stiffness, there was no statistical difference between the initial shear stiffness of all of the implant designs. In terms of shear stiffness before dislocation, implant designs 4 and 5 were significantly better than implant design 1, which was significantly better than implant design 3. Implant design 4 had the highest shear stiffness before dislocation, but it is not significantly better than implant design 5. In terms of work done to dislocate the implant design, implant design 1 was proven to be

significantly better than implant design 4, which was proven to be significantly better than implant design 5, which was proven to be significantly better than implant design 3. Implant design 1 was better than the next best implant (implant design 4) by 25%.

Lastly, all of the implants were tested in shear while bonded and positioned on a 30° decline. ANOVA and LSD tests were done on the data obtained, and the data provided sufficient evidence to statistically prove that at least one implant design was significantly different than the other implant designs in terms of failure force, failure distance, shear stiffness before dislocation, and work done. There was no statistical difference between the implant designs in terms of initial shear stiffness. In terms of failure force, implant design 1 was proven to be significantly better than implant design 4, which was proven to be significantly better than implant designs 5 and 3. Implant design 1 had the highest failure force at 23.06N, it was statistically significantly better than the next best implant (design 4) by 44%. In terms of failure distance, implant design 1 was significantly better than implant designs 4, 5, and 3 by 23%, 35%, and 68% respectively. In terms of initial shear stiffness, there was no statistical difference between the initial shear stiffness of all of the implant designs. In terms of shear stiffness before dislocation, implant designs 1, 5, and 3 were significantly better than implant design 4. Implant design 1 had the highest shear stiffness before dislocation, but it is not significantly better than implant designs 5 and 3. In terms of work done to dislocate the implant design, implant design 1 was proven to be significantly better than implant design 4, which was proven to be significantly better than implant design 5, which was proven to be significantly better than implant design 3. Implant design 1 was better than implant designs 4, 5, and 3 by 53%, 74%, and 91% respectively.

Now the effects of the various positions that the implant was tested in (flat and unbonded, flat and bonded, on an incline, and on a decline) will be examined and ranked (refer to Table 4.4). When looking at implant design 1 in terms of failure force, failure distance, initial shear stiffness, shear stiffness before dislocation, and work needed to dislocate the implant, the following observations were made. When looking at failure force, it is highest when the implant design1 is placed on an incline. The incline failure force is significantly better than the failure forces for the other 3 implant positions (bonded, placed on a decline, and placed flat). When looking at failure distance, it was largest when this implant design was in the flat unbonded position and it is significantly larger than failure distance yielded by the other positions. Initial shear stiffness is not affected by implant position. When looking at shear stiffness before dislocation, this implant design had the highest shear stiffness before dislocation in the flat and unbonded or flat and bonded position, the shear stiffness for these positions are significantly better than the shear stiffness for the other two positions. When looking at work needed to dislocate the implant, the most work was needed to dislocate the implant the when the implant was in the flat unbonded or inclined positions, significantly more than if the implant were in the bonded or declining position.

When looking at implant design 3 in terms of failure force, failure distance, initial shear stiffness, shear stiffness before dislocation, and work needed to dislocate the implant, the following things were observed. When looking at failure force, it is highest when the implant is placed flat either bonded or unbonded. When the implant is placed flat, the failure force is significantly higher than the failure forces of the implant when it is inclined or declined. When looking at failure distance, it was largest when this implant

design was in the inclined position, it is significantly larger than failure distance yielded by the implants while they were in the flat position (bonded or unbonded), and implants in the flat position yield significantly larger failure distances than implants in the decline positions. Initial shear stiffness is not affected by implant position. When looking at shear stiffness before dislocation, the implant design had the highest shear stiffness before dislocation in the flat and unbonded or the inclined position, the shear stiffness for these positions are significantly larger/better than the shear stiffness for the other two positions. When looking at work needed to dislocate the implant, the most work was needed to dislocate the implant the when the implant was in the inclined position, followed by the implant in the flat position (either bonded or unbonded), and it took the least work to dislocate the implant if it was on a decline.

When looking at implant design 4 in terms of failure force, failure distance, initial shear stiffness, shear stiffness before dislocation, and work needed to dislocate the implant, the following things were observed. When looking at failure force, it is highest when the implant is placed on an incline, however it is not statistically better than the results obtained when the implant is placed in the flat and unbonded position. The failure force of the implant in the flat bonded and unbonded positions are statistically similar to each other, but of these two positions only the failure force of the implant in the flat and bonded position is significantly less than the failure force of the implant in the inclined position. The implant yields the worst failure force in the declined position. When looking at failure distance, it was largest when this implant design was either in the flat and bonded or flat and unbonded positions, it is significantly larger than failure distance yielded by the implants while they were in the inclined or declined position. Initial shear

stiffness is not affected by implant position. When looking at shear stiffness before dislocation, the implant design had the highest shear stiffness before dislocation in the flat and unbonded, the flat and bonded, or the inclined positions, the shear stiffness before dislocation for these positions are significantly larger/better than the secondary lobe of the implant when it is in the declined position. When looking at work needed to dislocate the implant, the most work was needed to dislocate the implant when the implant was in the flat and unbonded position or in the inclined position, followed by the implant in the flat and bonded position, and it took the least work to dislocate the implant if it was on a decline.

When looking at implant design 5 in terms of failure force, failure distance, initial shear stiffness, shear stiffness before dislocation, and work needed to dislocate the implant, the following observations were made. When looking at failure force, it is highest when the implant is placed on an incline, however it is not statistically better than the results obtained when the implant is placed in the flat and unbonded position. The failure force of the implant in the flat bonded and unbonded positions are statistically similar to each other, but of these two positions only the failure force of the implant in the flat and bonded position is significantly less than the failure force of the implant in the inclined position. The implant yields the worst failure force in the declined position, however the failure force of the implant when it is flat and unbonded and when it is on a decline are not significantly different. When looking at failure distance, it was largest when this implant design was placed in an inclined position; it is significantly larger than failure distance yielded by the implants while they were in a flat bonded or a flat and unbonded position. Placement on a decline yielded the worst failure force. Initial shear

stiffness is not affected by implant position. When looking at shear stiffness before dislocation, it was largest when this implant design was placed in a flat and bonded position; it is significantly larger than shear stiffness before dislocation yielded by the implants while they were in inclined or flat and unbonded positions. Shear stiffness before dislocation is the least when the implant is placed on a decline, significantly less than when the implant is placed in all of the other positions. When looking at work needed to dislocate the implant, it was largest when this implant design was placed in an inclined position; it is significantly larger than shear stiffness before dislocation yielded by the implants while they were in flat and unbonded or flat and bonded positions. Work needed for dislocation is the least when the implant is placed on a decline, significantly less than when the implant is placed in all of the other positions.

Since the tests under heavy load could only be performed once each (the weight damaged the implants because for testing purposes they were made out of ABS), there was no statistical analysis done on the results. Under heavy compressive load, implant design 4 definitely outperforms the other implant designs. It took 18% more force to dislocate than the next best implant design (implant design 5), it was 58% better than the next best implant design (implant design 3) in terms of failure distance, and it required 83% more work to dislocate the implant than the next best implant design (implant design 5). When looking at force required to dislocate the implant designs under heavy compression, implant design 4 performed the best (as previously stated), followed by implant design 5, then implant design 1, and lastly implant design 3. When looking at distance that each implant design traveled before complete dislocation under heavy compression, implant design 4 also performed the best (as previously stated), followed by

implant design 3, then implant design 1, and lastly implant design 5. When looking at work required to dislocate the implant designs under heavy compression, implant design 4 also performed the best (as previously stated), followed by implant design 5, then implant design 3, and lastly implant design 1. As the implants approached their various points of dislocation, shear stiffness increased for implant designs 1 and 3 but decreased for implant designs 4 and 5. Implant design 1 was the only implant design that completely broke during testing while the other implants were only structurally compromised by the heavy load. These results are especially significant because they are an indicator of the reactions to expect from the implant designs under more realistic loading conditions similar to loads they would encounter in the spine (Figures 4.21-4.24).

Under 500g of compression, when looking at the failure force at which the various implants dislocated under, overall, implant design 1 had the highest/best failure force in all instances but except for then it was in the flat and unbonded position, then it had the second highest failure force. Implant design 4 consistently had the second highest failure force except for when it was in the flat and unbonded position; in that position it was statistically tied with implant design 5 for highest failure force. Implant design 5 had the next highest failure forces, followed by implant design 3. Under 60lb of compression, implant 4 had the highest/best failure force, followed by implants 5, 1, the 3. Under 500g of compression, when looking at the failure distance, overall, implant design 1 had the highest/best failure distance or was not statistically significantly different from the implant that had the highest failure distance all of the time. Implant design 4 had the 2nd highest failure distance half of the time, the 3rd highest failure distance a quarter of the

time, and 4th highest failure distance a quarter of the time. Implant design 5 had the highest failure distance (or was not significantly different from the implant design that had the highest failure distance) half of the time, had the second highest failure distance (or was not significantly different from the implant design that had the second highest failure distance) one quarter of the time, and had the 3rd highest failure distance one quarter of the time. Implant design 3 had the lowest/worst failure distance in all instances except when it was on an incline, and then it had the next lowest failure distance. Under 60lb of compression, implant design 4 had the farthest failure distance, followed by implant designs 3, 1, the 5. There was no significant difference in the initial shear stiffness of the implants under any circumstances. Under 500g of compression, when looking at shear stiffness before dislocation, overall, implant design 1 had the highest shear stiffness one quarter of the time and had the second highest shear stiffness or (or was not significantly different from the implant design that had the second highest shear stiffness) three quarters of the time. Implant design 4 had the highest shear stiffness (or was not significantly different from the implant design that had the highest shear stiffness) three quarters of the time and it had the lowest shear stiffness one quarter of the time. Implant design 5 had the highest/best shear stiffness (or was not significantly different from the implant design that had the best shear stiffness) three quarters of the time and had the second highest shear stiffness (or was not significantly different from the implant design that had the second highest shear stiffness) one quarter of the time. Implant design 3 had the lowest/worst shear stiffness in all instances except for when it was placed on a decline, then it had the second lowest shear stiffness. Under 60lb of compression, implant design 1 had the highest shear stiffness before dislocation, followed

by implant designs 5, 3, the 4. Under 500g of compression, when looking at work needed to dislocate the implant, overall, implant design 1 required the most work to dislocate/ was best all of the time. Implant design 4 was second best all of the time. Implant design 5 was third best (or was not significantly different from the implant design that was third best) all of the time. Implant design 3 was worst (or was not significantly different from the implant design that was worst) in all instances. Under 60lb of compression, implant design 4 took the most work to dislocate, followed by implant designs 5, 3, the 1.

The most important criteria to consider for this experiment are work needed to dislocate the implant and shear stiffness before dislocation. Work needed for dislocation takes into account force needed for dislocation and distance needed for dislocation so it is a very useful criterion to consider. Shear stiffness is important to consider because vertebra are not supposed to move in shear in relation to one another and unless an implant design can effectively resist shear forces, it will not be feasible. Shear stiffness before dislocation is deemed more important than initial shear stiffness because initially, when shear forces are just beginning to be generated between two vertebra, primary stability comes from the annulus fibrosus. Very small shear forces can be resisted by the annulus; but the larger the shear force on the vertebra, the more the implant needs to provide stability and the stiffer the implant needs to be in shear. Considering the values obtained for work needed to shear an implant design under 500g of compression, implant design 1 required the most work to cause dislocation (was the best) because it was the most pointed implant design (see Figure 3.1). Followed by implant design 4 which was the second most pointed implant design (see Figure 3.4), followed by implant design 5 because it had the most surface area (see Figure 3.5), and lastly implant design 3 (see

Figure 3.3). Under heavy compression implant design 4 required more than 5 times more work to shear than any other implant design. Even though implant design 1 was slightly better than implant design 4 under 500g of compression in terms of work, implant design 4 would still be the better choice because it far outperformed implant 1 under 60lbs of compression, a load much more similar to the loads that will be placed on it under normal physiological conditions. Considering the values obtained for shear stiffness of the implants before dislocation under 500g of compression, implant design 5 had the greatest shear stiffness/ was best (or was not statistically different from the implant design that had the greatest shear stiffness) in every position. The next statistically best implant design in this case was implant design 4 which had the greatest shear stiffness (or was not statistically different from the implant design that had the greatest shear stiffness) in every position except the declined position where it performed the worst. Under heavy compression implant designs 1 was stiffest, followed by 5, then 3, then 4. However, all of the stiffness values stayed within the same range with the best implant design being only about 13% stiffer than the worst implant design. Even though implant design 5 outperformed implant design 4 under 500g of compression in terms of shear stiffness, implant design 4 would still be the better choice because even though it was slightly less stiff than design 5, its smaller surface area would make it much less susceptible to wear than implant design number 5. Under 60lbs of compression all of the implant designs had similar stiffness; so if they are all similar, implant 4 is still the best choice because of its superiority in other areas.



Figure 4.1. Picture of bottom fixation device used in setup for testing in shear.



Figure 4.2. Picture of top fixation device used in setup for testing in shear.

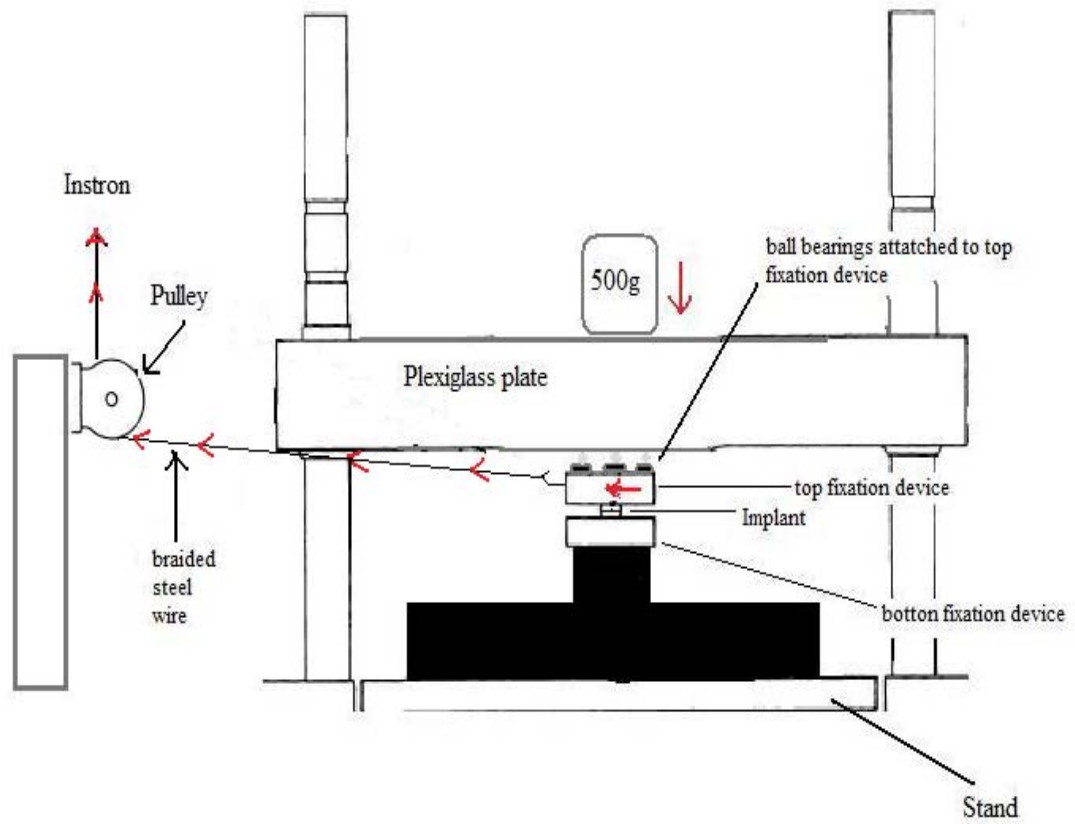


Figure 4.3. Drawing of setup for testing in shear.

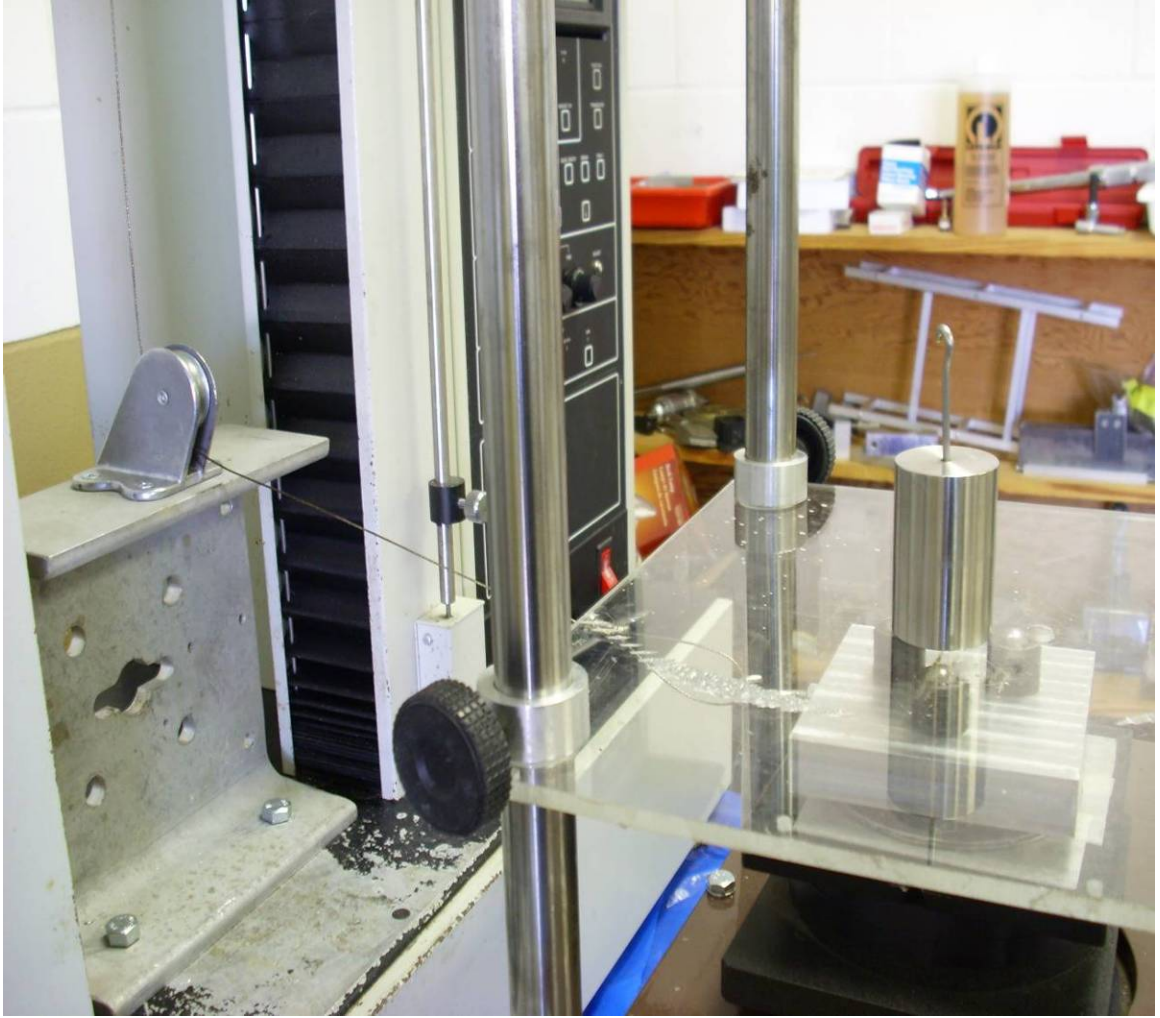


Figure 4.4. Picture of setup for testing in shear.

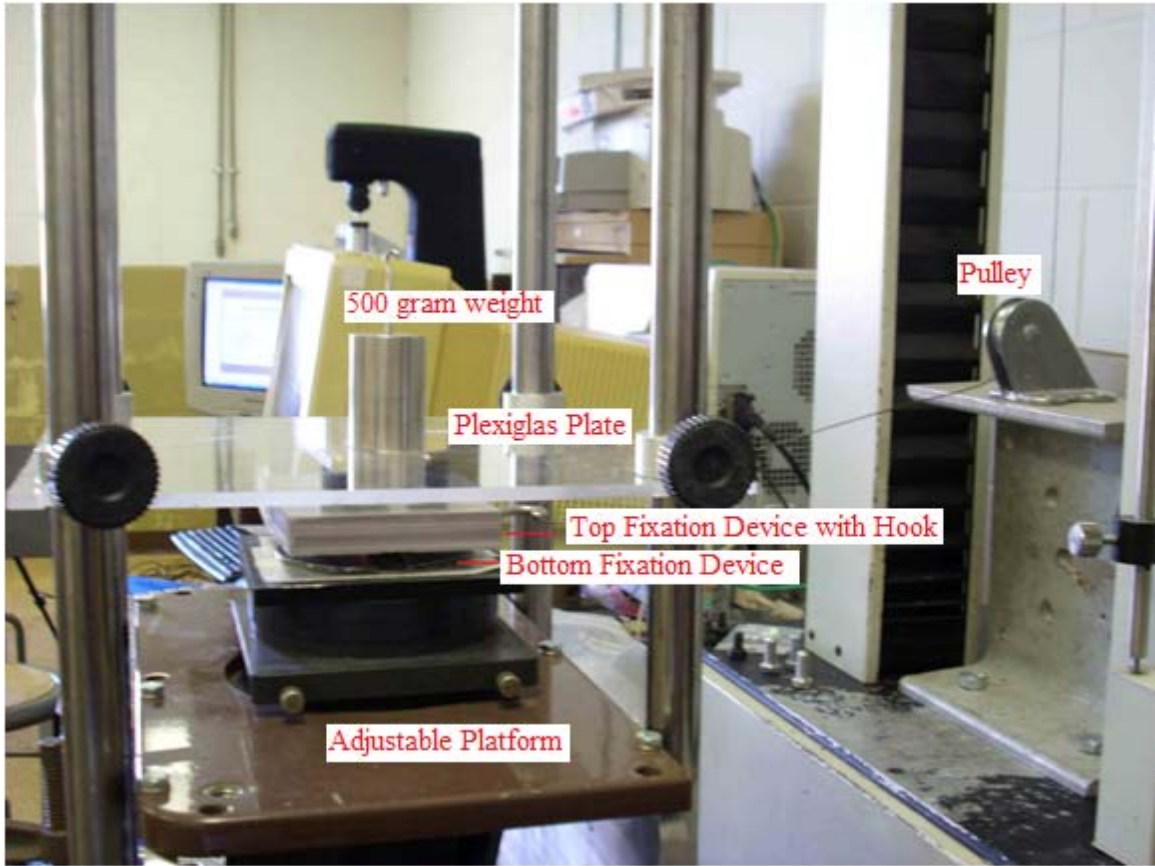


Figure 4.5. Picture of setup for testing in shear.

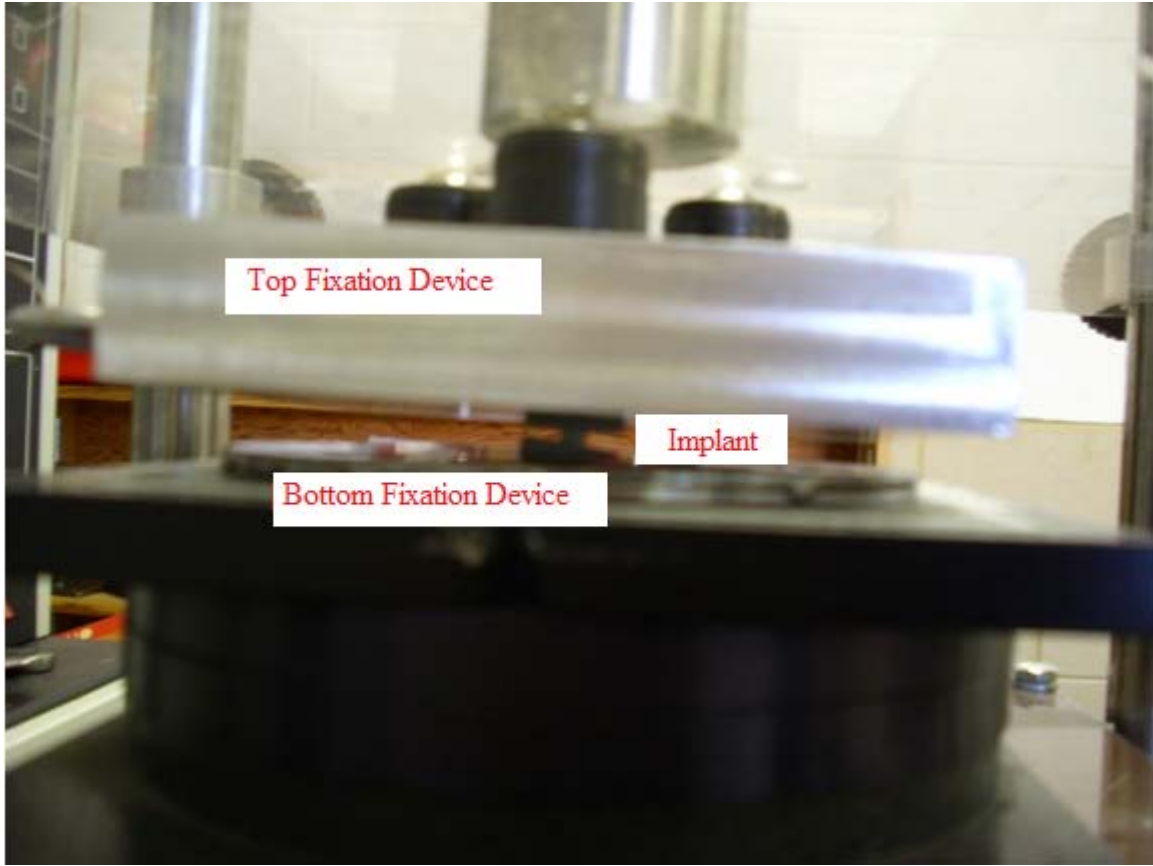


Figure 4.6. Picture of setup for testing in shear.

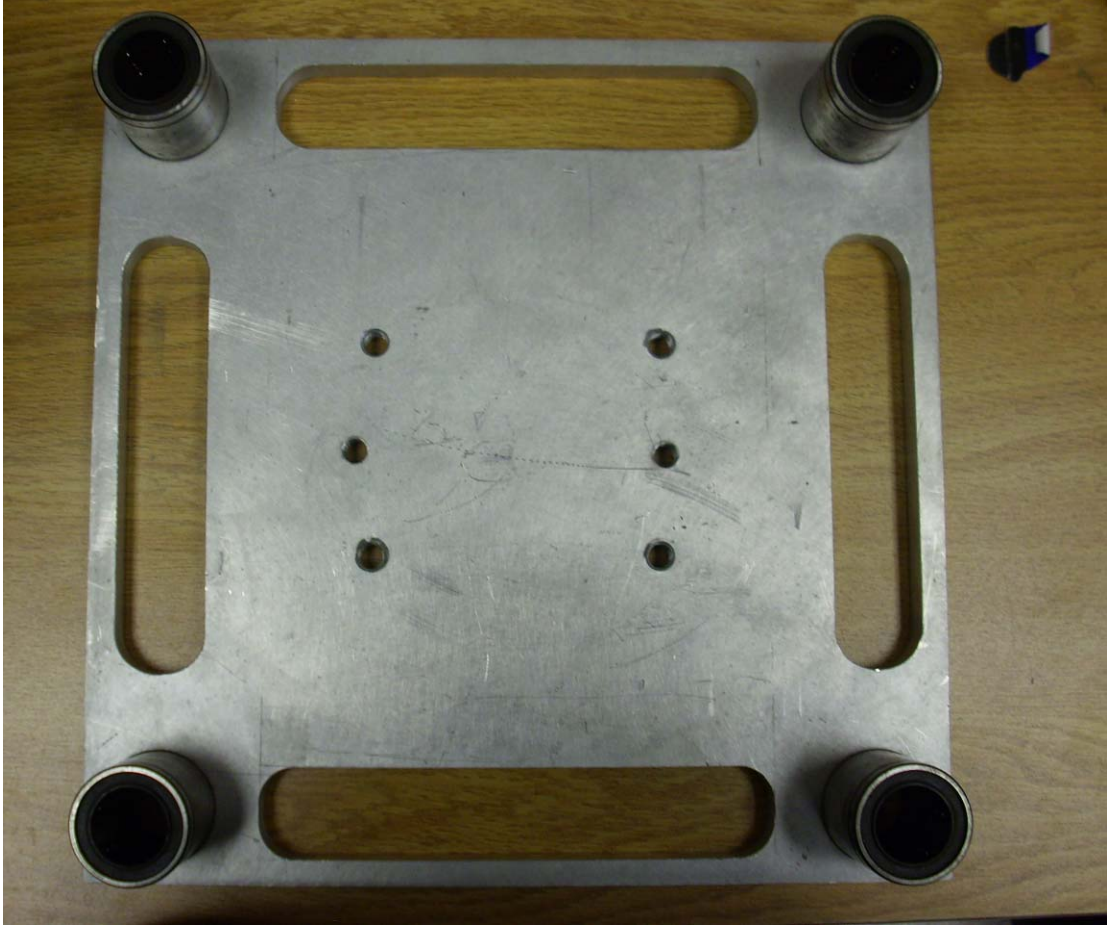


Figure 4.7. Picture of heavy plate used for testing in shear.

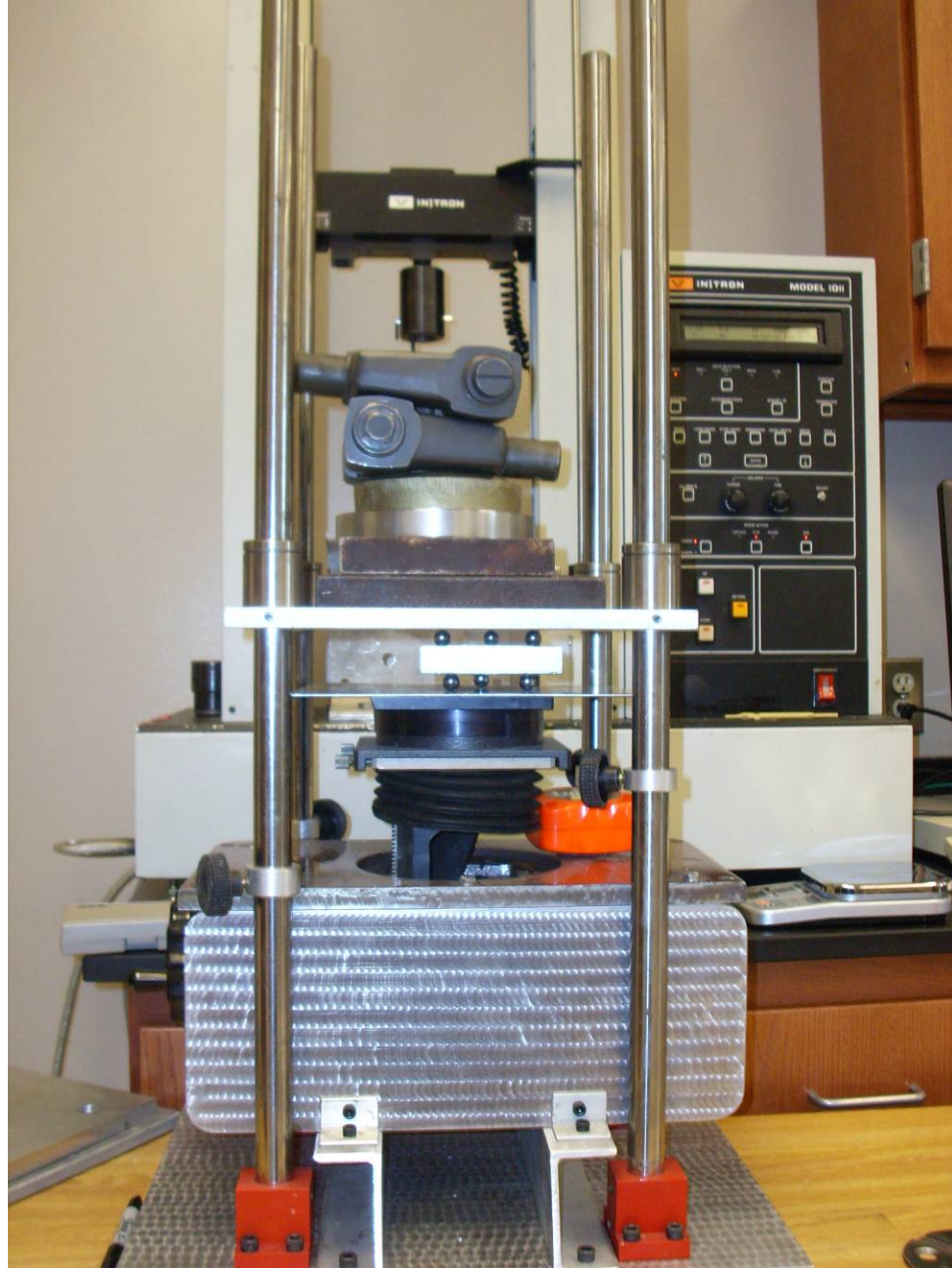


Figure 4.8. Picture of setup for testing in heavy shear.

Table 4.1. Example of preliminary result table for testing in shear.

	mm	kn	mm	n	Individual Areas
1		0			
2		0	0.000	1.75	0.00000
3		0	0.000	1.75	0.00000
4		0	0.000	1.75	0.00000
5		0	0.000	2.00	0.00080
6	0.0004	0.002	0.000	2.00	0.10280
7	0.0518	0.002	0.052	2.00	0.05140
8	0.0775	0.002	0.078	2.00	0.02460
9	0.0898	0.002	0.090	2.00	0.04600
10	0.1128	0.002	0.113	2.00	0.04080
11	0.1332	0.002	0.133	2.00	0.03358
12	0.149	0.00225	0.149	2.25	0.03803
13	0.1659	0.00225	0.166	2.25	0.03645
14	0.1821	0.00225	0.182	2.25	0.04433
15	0.2018	0.00225	0.202	2.25	0.03735
16	0.2184	0.00225	0.218	2.25	0.03485
17	0.2348	0.002	0.235	2.00	0.03421

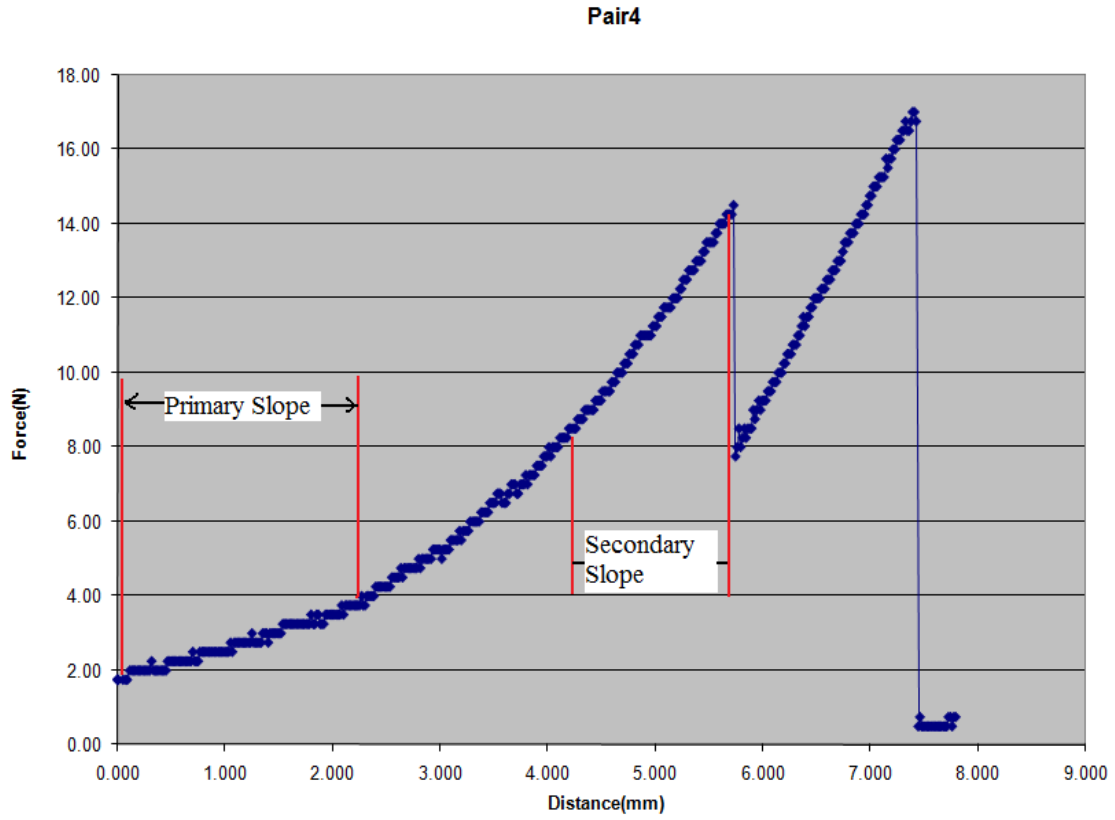
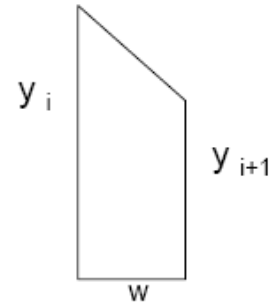


Figure 4.9. Sample diagram of force-distance graph.

$$\text{Trapezoid area} = \frac{1}{2} (y_i + y_{i+1}) W$$



Area under a curve (trapezoidal rule) = sum all trapezoids

$$\begin{aligned} \text{Area} = & \frac{W}{2} (y_0 + y_1) + \frac{W}{2} (y_1 + y_2) + \frac{W}{2} (y_2 + y_3) \\ & + \dots + \frac{W}{2} (y_{n-1} + y_n) \end{aligned}$$

Figure 4.10. Trapezoidal Integration Equation⁷².

Table 4.2. Results table for testing in shear.

Sample Group	Average Failure Force (N)	Average Failure Distance (mm)	Average Primary Slope	Average Secondary Slope	Average Work(N/mm)
Pair 4	16.13	8.739	0.8487	3.3153	73.8353500
Pair 5	5.75	8.198	0.7291	2.6446	43.4326500
Pair 3	5.92	6.363	0.8454	1.2719	24.1009667
Pair 1	15.40	11.254	0.7182	3.1220	115.3305280
STPair 1	20.58	8.739	0.8078	2.2215	75.8466067
GluPair 1	19.08	8.085	0.8177	2.7323	70.4207400
GluPair 3	5.95	6.735	0.7694	0.9283	25.3964780
GluPair 4	13.70	7.107	0.8046	3.7098	49.5414120
GluPair 5	5.00	8.189	0.7828	4.0283	42.8980000
UpPair 1	23.06	9.526	0.8060	2.1761	95.1688060
DwnPair 1	18.75	8.526	0.8418	2.3324	76.3310920
UpPair 3	4.50	9.142	0.6863	1.2979	42.0266029
DwnPair 3	3.57	2.745	0.7706	0.9462	7.3474986
UpPair 4	18.79	8.370	0.7983	3.1670	71.2235900
DwnPair 4	10.54	6.556	0.7231	2.6510	35.8472500
UpPair 5	6.40	9.759	0.7514	2.7909	60.5738620
DwnPair 5	4.70	5.503	0.8046	1.8513	19.9547400

Table 4.3. Result table for testing in shear under heavy load

Sample Group	Samples Under Heavy Compression				
	Average Failure Force (N)	Average Failure Distance (m)	Average Primary Slope	Average Secondary Slope	Average Work(N/mm)
Baseline	6.25	27.751001	1.187614607	1.256953824	128.9156219
pair 1	117.5	14.0974	5.064864813	29.07922449	349.3457544
pair 3	100	18.1154	16.64226943	26.80901911	670.2133731
pair 4	288.75	43.507599	28.69903084	25.16295048	7548.240062
pair 5	237.5	13.967501	31.81678333	27.21507971	1312.839261

Table 4.4. Statistical ranking of the various implant designs

Statistical Analysis of Results For Shear Testing under 500g of Compression					
Testing Position	Failure Force	Failure Distance	Initial Shear Stiffness	Shear Stiffness Before Dislocation	Work required for Dislocation
Flat and Unbonded	4+5, 1+3	1, 4+5, 3	SAME	4+1+5, 3	1, 4, 5+3
Flat and Bonded	1, 4, 3+5	5+1, 4, 3	SAME	5+4, 1, 3	1, 4, 5, 3,
At a 30° Incline	1, 4, 5, 3	5+1, 3, 4	SAME	4+5, 1, 3	1, 4, 5, 3
At a 30° Decline	1, 4, 5+3	1, 4, 5, 3,	SAME	1+5, 3, 4	1, 4, 5, 3
The numbers represent their corresponding implant designs. For example, 1 refers to implant design 1					
The implant designs are ranked from right to left, best performance to worst performance					
A + sign means that there is no statistical significant difference between two implant designs					
SAME means that there is no statistical Difference between any of the implant designs					

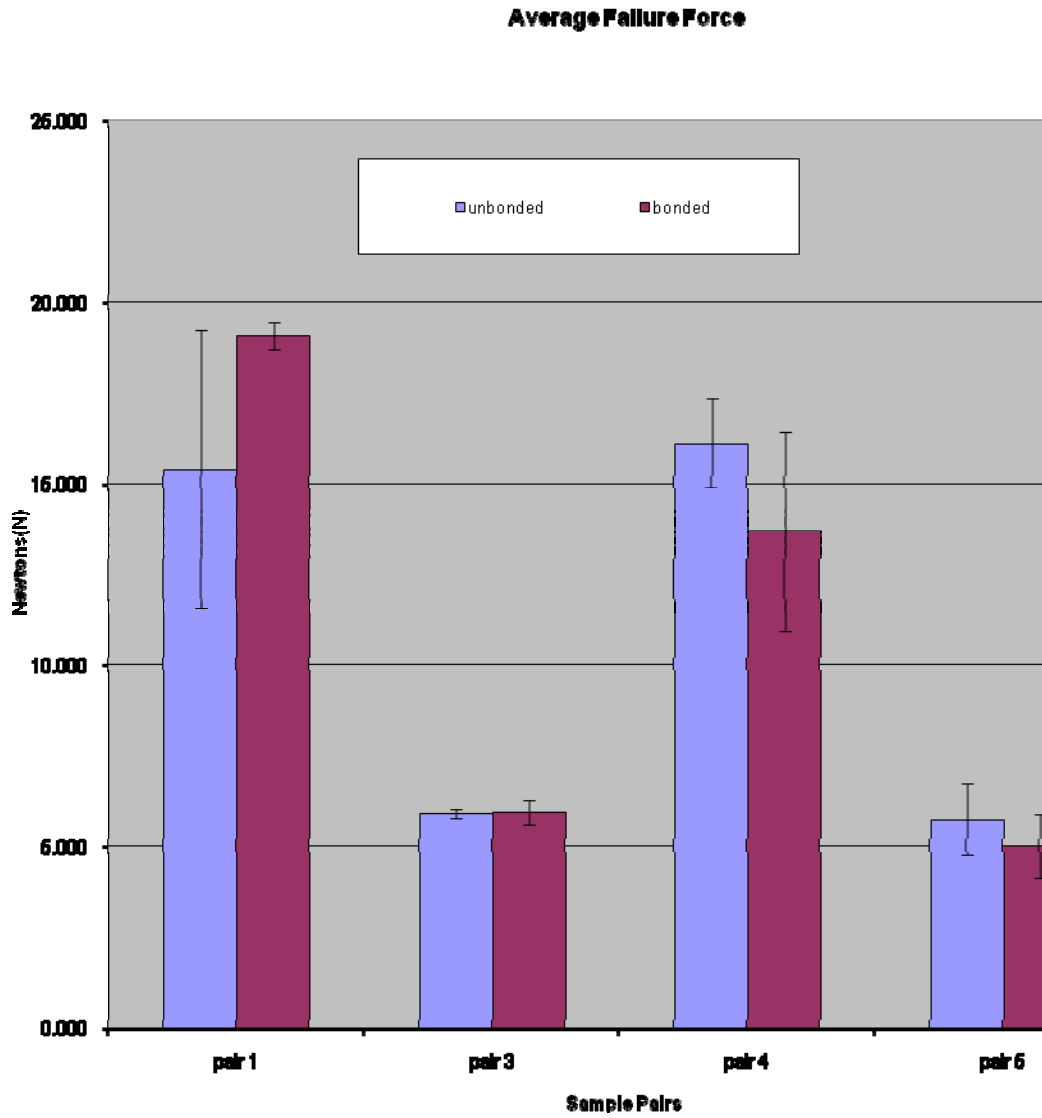


Figure 4.11. Graph of comparison of average failure forces in implant designs in bonded and unbonded testing.

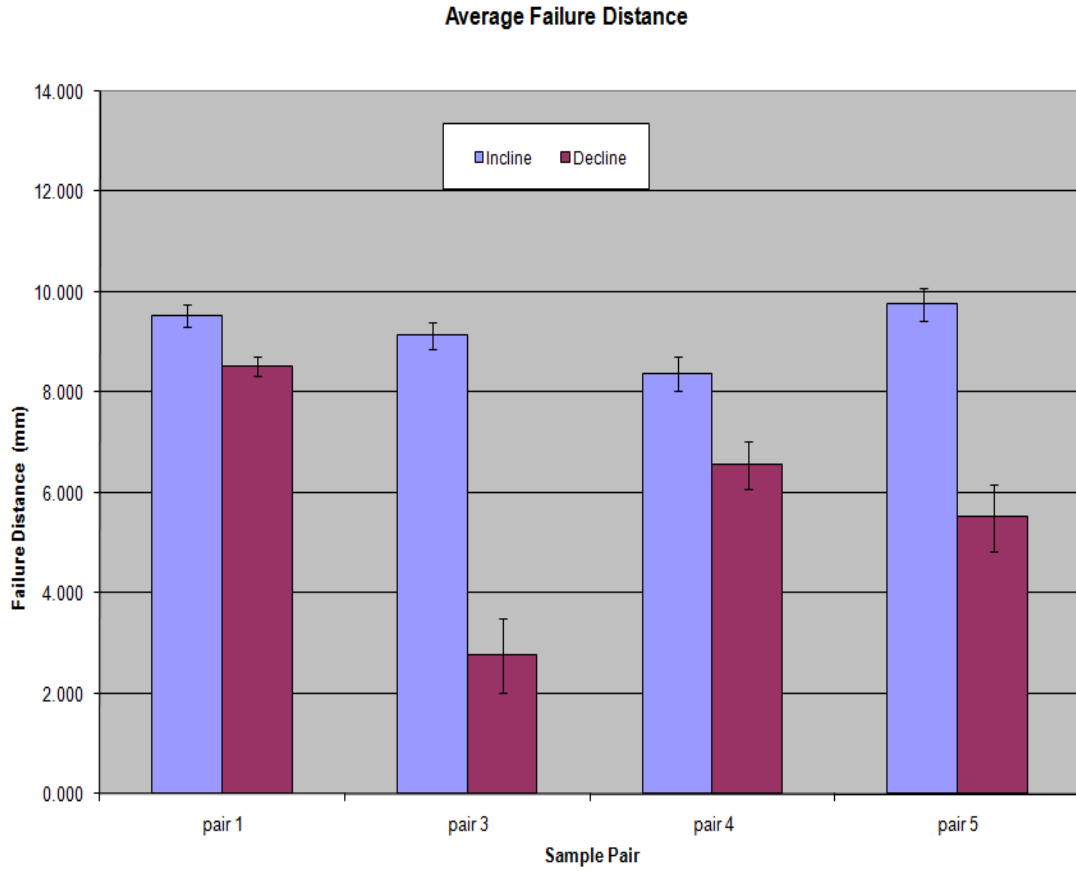


Figure 4.12. Graph of comparison of average failure forces in implant designs in testing on an incline and on a decline.

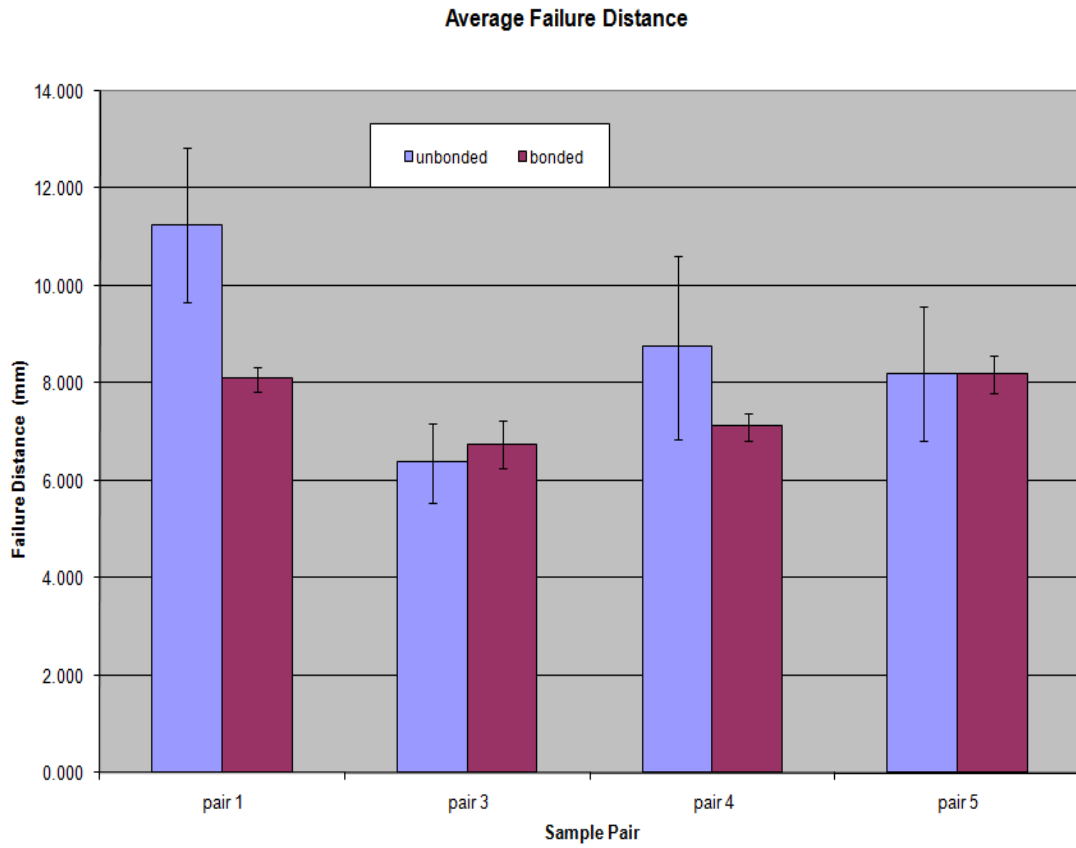


Figure 4.13. Graph of comparison of average failure distance in implant designs in bonded and unbonded testing.

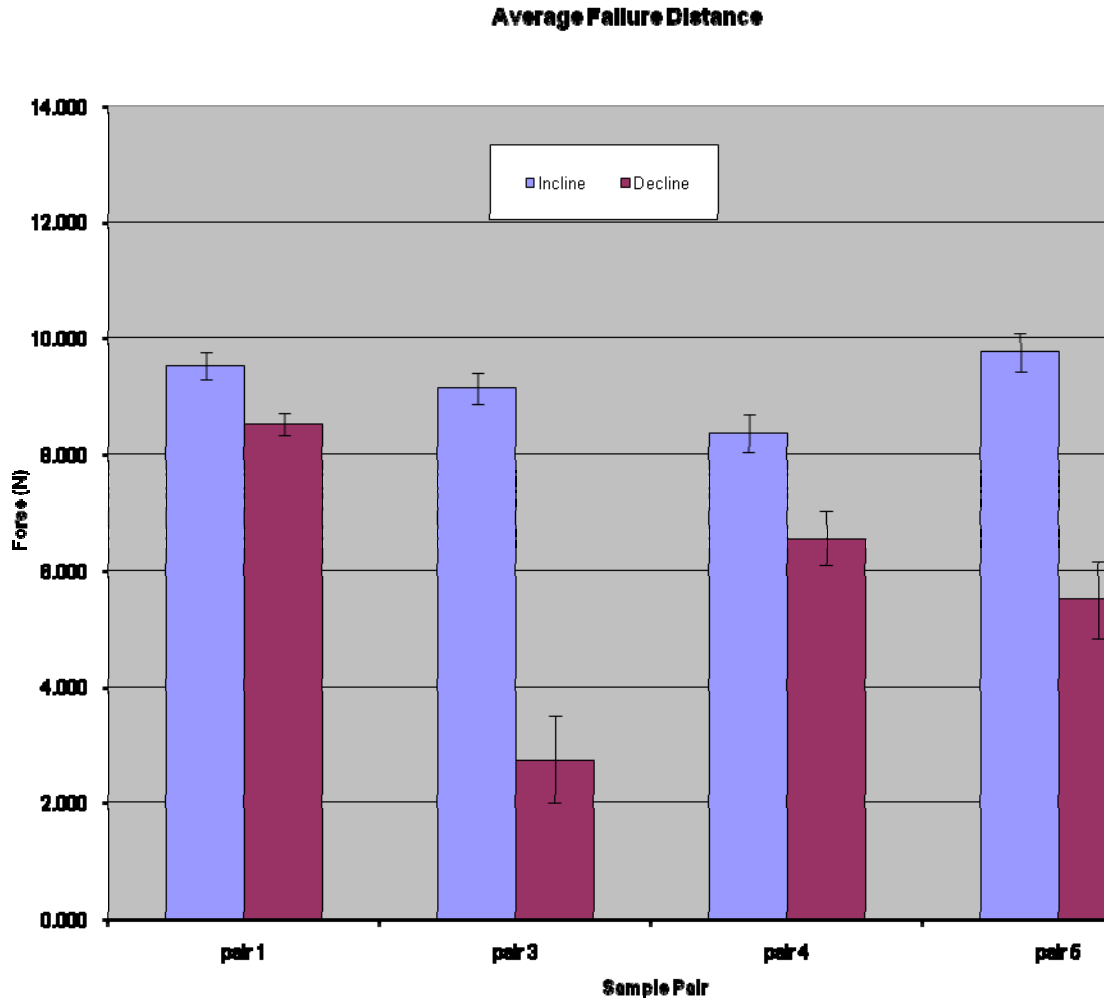


Figure 4.14. Graph of comparison of average failure distance in implant designs in testing on an incline and on a decline.

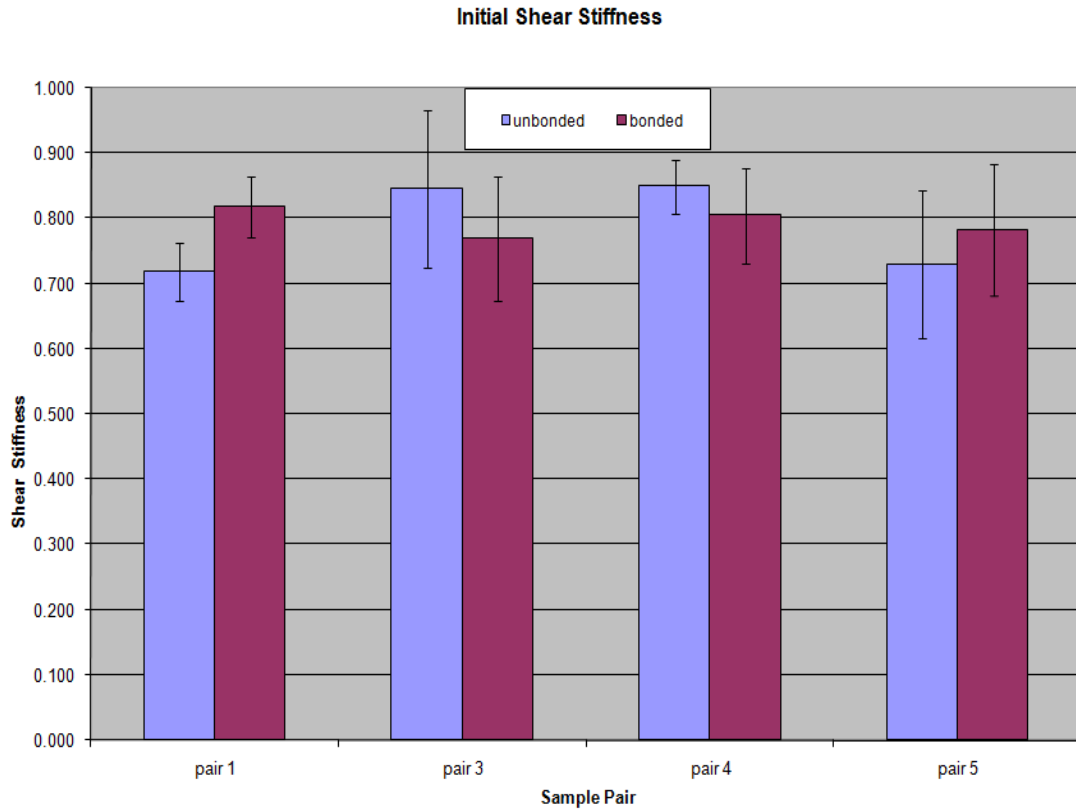


Figure 4.15. Graph of comparison of average initial shear stiffness in implant designs in bonded and unbonded testing.

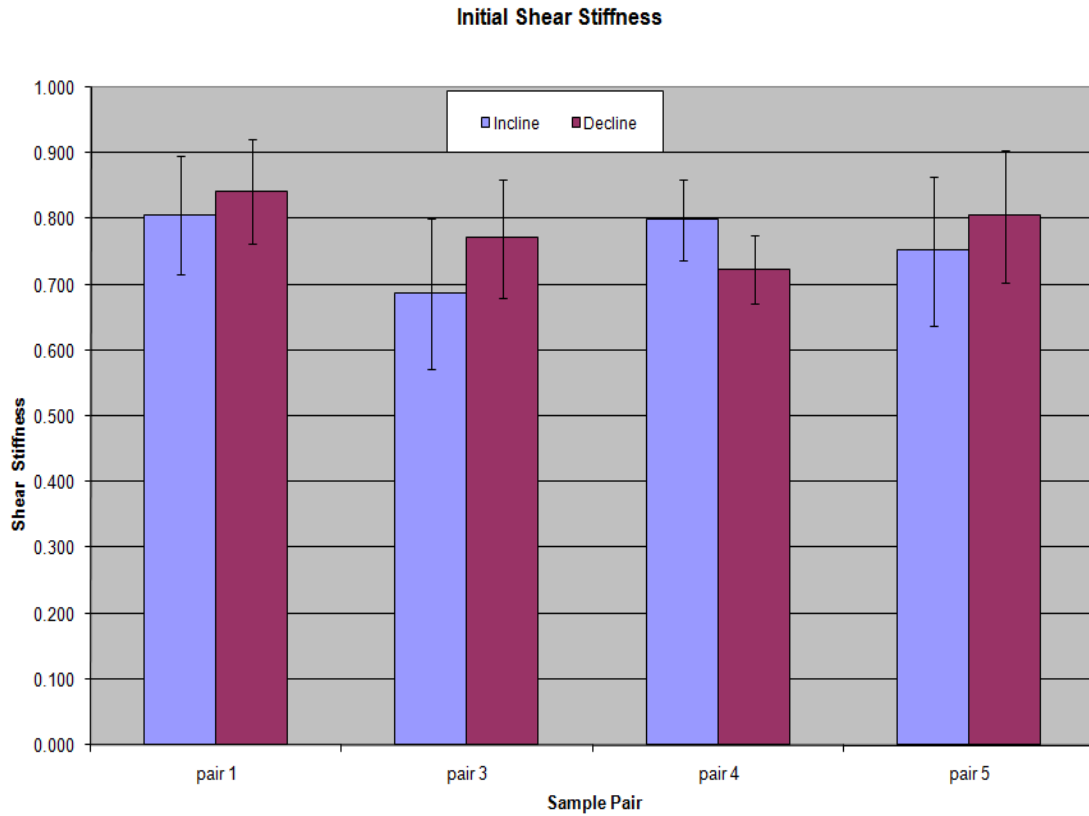


Figure 4.16. Graph of comparison of average initial shear stiffness in implant designs in testing on an incline and on a decline.

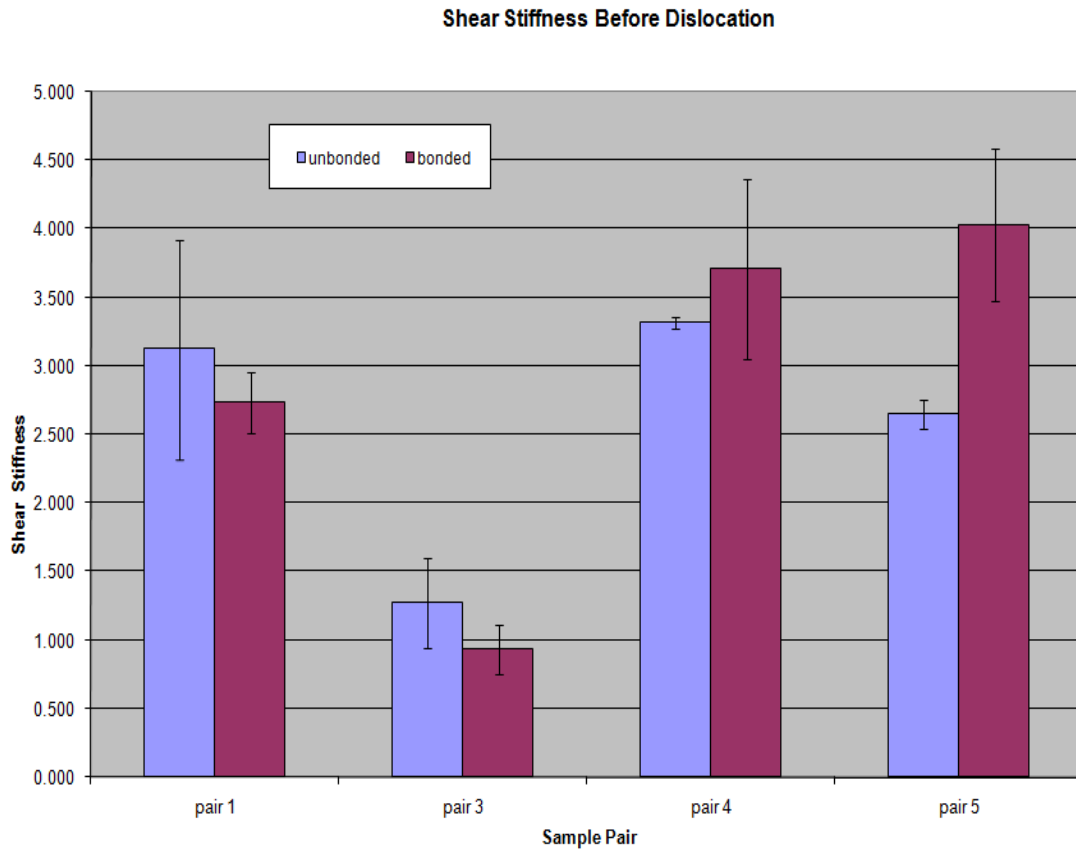


Figure 4.17. Graph of comparison of average shear stiffness before dislocation in implant designs in bonded and unbonded testing.

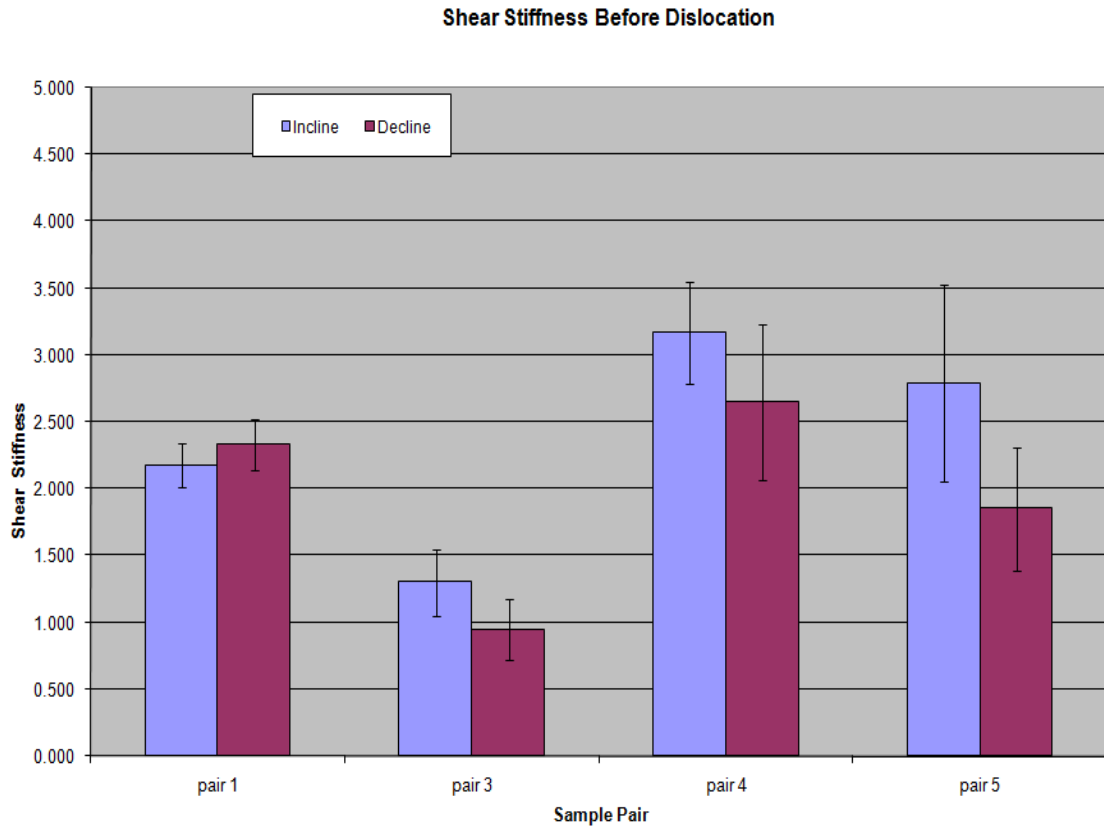


Figure 4.18. Graph of comparison of average shear stiffness before dislocation in implant designs in testing on an incline and on a decline.

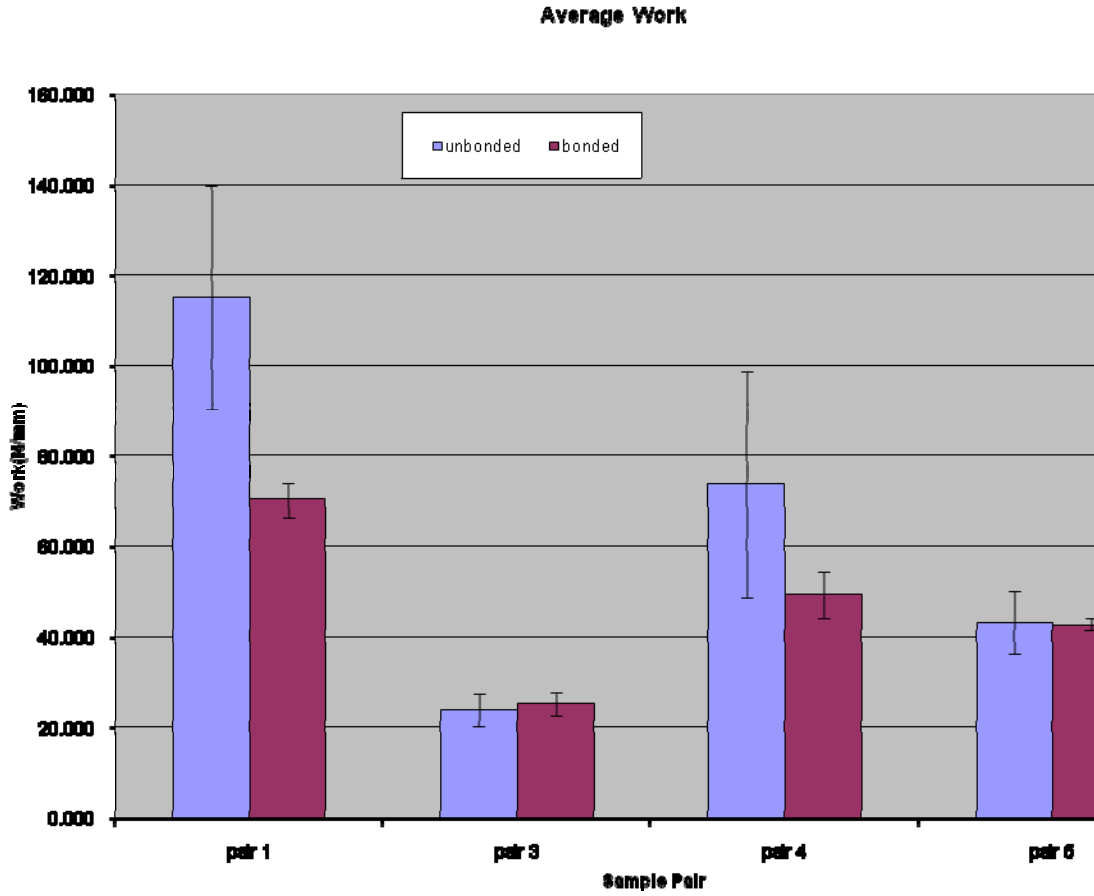


Figure 4.19. Graph of comparison of average work needed for dislocation for implant designs in bonded and unbonded testing.

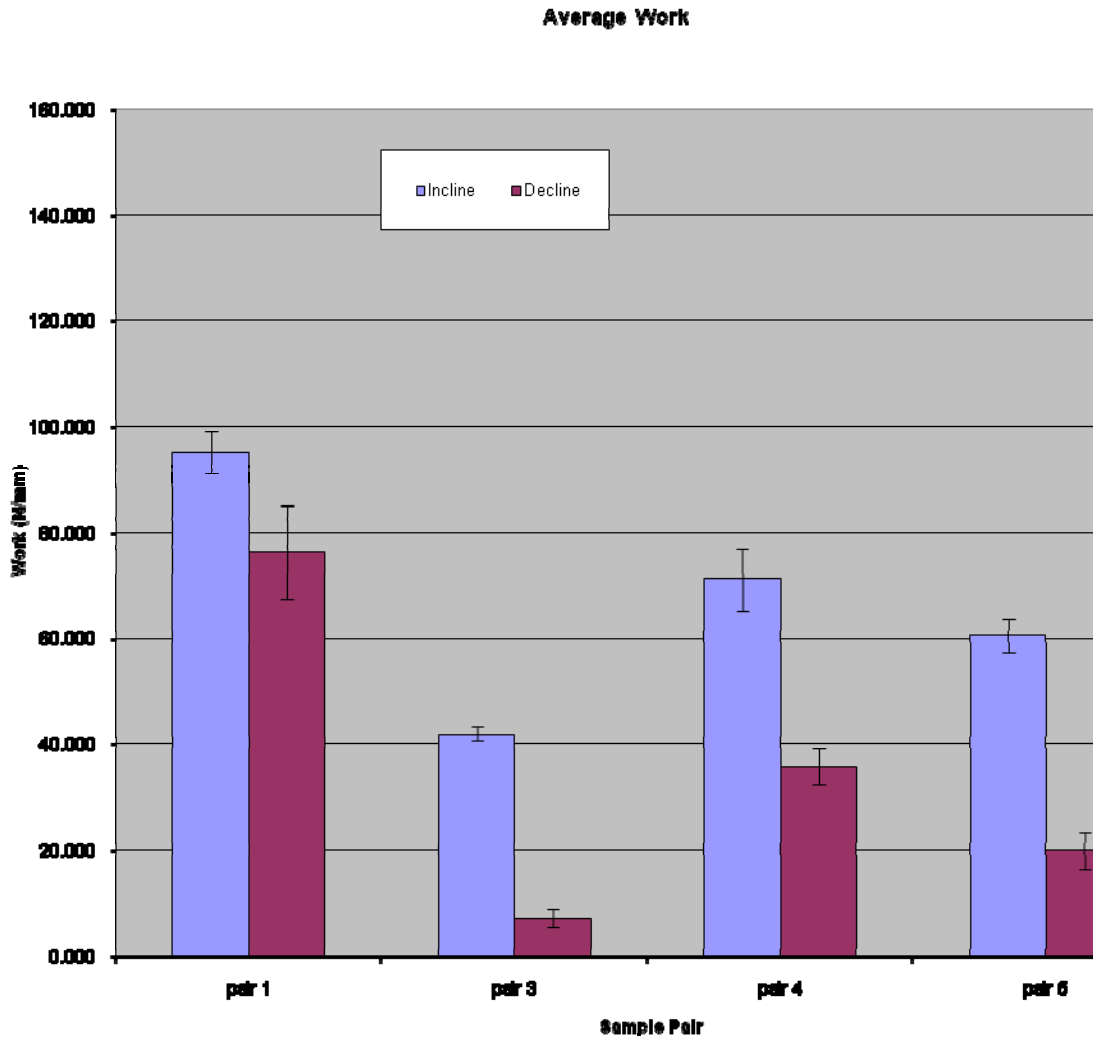


Figure 4.20. Graph of comparison of average work needed for dislocation in implant designs in testing on an incline and on a decline.

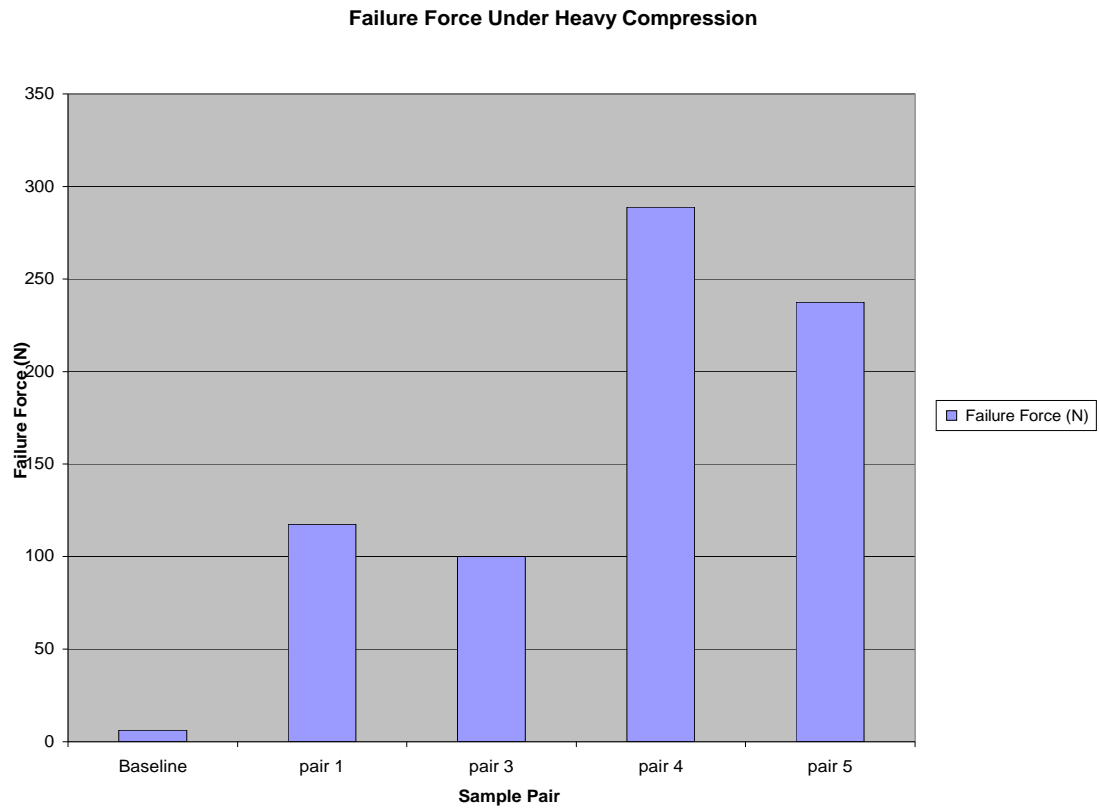


Figure 4.21. Graph of comparison of average failure forces in implant designs in testing under heavy compression.

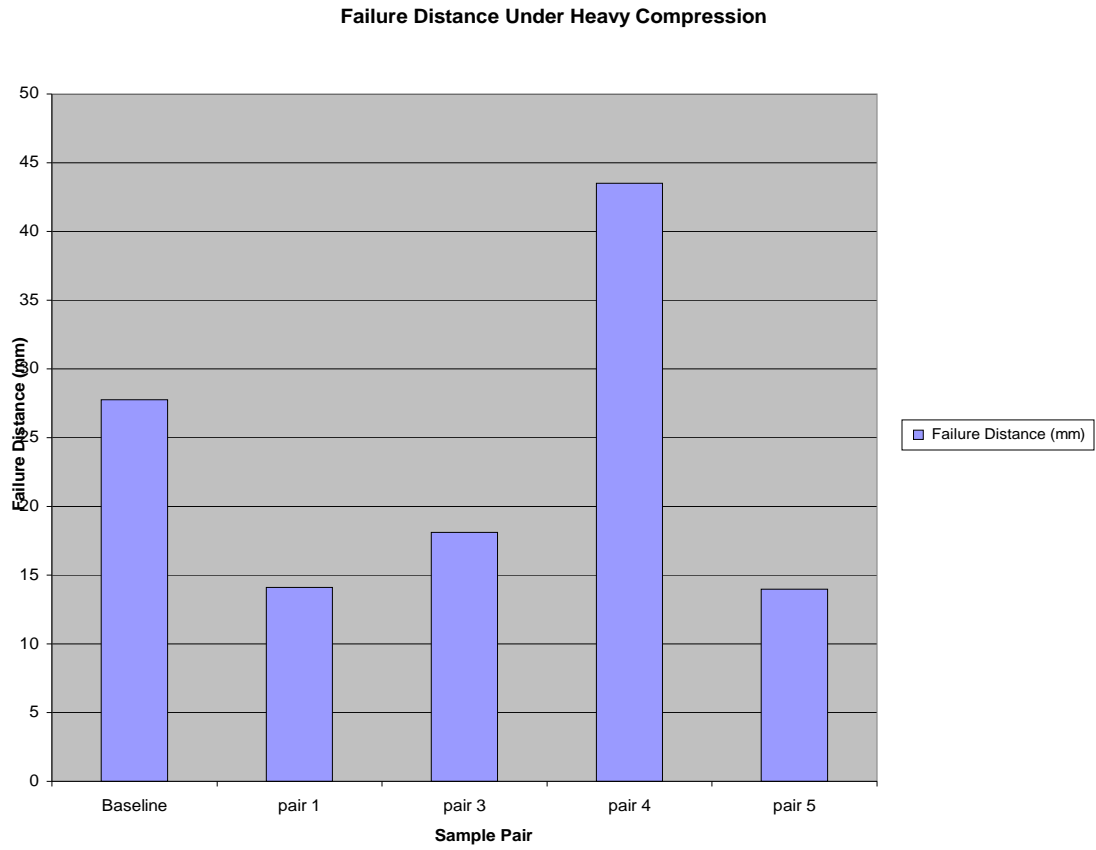


Figure 4.22. Graph of comparison of average failure distance in implant designs in testing under heavy compression

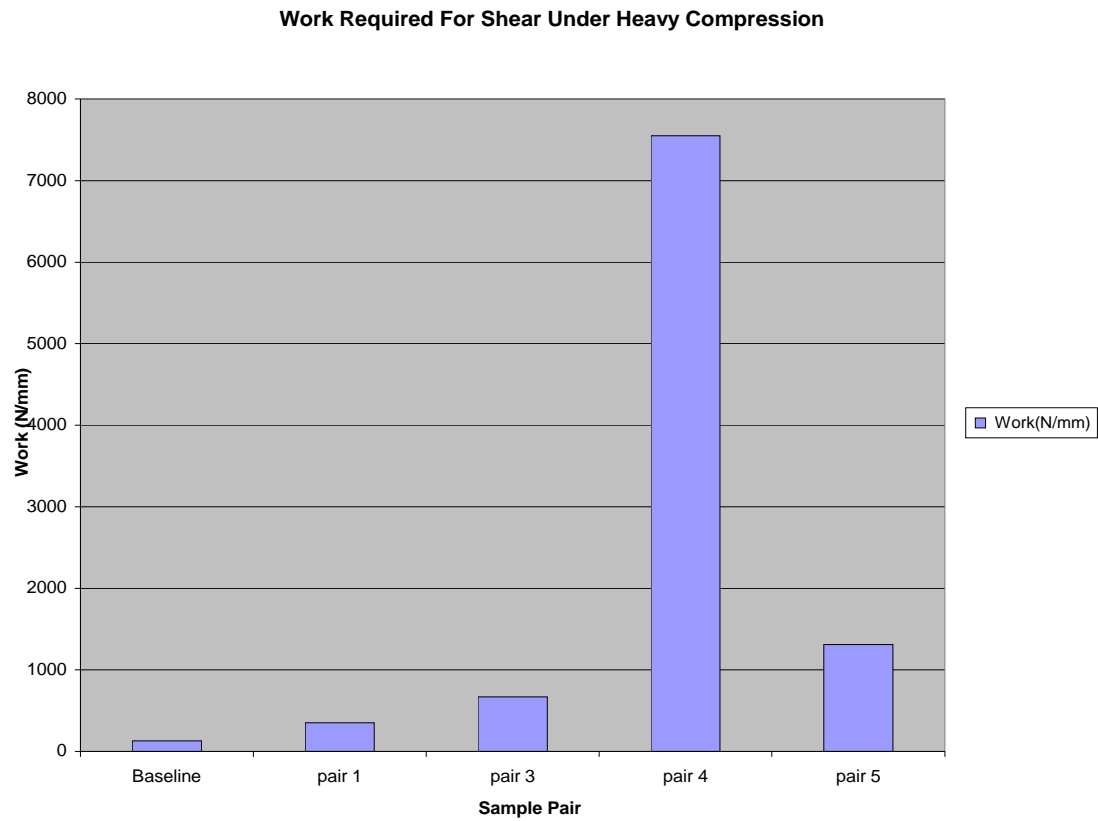


Figure 4.23. Graph of comparison of average work required for dislocation in implant designs under heavy compression.

Shear Stiffness Under Heavy Compression

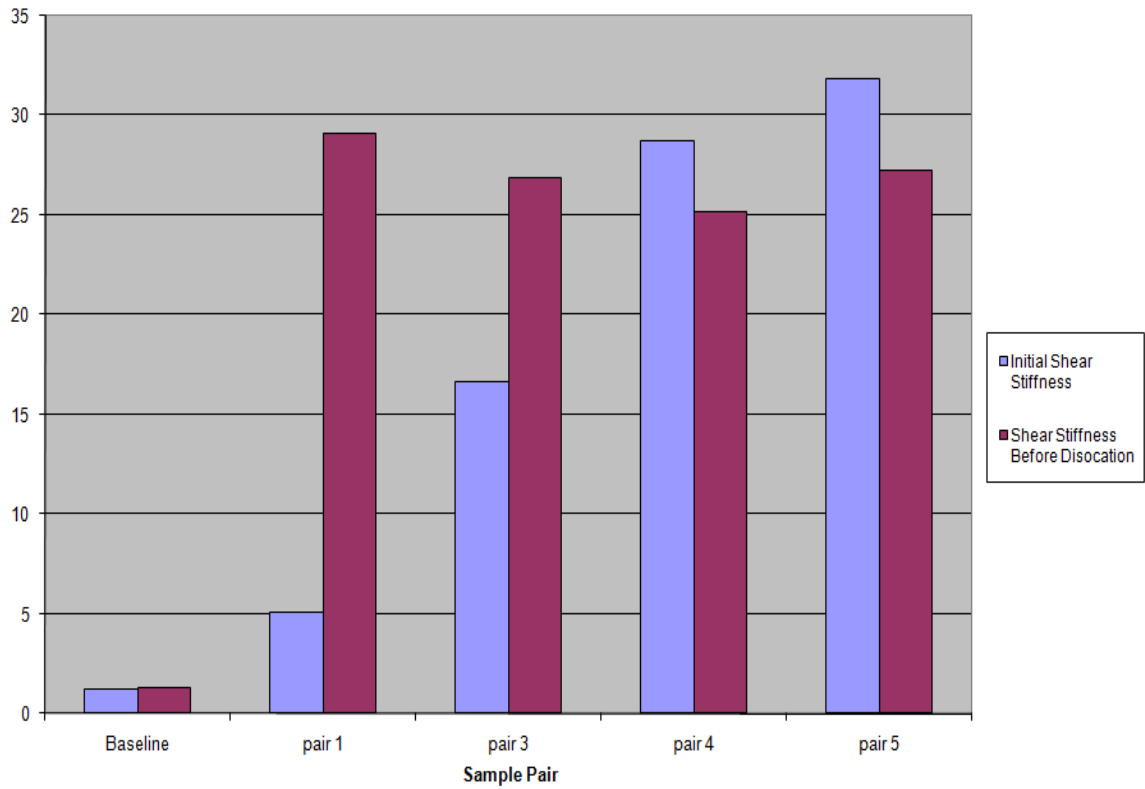


Figure 4.24. Graph of comparison of average initial shear stiffness and shear stiffness before dislocation on implant designs in testing under heavy compression.

CHAPTER V

TORSIONAL TESTING

5.1 Machinery and Setup

Torsion testing was conducted using the LabVIEW in conjunction with a custom electropneumatic regulator, a torsional pneumatic cylinder, a multimeter, a breakout box, multiple BNC cables, an air pressure regulator, three air hose, and pressurized air. An adjustable platform was placed on a table near a pressurized air source and a computer capable of running the LabVIEW data capture program. A torsional pneumatic cylinder (similar to a regular pneumatic cylinder but instead of providing linear force, it provides torsional force when used with compressed air) was secured to the adjustable platform (as seen in Figure 5.1). A paper ruler was taped to the cylinder so that the distance it rotated during each test could be recorded. The same circular (156g, 3.94in diameter, .14 in thick) fixation device (seen in Figure 4.1) designed to secure the bottom half of an implant during shear testing was also used to secure the bottom half of the implant during torsional testing. This fixation device was placed on top of washers and secured to the torsional pneumatic cylinder with screws. The same square (533g, 4in x 4in, .75in thick) fixation device (seen in Figure 4.2) designed to secure the top half of the implant during shear testing was also used to secure the top half of the implant during torsional testing. The top fixation device was firmly screwed to the bottom of the same (600g, 1ft x 1ft,

.25in thick) Plexiglas plate that was used during shear testing and the top fixation device was placed onto the bottom fixation device with the implant between them. This setup can be seen in Figures 5.2. and 5.3. A 500g weight was then placed on top of the Plexiglas plate; the weight places some compressive force on the implant when it is set in the fixation device. Running from the torsional pneumatic cylinder to the custom electropneumatic regulator was a white air hose; this hose provides the air necessary to turn the torsional platform during testing. A second white air hose ran from the custom electropneumatic regulator to the outlet of an air pressure regulator that was set to 5psi, all torsional tests were run at 5psi. A third hose ran from the inlet of the pressure regulator to a source of compressed air. Also, simultaneously running from the custom electropneumatic regulator was a cable to connect it to the desktop computer, a BNC cable that connected it to a breakout box (a device in which a multi-cable electric line is split into its component cables in order to allow for testing or signal enhancement), and a multimeter (which made sure the voltage readings that were coming into the custom electropneumatic regulator was correct). This complex setup can be seen in Figure 5.4.

Torsional tests were also performed using a $\pm 50\text{N}$ tension compression load cell. Before the tests the load cell was calibrated; after the load cell was calibrated, it was attached to the original torsion setup with a vertical metal bar. Then the bottom fixation device was modified (Figure 5.5), a bar was welded to it so that when the fixation device turned, the bar would press against the load cell and give a voltage reading which was recorded by the LabVIEW program. This voltage was later used to calculate torque.

5.2 Methods and Materials

Implant design 2 was excluded from torsional testing as well; implant designs 1, 3, 4, and 5 were tested as planned. During testing, a steady air pressure (set to 5psi with the air pressure regulator) flowed into the custom electropneumatic regulator from the pressurized air source. Voltages, ranging from 0.9-1.07 were also sent to the electropneumatic regulator using the LabVIEW program on the desktop computer the electropneumatic regulator was connected to. Since there was a steady air pressure going to the electropneumatic regulator, each time a voltage was sent to the regulator, compressed air flowed through the air hose connecting the electropneumatic regulator to the torsional pneumatic cylinder causing the cylinder to try to rotate. The degree of rotation depended on the voltage sent to the electropneumatic regulator. BNC cables also connected the multimeter to the custom electropneumatic regulator, so each time a voltage was sent to the regulator it was also displayed on the multimeter. This was done to insure that there was no electrical error and, the correct voltages that caused the various rotations of the torsional pneumatic cylinder were noted.

All of the four implant designs in turn were bonded into the top and bottom fixation devices, with the Plexiglas plate on top and a 500g weigh placing the implants under slight compression, and a paper ruler was placed around the revolving portion of the torsional pneumatic cylinder so that the distance that the implant revolved when subjected to various voltages could be recorded (the setup is displayed in Figure 5.3). Voltages were sent through the electropneumatic regulator starting at 0 V and increasing in 0.1 volt increments. The torsional pneumatic cylinder did not rotate at less than 0.9V for any of the implant designs and all of the implant designs dislocated by or before

1.07V so torsion was never tested above 1.07V. Since the top and bottom of all of these implant designs are corresponding/complementary shapes that fit snugly together under compression, when one half of an implant was shifted to a point where it would not go back into proper position if released from all stresses, the two halves were considered to have dislocated and the test was ended (Figure 5.6). Each voltage (0.9-1.07V) was sent from LabVIEW and then the distance of rotation that it caused on the torsional pneumatic cylinder was recorded. This test was done for each implant when it was in the center of the top and bottom fixation devices and the tests were repeated then the implants were 3mm, 6mm, and 9mm off center from the axis of rotation in their fixation devices. An illustration of what it means for an implant to be off center can be seen in Figure 5.7.

After all of the implants were tested at center and 3mm, 6mm, and 9mm off center and distance of rotation was recorded for all of the voltages tested (0.9-1.07) on each implant, another set of testing was done using a $\pm 50\text{N}$ tension compression load cell and a modified bottom fixation device (Figure 5.5). The idea behind testing with a load cell was this: when a load cell is placed under pressure, it produces a voltage. So when the load cell was vertically fixed to the modified torsional setup and voltage was run through the electropneumatic regulator, the torsional pneumatic cylinder turned and the bar welded onto the modified bottom fixation device pressed against the load cell. For each voltage that was run into the electropneumatic regulator by LabVIEW, the bar pressed on the load cell and the load cell output a voltage, yielding a table of voltage in and voltage out. This data was turned into more useful information by doing a calibration of the load cell. The voltages obtained from that calibration were used to calculate the torques at specific voltages. A table was then made of voltage vs. torque (a sample of which can be

seen in Table 5.1). That table was subsequently graphed (Figure 5.8), the equation from that graph could be used to find the torque at any voltage. That equation was used ultimately to find the torque at all of the voltages that were input during the first round of testing where a voltage was entered into LabVIEW and the torsional pneumatic regulator turned a certain distance.

5.3 Results and Analysis

The torsional pneumatic cylinder did not rotate at less than 0.9V for any of the implants and 1.07 volts was the highest voltage required for dislocation or complete rotation. For the first set of testing without the load cell, voltages entered into LabVIEW and the amount of torsion those voltages caused on the torsional pneumatic cylinder were calculated. These voltage and torque values were calculated for each implant in the centered position, at 3mm offset, 6mm offset, and 9m offset. Using the equation found by graphing voltage vs. torque, the torque was found for each voltage entered into LabVIEW. The degree of rotation for each distance moved was also found using the circumference of the torsional portion of the torsional pneumatic cylinder as well as the distance that the torsional portion rotated during each test. Voltage entered from LabVIEW (voltage in) and the other two calculated results (torque and degreed of rotation) were all grouped together in tables. A sample of this data can be seen in Table 5.2.

Ultimately, the minimum torque required to begin movement of each implant at the centered position and at 3mm offset, 6mm offset, and 9mm offset was recorded and graphed. The maximum torque required for dislocation of each implant at the centered

position and at 3mm offset, 6mm offset, and 9mm offset was also recorded and graphed. These graphs can be seen in Figures 5.9-5.16. A statistical ranking of the various implant designs can be seen in Table 5.3.

Physiologically, vertebrae are supposed to rotate in relation to one another; ideally, the best implant design will be stiff in shear and low in torsional resistance. Since any resistance to torque would be due to friction between the two halves of the implant, the ideal implant design would rotate freely. For these torsional tests the best implant design is the one which requires the least torque to move. The minimum torque required for movement stayed within the same range (about 1.6- 2.0 Nm) for all of the implant designs. When the implants were centered, implant designs 1 and 3 required the least torque to begin torsion, they were 5% better than the next best implant which was implant design 4, design 4 was also 5% better than the worst implant design which was implant design 5. This makes sense because the sharpest implants required the least torque to begin movement and the flatter the implants got (or more surface area they had), the more torque was required for movement (to review the implant shapes please see figures 3.1-3.5). When the implant designs were offset 3mm from the center of the fixation device, implant design 3 required the least torque for movement, 10% less than implant design 5. Implant design 5 required 5% less torque than implant design 1, and implant design 1 required 10% less torque for movement than implant design 4. When the implant designs were 6mm offset, implant design 3 required the least torque for movement, 10% less than implant design 5, then implant design 4, and lastly implant design 1. When the implant designs were 9mm offset, implant design 1 took the least torque to initiate movement, 28% less than implant designs 3 and 5 which took 5% less torque to move than implant

design 4. When considering minimum torque required for movement, implant design 3 was the most consistent in low resistance to torsional movement despite the positioning, followed by implant designs 5, then 1, then 4. This was surprising because since implant design 3 has the second broadest surface area of all of the implant designs, it was expected to take more torque to move than the sharper implant designs (implant designs 1 and 4) ANOVA and LSD tests along with paired effects comparison were used to determine the effects of implant design and location of the implant (offset) on each other. It was determined that pair and position significantly interact to affect the response of torque. The best combinations to provide the minimum amount of torque required for minimum movement were found to be the combinations of implant design 3 at 3mm offset and implant design 3 at 6mm offset. The statistical analysis shows that overall (looking at all positions for this test), implant design 3 resists torque the least for minimum torque required to just move the implant.

The minimum torque values required for full rotation (or dislocation if the implants were placed off center) varied greatly (from about 15-25 N.m) When the implants were centered, implant designs 1 and 3 still required the least torque to dislocate the implant, 5% less than implant design 4, implant design 5 required the most torque for dislocation. The results for all four implant designs for minimum torque required to move the implants and the results for all four implant designs for the maximum torque needed to dislocate them are almost identical sets of data when the implant is centered (Figures 5.9 and 5.13). The implant designs all behave the same with respect to one another except of course all of the minimum torque values required for dislocation or full rotation of the implants are higher in all cases than the minimum torque values required for movement

of the implants. When the implant designs were offset 3mm from the center of the fixation device, implant design 3 required the lowest torque, 17% less than implant design 5, which required 18% less torque for movement than implant designs 4 and 1. When the implant designs were offset 6mm from the axis of rotation, implant design 3 again required the least torque for movement, followed by implant design 5, then designs 4 and 1 which required the same amount of torque. When the implant designs were 9mm offset, implant design 1 required the least amount of torque for movement, 5% less than implant design 5, which required 5% less torque than implant designs 3 and 4 which required the most torque for movement. ANOVA and LSD tests along with paired effects comparison were used to determine the effects of implant design and location of the implant (offset) on each other. It was determined that pair and position significantly interact to affect the response of torque. Implant design 3 at 3mm offset was found to be the combination that required the least torque to fully rotate. The statistical analysis shows that overall (looking at all positions), implant design 3 resists torque the least for minimum torque required for movement, followed by implant design 5, then implant design 4, then implant 1. The statistical analysis shows that overall (looking at all positions for this test), implant design 3 still resists torque the least for minimum torque required for full rotation.

Implant designs 3 and 5 are less resistant to torsional stresses than implant 4; however, implant design 4 may still be the best implant choice. Implant design 4 is more stable than designs 3 and 5, and it can accommodate bending movements without sliding like implant designs 3 and 5 have to do because of their large surface areas. Sliding is a major concern because the more sliding that occurs over a larger surface area, the more

wear that takes place. Since these implants are meant to be places into patients with significantly intact annulus fibrosus (typically young people), the longevity of these implants are a definite concern and the larger the surface area, the worse the implant performs in terms of wear over time.

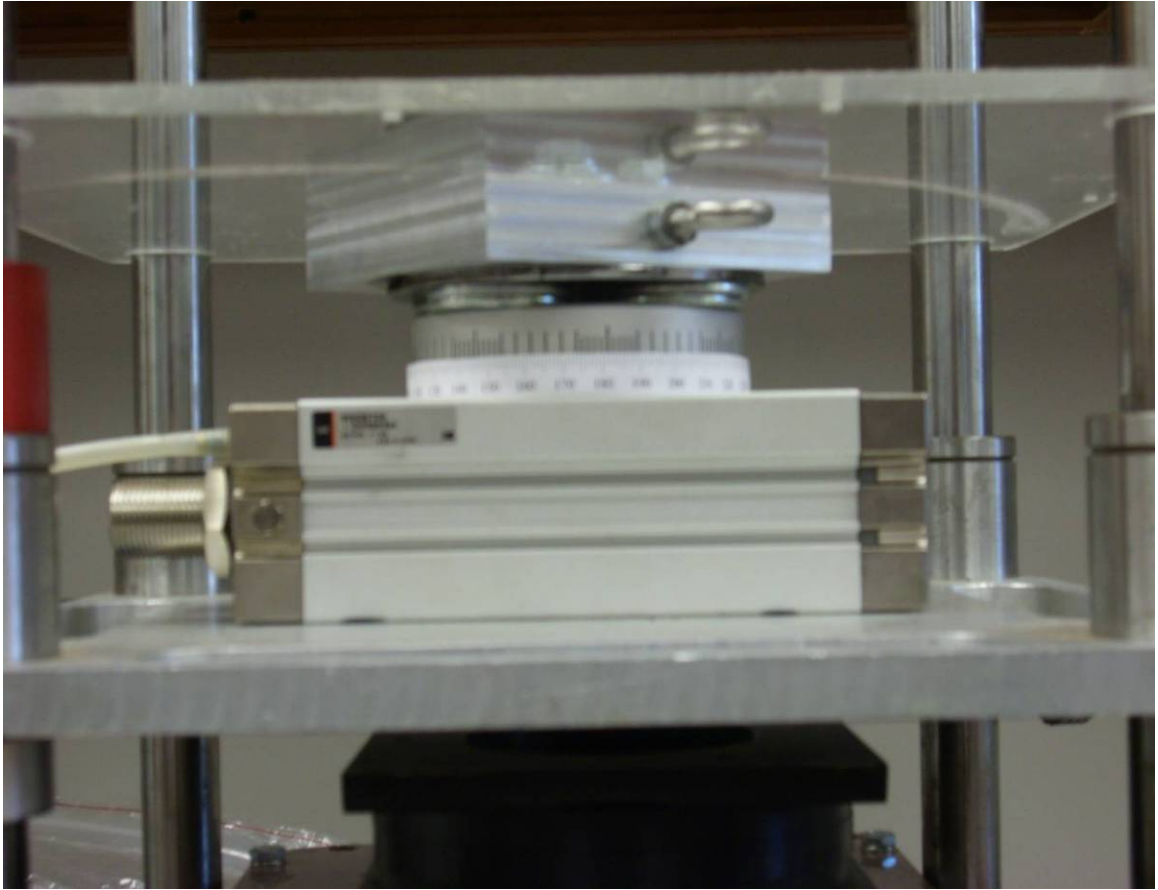


Figure 5.1. A torsional pneumatic cylinder attached to an adjustable platform

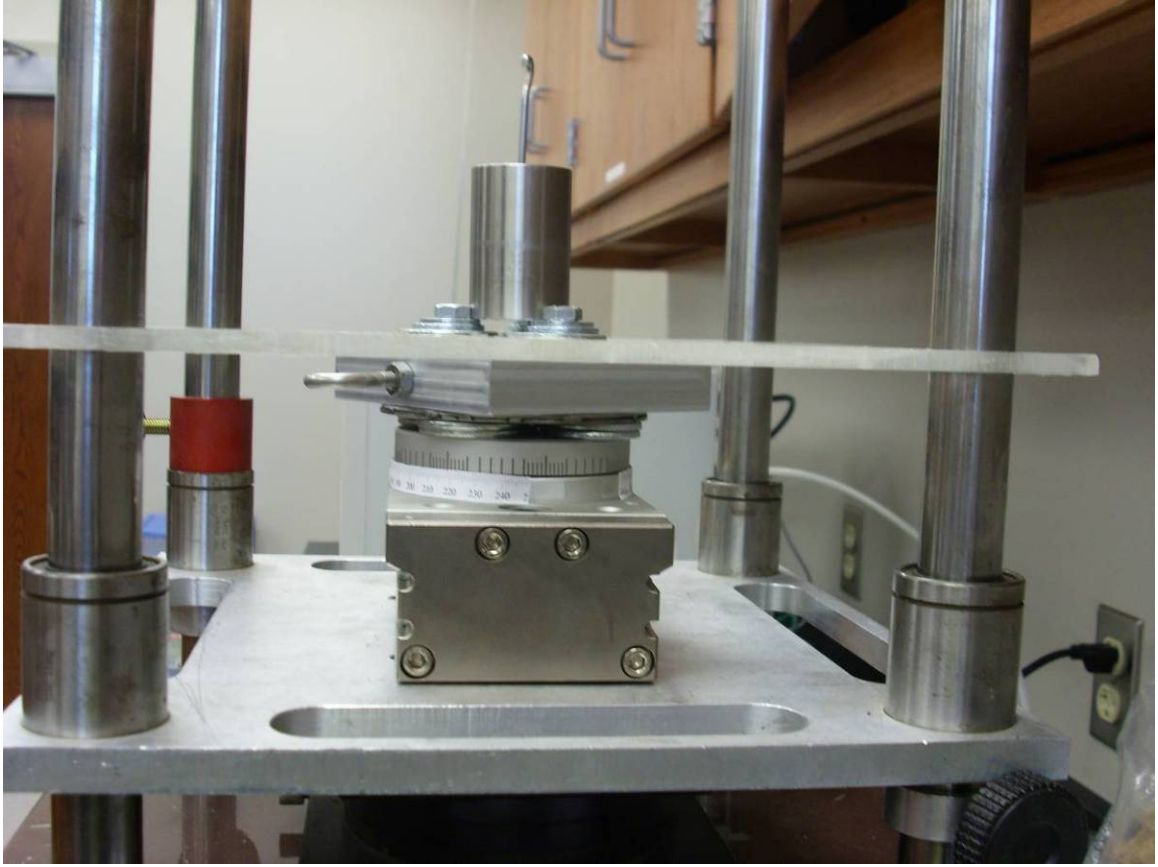


Figure 5.2. Side view of the implant fixation devices for torsional testing

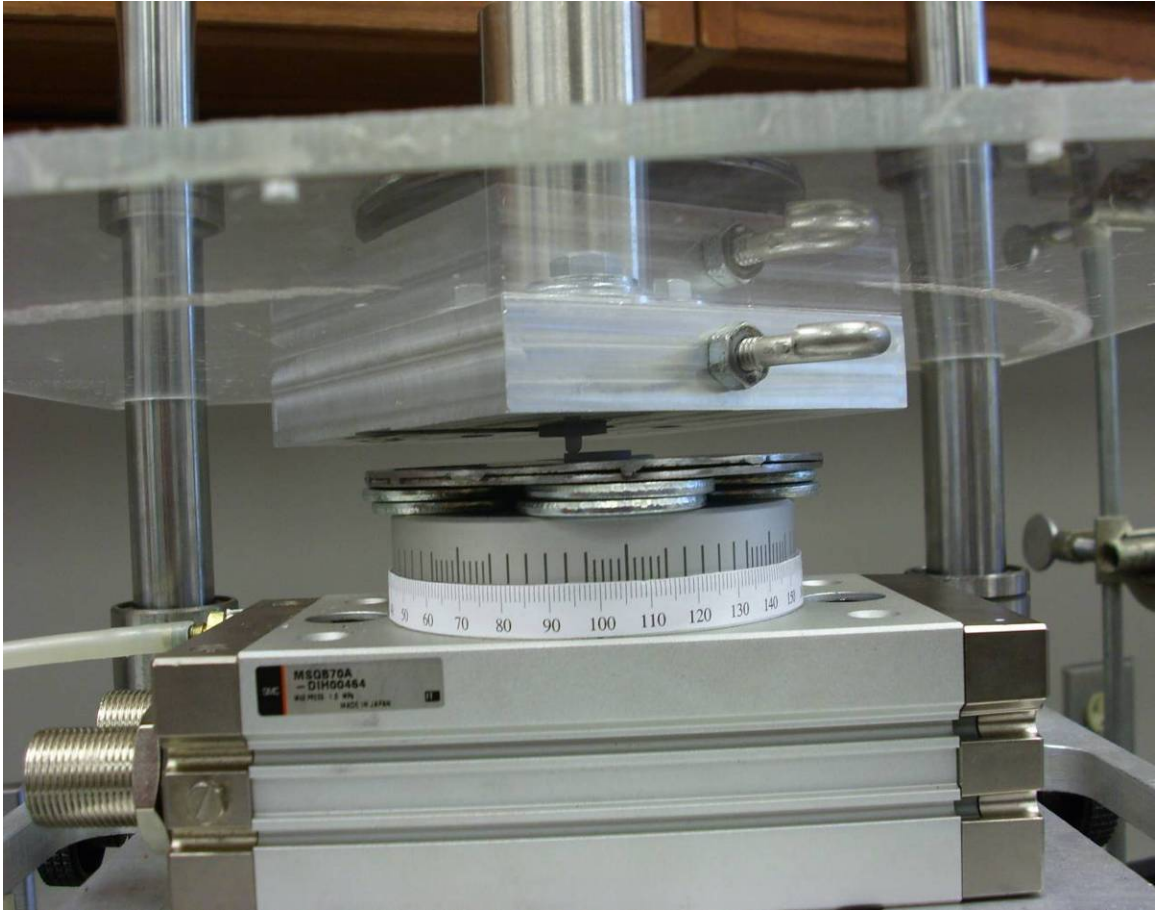


Figure 5.3. Front view of the implant fixation devices for torsional testing

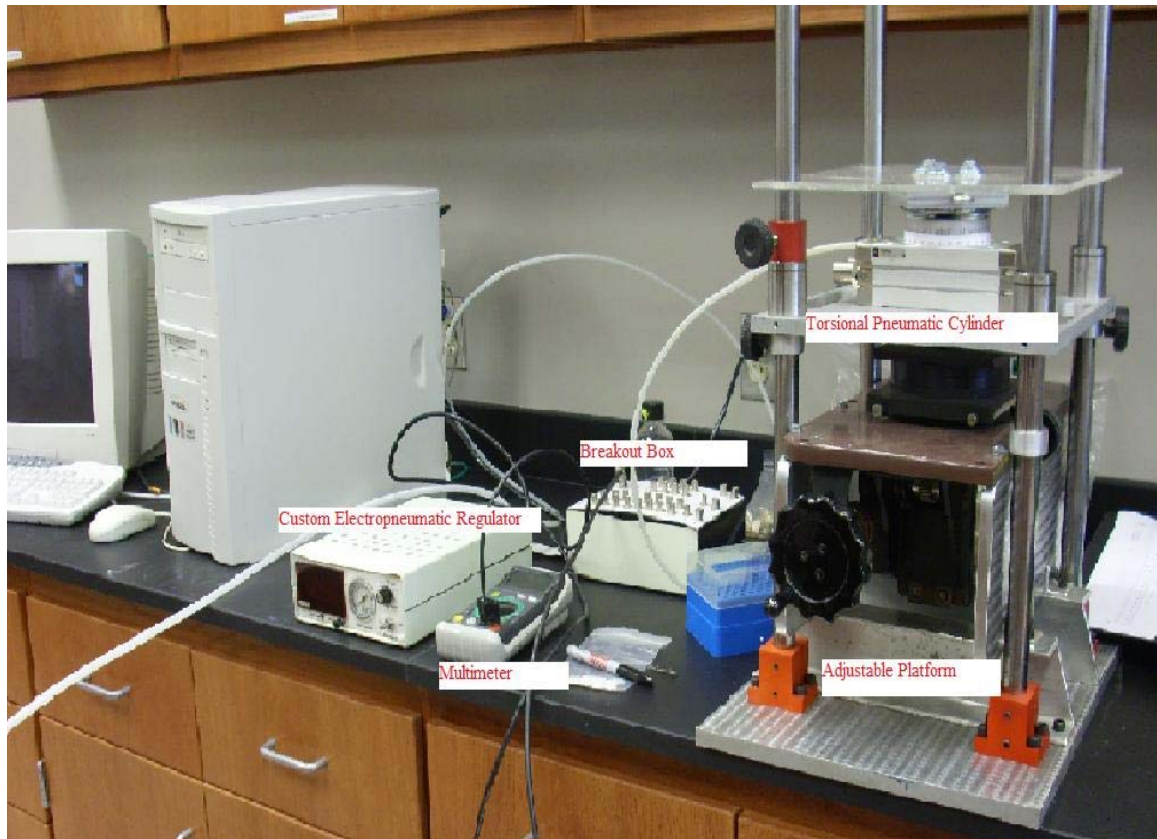


Figure 5.4. Setup for torsional pneumatic torsional testing.



Figure 5.5. Modified bottom fixation device for torsional testing with a load cell

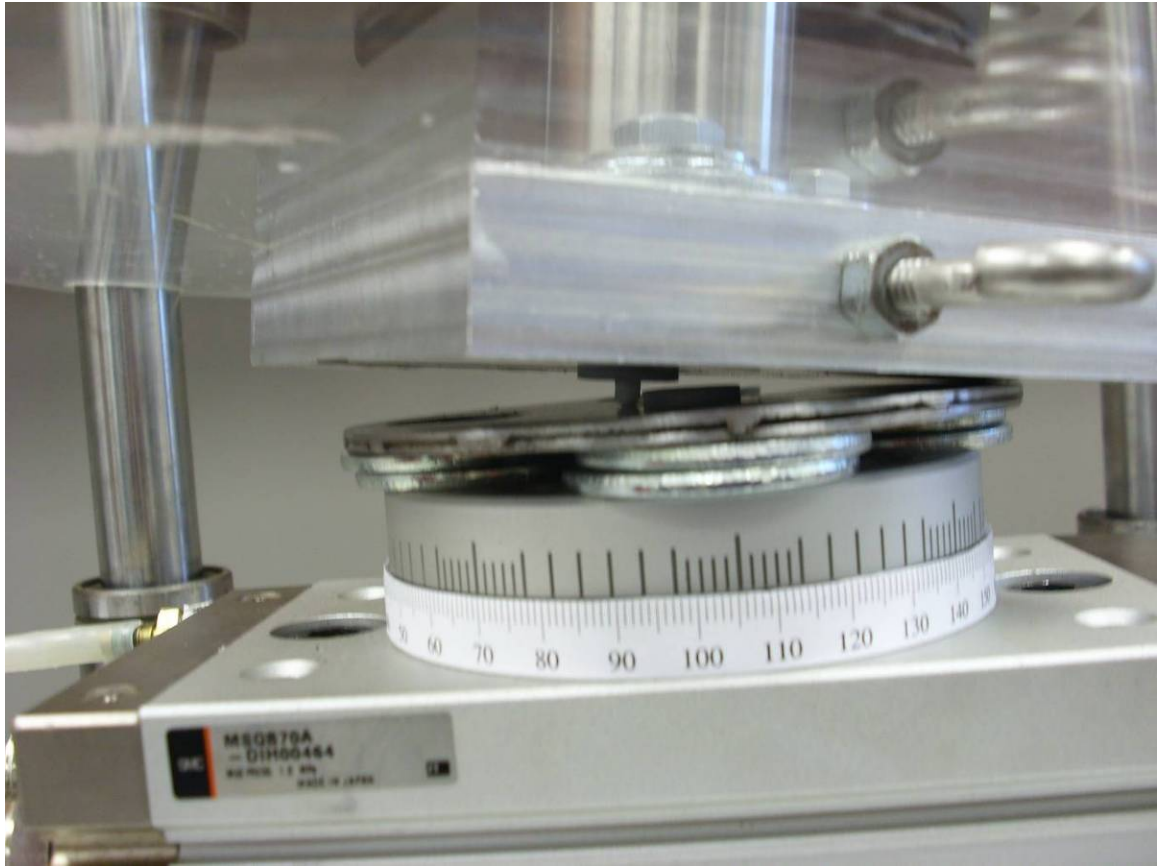


Figure 5.6. Picture of Implant after dislocation in torsional testing

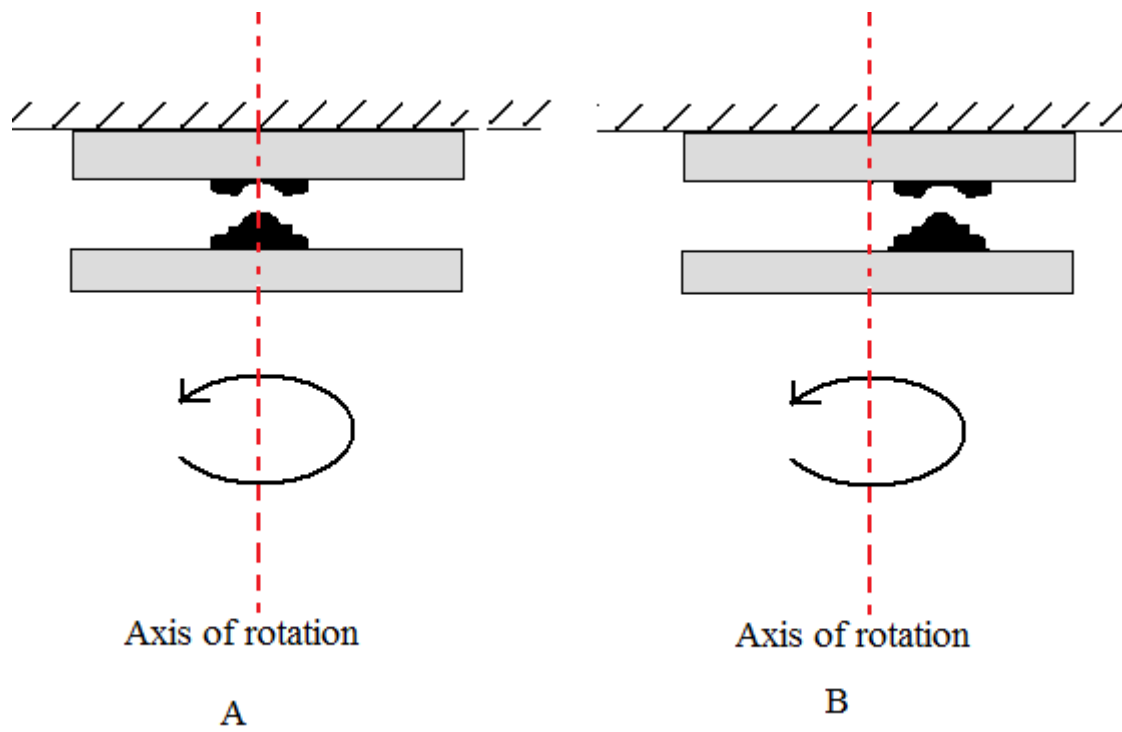


Figure 5.7. A) Side view of an illustration of an implant that is centered
 B) Side view of an illustration of an implant that is off centered

Table 5.1. Table of voltage entered in LabVIEW and resulting torque

Voltage In (V)	Torque (N.m)
0.005	0.138375
0	0.132125
0	0.132125
0	0.138375
0	0.132125
0	0.132125
0.005	0.132125
0	0.138375
0	0.132125
0	0.132125
0	0.132125
0.947	0.132125
0.947	0.132125
0.952	0.132125
0.952	0.132125
0.952	0.132125
0.957	0.138375
0.957	0.138375

At Supply Pressure of 5psi

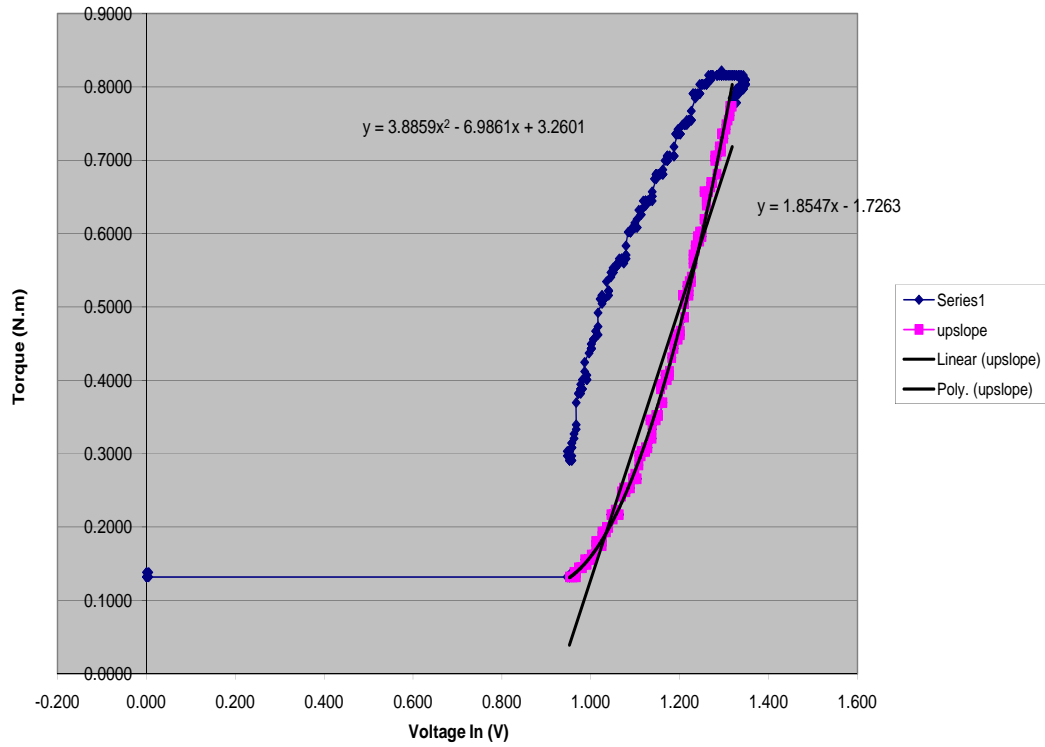


Figure 5.8. Graph of the voltage entered in LabVIEW and the resulting torque.

Table 5.2. Voltage entered in LabVIEW and the resulting torque and degrees of rotation

Implant 1		5 psi	
500g weight			
Voltage (V)	Torque (N.m)	Degrees of Rotation (°)	
0.90	0.1202	0.00	
0.91	0.1207	0.00	
0.92	0.1219	0.00	
0.93	0.1239	0.00	
0.94	0.1267	0.00	
0.95	0.1303	0.00	
0.96	0.1347	0.00	
0.97	0.1398	0.00	
0.98	0.1457	0.00	
0.99	0.1524	0.00	
1.00	0.1599	0.00	
1.01	0.1681	0.00	
1.02	0.1772	17.75	
1.03	0.1870	133.10	

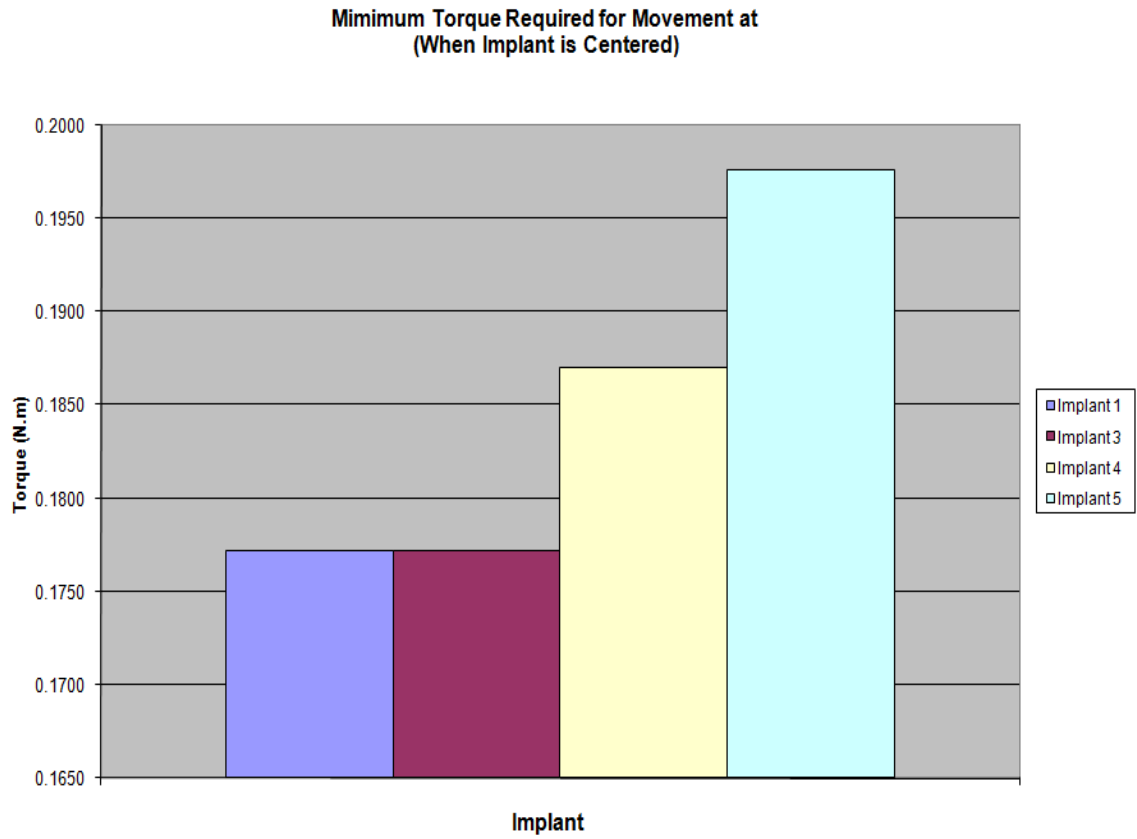


Figure 5.9. Graph of minimum torque required for movement when the implant is centered

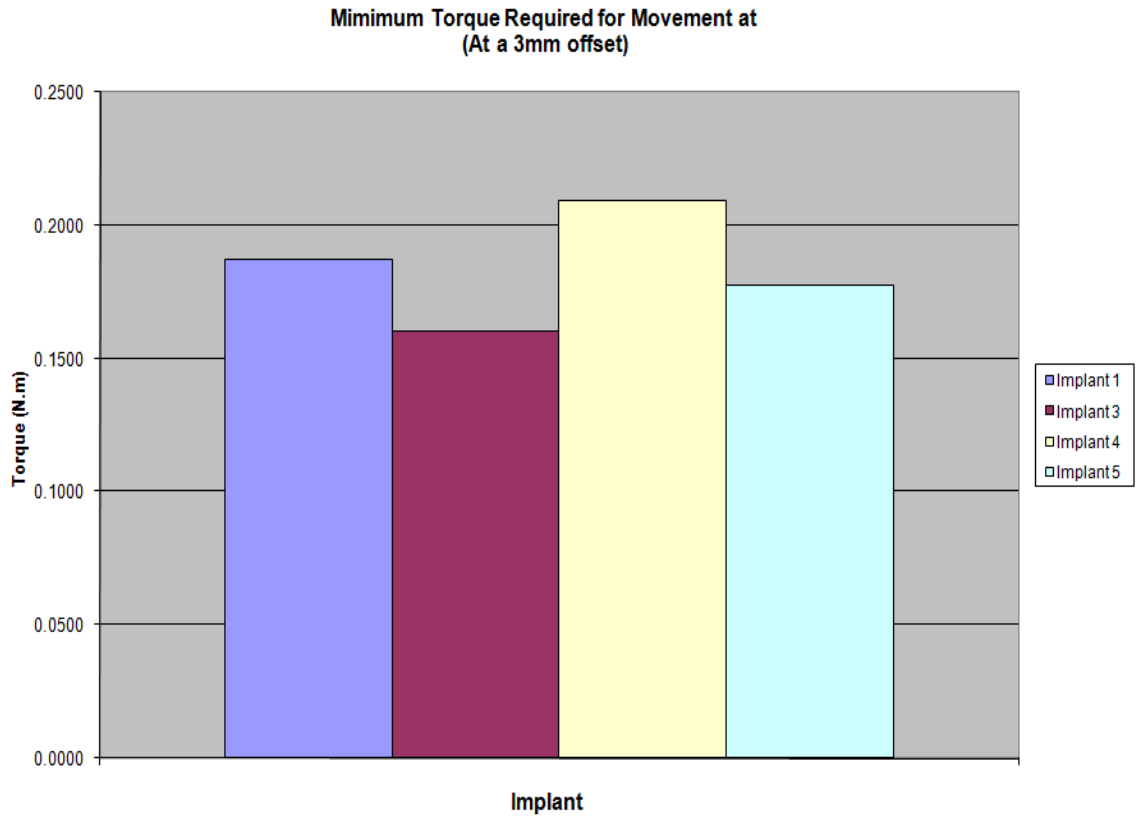


Figure 5.10. Graph of minimum torque required for movement when the implant is at a 3mm offset.

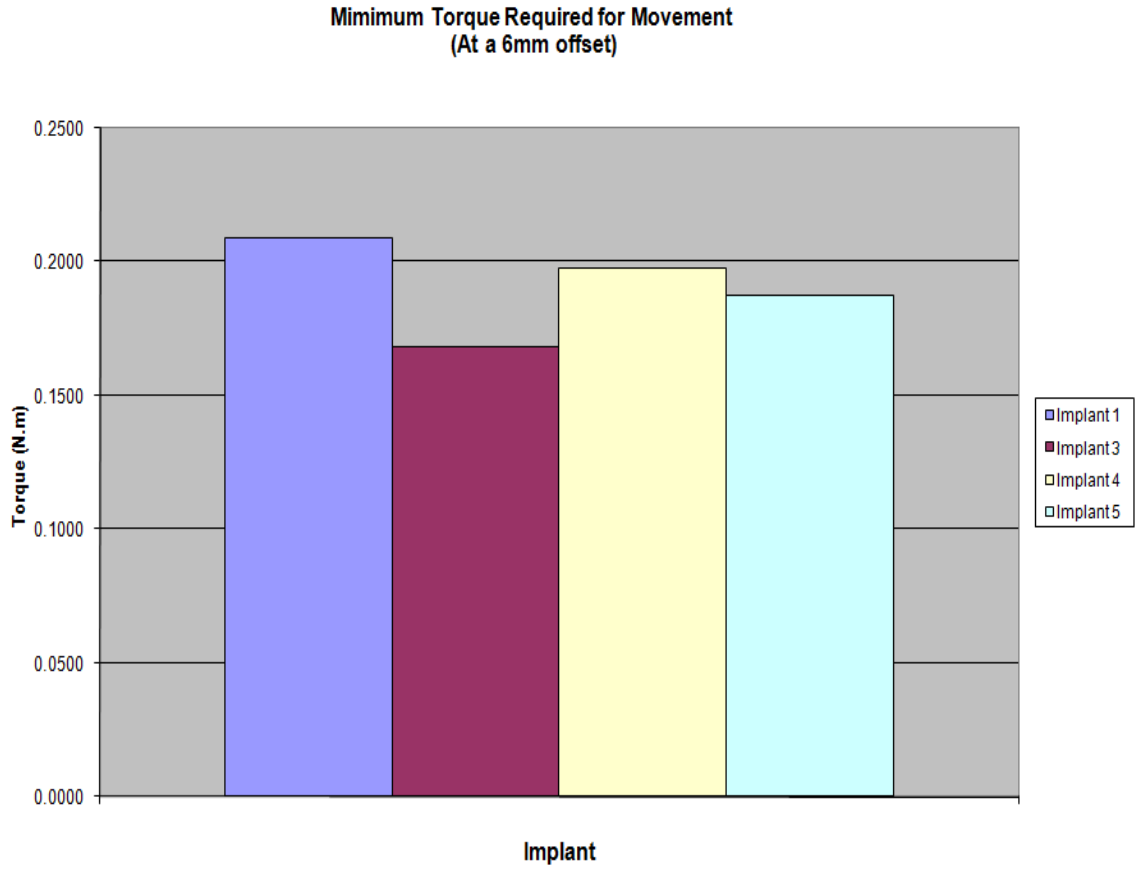


Figure 5.11. Graph of minimum torque required for movement when the implant is at a 6mm offset

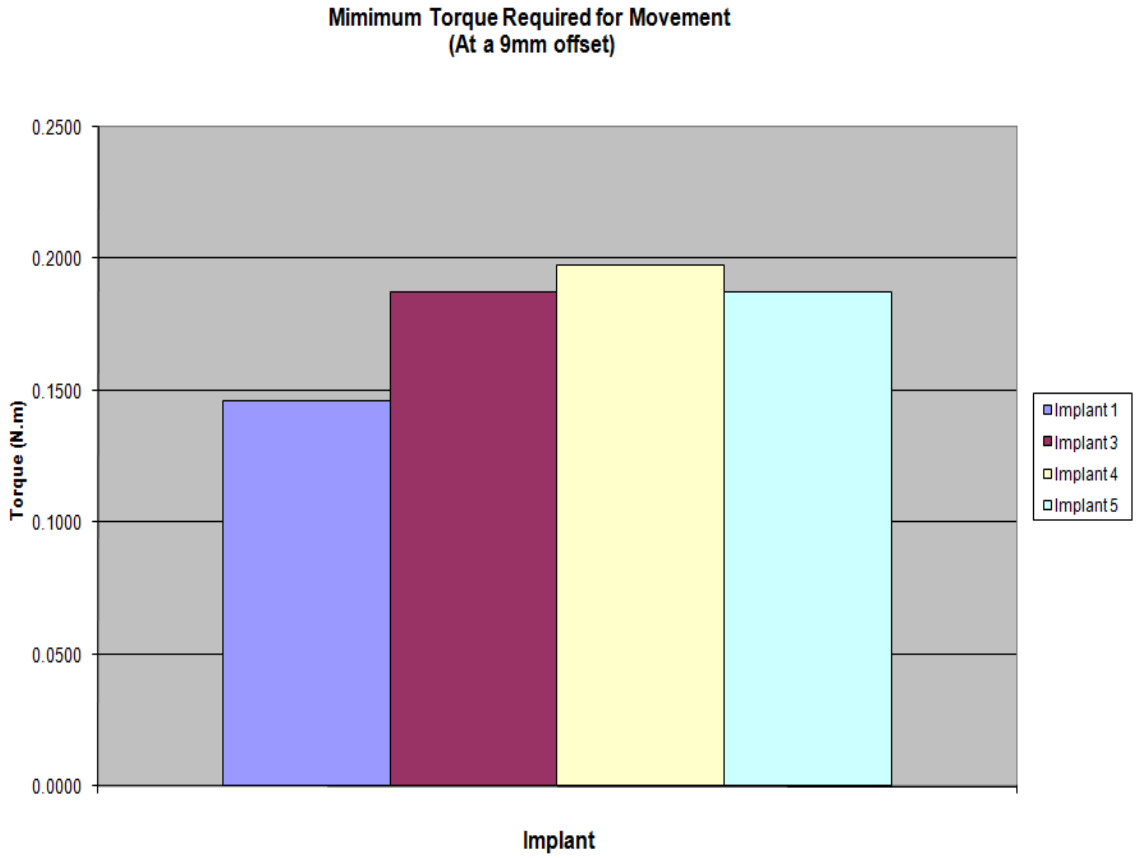


Figure 5.12. Graph of minimum torque required for movement when the implant is at a 9mm offset

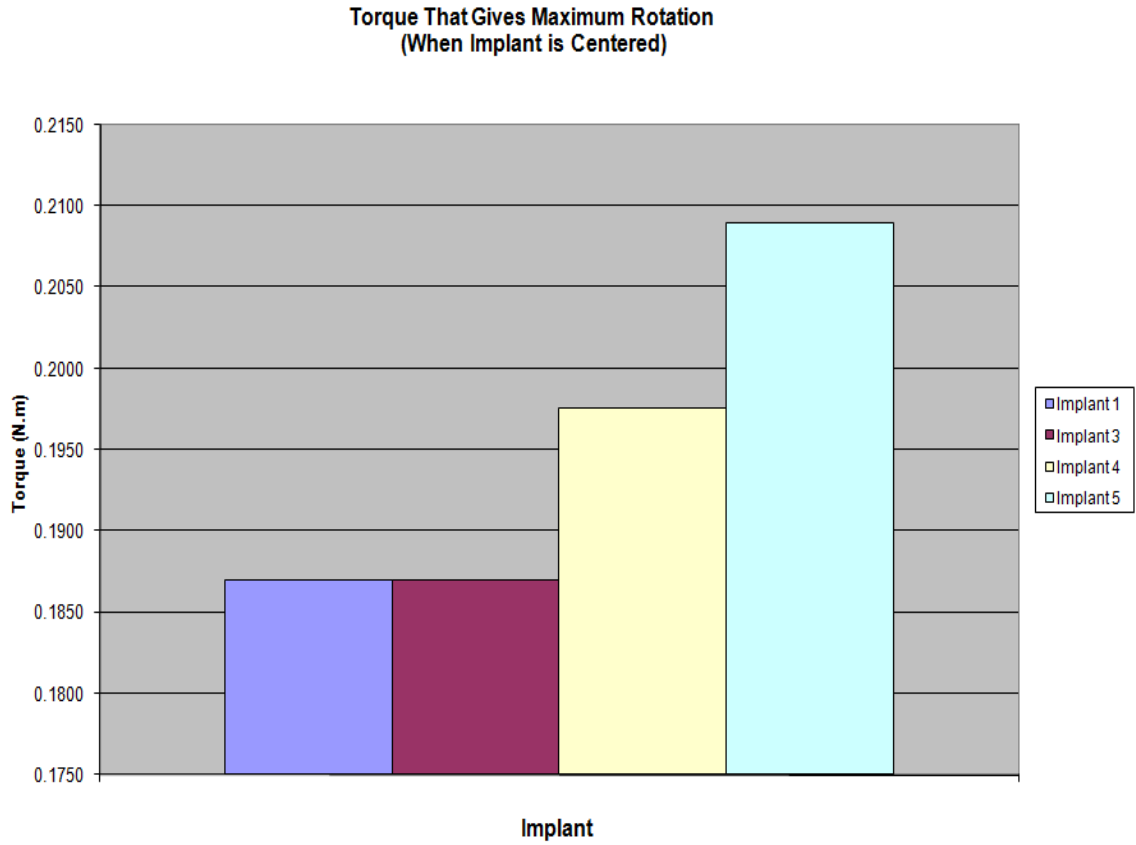


Figure 5.13. Graph of maximum torque required for implant dislocation when the implant is centered

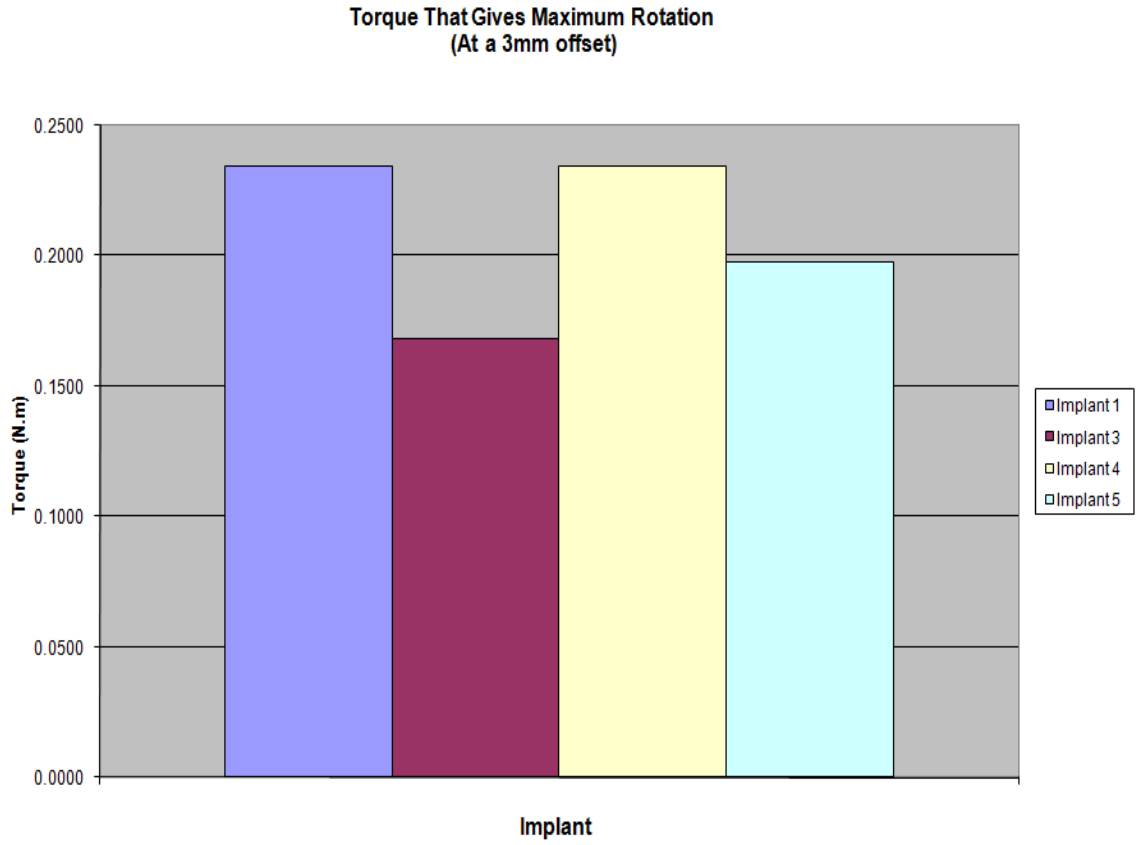


Figure 5.14. Graph of maximum torque required for dislocation when the implant is at a 3mm offset

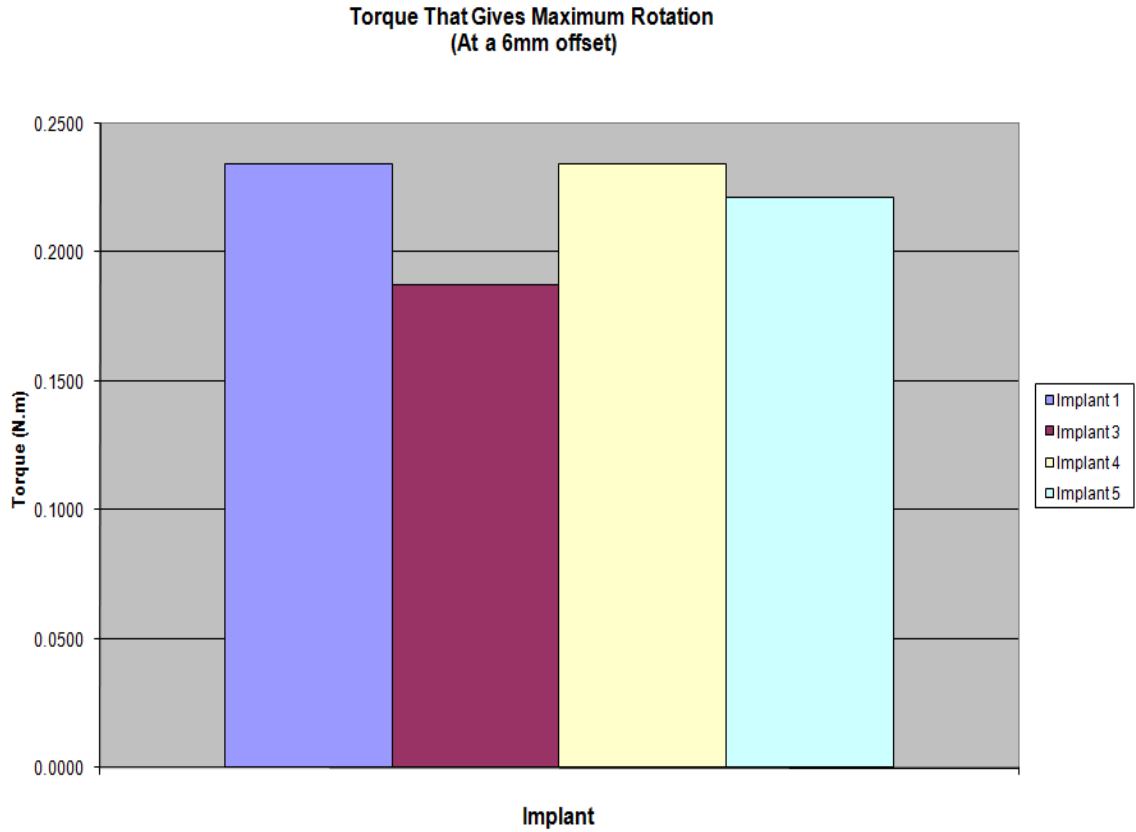


Figure 5.15. Graph of maximum torque required for dislocation when the implant is at a 6mm offset.

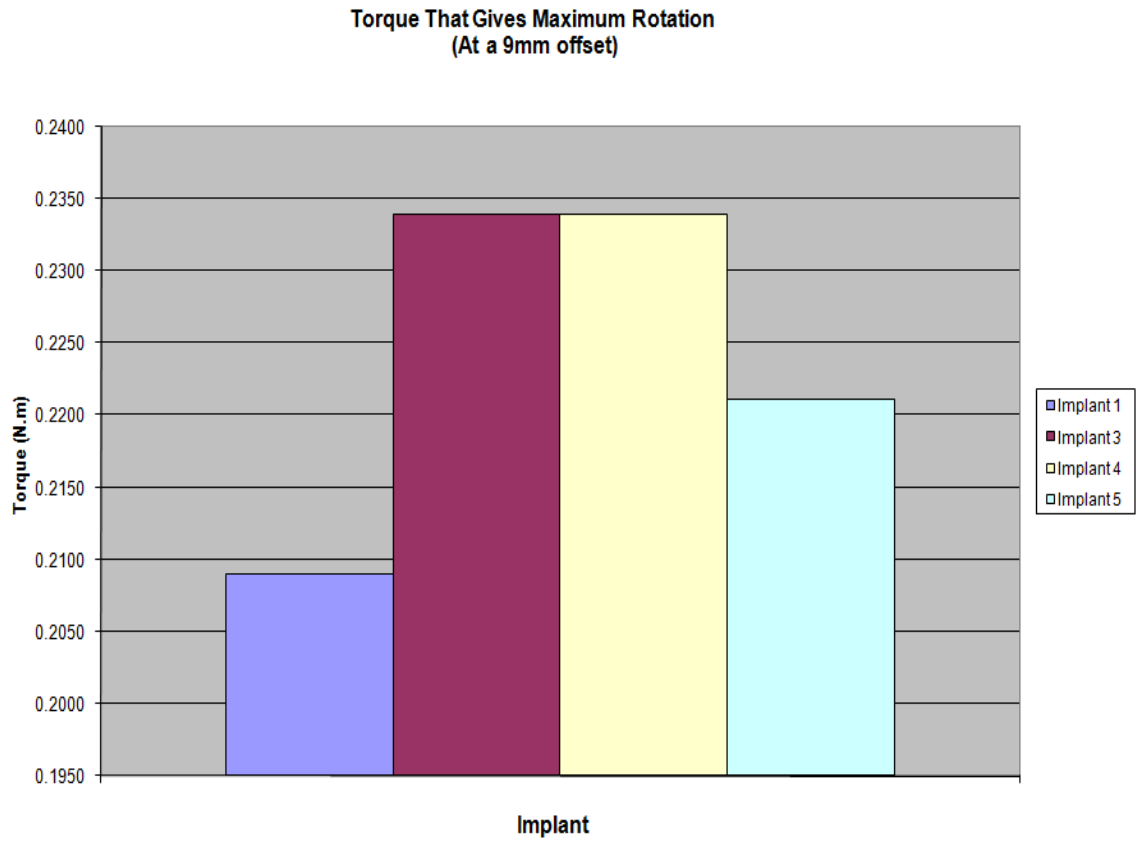


Figure 5.16. Graph of maximum torque required for dislocation when the implant is at a 9mm offset

Table 5.3. A statistical ranking of the various implant designs

Statistical Analysis of Results For Torsional Testing under 500g of Compression			
<u>Testing Position</u>	<u>Minimum Torque Required for Movement</u>	<u>Minimum Torque Required for Full Rotation</u>	
Centered	3 + 1, 4, 5	3 + 1, 4, 5	
3mm offset	3, 5, 1, 4	3, 5, 4 + 1	
6mm offset	3, 5, 4, 1	3, 5, 4 + 1	
9mm offset	1, 5 + 3, 4	1, 5, 3, 4	
<p>The numbers represent their corresponding implant designs. For example, 1 refers to implant design 1</p> <p>The implant designs are ranked from right to left, best performance to worst performance</p> <p>A + sign means that there is no statistical significant difference between two implant designs</p> <p>SAME means that there is no statistical Difference between any of the implant designs</p>			

CHAPTER VI

CONCLUSION

This work proposed the creation of idealized models to determine the shape of nuclear implant best suited to resist the standard shear and torsional stresses that are generated in the lumbar spine. More specifically to select which one of four rigid two part nuclear implants drawn in predetermined shapes would serve best as a substitute for a degenerated nucleus pulposus in intervertebral discs. It is the conclusion as determined by various in vitro mechanical tests that implant design 4 is the implant design most resistant to shear. And implant design 3 is the implant design least resistant to torsional stress. Therefore, a combination of implant design 3 and implant design 4 might be optimal in terms of shear, torsion, wear, and stability

Results show that the standard deviations for all of the shear tests are relatively small, and since many tests were run; the conclusion is that the obtained data is accurate. Tests were performed in shear under numerous conditions. The implant designs were tested in plain shear to see how well they resisted shear forces. They were then tested in a bonded state to see if fixation to the vertebra would interfere with their mechanical function. Lastly, they were tested on an incline and a decline to observe how the likely phenomenon of subsidence or tilted insertion would affect their mechanical properties.

Considering the values obtained for work needed to shear an implant design under 500g of compression, implant design 1 required the most work to cause dislocation (was the best) because it was the most pointed implant design (see Figure 3.1). Followed by implant design 4 which was the second most pointed implant design (see Figure 3.4), followed by implant design 5 because it had the most surface area (see Figure 3.5), and lastly implant design 3 (see Figure 3.3). Under heavy compression implant design 4 required more than 5 times more work to shear than any other implant design. Even though implant design 1 performed better than implant design 4 under 500g of compression in terms of work, implant design 4 would still be the better choice because it was not much worse than implant design 1 under 500g of compression and it far outperformed implant 1 under 60lbs. of compression, a load much more similar to the loads that will be placed on it under normal physiological conditions. Considering the values obtained for shear stiffness of the implants before dislocation under 500g of compression, implant design 5 had the greatest shear stiffness/ was best (or was not statistically different from the implant design that had the greatest shear stiffness) in every position except the flat, unbonded position. The next best implant design in this case was implant design 4 which had the greatest shear stiffness (or was not statistically different from the implant design that had the greatest shear stiffness) in every position except the declined position where it performed the worst. Under heavy compression implant design 1 was stiffest, followed by 5, then 3, then 4. However, all of the stiffness values stayed within the same range with the stiffest implant design being only about 13% stiffer than the least stiff implant design. Even though implant design 5 outperformed implant design 4 under 500g of compression in terms of shear stiffness,

implant design 4 would still be the better choice because even though it was slightly less stiff than design 5, it would still be stiff enough to resist any shear stresses that would physiologically be generated in the lumbar spine, and its smaller surface area would make it much less susceptible to wear than implant design number 5. Under 60lbs of compression all of the implant designs had similar stiffness; so if they are all similar, implant 4 is still the best choice because of its superiority in other areas.

The best combinations to provide the minimum torque required for movement were found to be the combinations of implant design 3 at 3mm offset and implant design 3 at 6mm offset. Implant design 3 at 3mm offset was found to be the combination that required the least torque to fully rotate. The statistical analysis shows that overall (looking at all positions), implant design 3 resists torque the least for minimum torque required for movement, followed by implant design 5, then implant design 4, then implant 1. The statistical analysis also shows that overall (looking at all positions), implant design 3 still resists torque the least for minimum torque required for full rotation, followed by implant design 5, then implant design 4, then implant 1.

Implant design 3 clearly allowed the most rotation. Implant design 5, because of its large surface area was the only implant design broad and shallow enough to have the beneficial characteristic of returning to its original position (not dislocating) when pulled for a distance then released from shear or torsional stresses. Despite these beneficial attributes, and while statistics show that implant designs 3 and 5 are less resistant to torsional stresses than implant 4, implant design 4 offers more stability than implant designs 3 and 5 and can accommodate bending movements without sliding like implant designs 3 and 5 have to do because of their large surface areas. Sliding is a major concern

because the more sliding that occurs over a larger surface area, the more wear that takes place. Since these implants are meant to be placed into patients with significantly intact annulus fibrosus (typically younger individuals), the longevity of these implants are a definite concern and the larger the surface area, the worse the implant performs in terms of wear over time. Therefore, a combination of implant design 3 and implant design 4 might be optimal in terms of shear, torsion, wear, and stability.

Although this study may reveal much about the mechanical properties of various incompressible intervertebral disc implants relating to the compressive behavior of the nucleus implanted intervertebral disc, there were limitations. The ABS thermoplastic with which the implant designs were reproduced during prototyping was not very stiff. This means that instead of the data gathered (like the data for forces needed for dislocation of an implant design and especially the data for the distance travelled before dislocation) being strictly the result of the shape of the implant designs as intended, these results also take into account the deformation of the ABS material. The material was not stiff enough to resist all deformation, especially under the 60 lb load. Another issue is that for this FDM prototyping method, the resolution in the z axis was 1/100th of an inch per inch. Since the implant designs were only 15mm long and 5-6mm tall, this resulted in uneven surfaces for all of the implant designs. The inner surfaces of the designs had to be manually polished (sanded smooth) which may have caused surface irregularities that might have affected the results of this experiment. The last main issue is that because of limited resources, only two sets (designs 1-5) of the implant prototypes could be ordered. This means that numerous tests were run on each of these two sets. After repeated shear and torsional testing on a material as potentially pliable as ABS thermoplastic, permanent deformation almost certainly took place and most likely influenced

the results. Also, since this was a laboratory study conducted using only fixation devices, these results only apply to in vitro environments.

The knowledge of the implant shapes and mechanics learned in this study have lead to a solid conclusion on the best interior shape for an implant of this type. The implant design should now be reproduced using various implantable materials suitable for this purpose and including suitable outer fixation devices. Once that has been done, functional spinal units should be obtained and there should be another round of shear and torsional laboratory testing to determine if this design is feasible in terms of wear and subsidence. This is very important because subsidence into the cartilaginous vertebral endplates has been a chief concern when dealing with all previously studied rigid nuclear intervertebral disc prosthesis. If subsidence is not excessive, the next step would be implanting the prosthetics into animal subjects to observe their function and obtain data that would be imperative in determining the longevity of an implant that will ultimately be used on people with intact annulus fibrosus.

REFERENCES CITED

- [1] Am Fam Physician. 2007 Dec 1;76(11):1669-76.
- [2] Manchikanti L. Epidemiology of Low Back Pain. Pain Physician 2000;3(2):167-92.
- [3] Pain. 2007 Oct;131(3):293-301. Epub 2007 Feb 20
- [4] Am Fam Physician. 2007 Nov 15;76(10):1497-502.
- [5] Sehgal N, Fortin JD. Internal Disc Disruption and Low Back Pain. Pain Physician 2000;3(2):143-57.
- [6] Coventry MB, Ghormley RK, Kernohan JW. The Intervertebral Disc: Its Microscopic Anatomy and Pathology. Part III. Pathologic Changes in the Intervertebral Disc. J Bone Joint Surg 1945;27A:460-74.
- [7] Markolf KL, Morris JM. The Structural Components of the Intervertebral Disc: A Study of Their Contributions to the Ability of the Disc to Withstand Compressive Forces. J Bone Joint Surg 1974;56A:675-87.
- [8] Anat J. Sagittal evaluation of elemental geometrical dimensions of human vertebrae (1985), 143, 115-120
- [9] Osti OL, Vernon RB, Moore R, Fraser RD. Annular Tears and Disc Degeneration in the Lumbar Spine. J Bone Joint Surg (Br) 1992;74B:678-82.
- [10] Kambin P, Savitz MH. Arthroscopic Microdiscectomy: An Alternative to Open Disc Surgery. The Mount Sinai Journal of Medicine 2000;67(4):283-7.
- [11] Bao QB, Yuan HA. Artificial Disc Technology. Neurosurgical Focus 2000;9(4):1-9.
- [12] Biomaterials, Volume 17, Number 12, June 1996 , pp. 1157-1167(11)
- [13] NucleusArthroplasty™ Volume III: Surgical Techniques & Technologies
Technology in Spinal Care
- [14] Eur Spine J (2002) 11 (Suppl. 2) :S154–S156

- [15] Burke T, Caputy A. Treatment of thoracic disc herniation: evolution toward the minimally invasive thoracoscopic technique. *Neurosurgical Focus* 2000; 9 (4):E9.
- [16] *Eur Spine J* (1998) 7 : 132–141
- [17] Markolf K. Deformation of the Thoracolumbar Intervertebral Joints in Response to External Loads: A BIOMECHANICAL STUDY USING AUTOPSY MATERIAL. *J Bone Joint Surg Am.* 1972;54:511-533.
- [18] Virgin W. Experimental Investigations into Physical Properties of Intervertebral Disc. *J Bone Joint Surg* 1951;33B:607.
- [19] JONCK L. M. The Mechanical Disturbances Resulting From Lumbar Disc Space Narrowing. *J Bone Joint Surg Br*, May 1961; 43-B: 362 - 375.
- [20] *Journal of Biomechanical Engineering.* 536 / Vol. 127, June 2005
- [21] *Acta Neurochir (Wien)* (1999) 141: 1083-1087
- [22] Hirsch C. The Reaction of Intervertebral Discs to Compression. *J Bone Joint Surg* 1955;37A:1188.
- [23] Brown T, Hanson R, Yorra A. Some Mechanical Tests on the Lumbo-Sacral Spine with Particular Reference to the Intervertebral Discs. *J Bone Joint Surg* 1957;39A:1135.
- [24] Roaf R. A Study of the Mechanics of Spinal Injuries. *J Bone Joint Surg* 1960;42B:810.
- [25] Mechanical Behavior of the Human Lumbar Intervertebral Disc with Polymeric Hydrogel Nucleus Implant: An Experimental and Finite Element Study: <http://worldcat.org/wcpa/ow/a8e30c86fa3372a2a19afeb4da09e526.html>
- [26] Injectable Bioadhesive Hydrogels for Nucleus Pulposus Replacement and Repair of the Damaged Intervertebral Disc: http://idea.library.drexel.edu/bitstream/1860/1315/1/Vernengo_Jennifer.pdf
- [27] Dahl M. et al. Dynamic Characteristics of the Intact, Fused, and Prosthetic-Replaced Cervical Disk.
- [28] Praemer A, Furner S, Rice DP. *Musculoskeletal Conditions in the United States.* 1st ed. Park Ridge: American Academy of Orthopaedic Surgeons, 1992.

- [29] Hoppenfeld S. *Physical Examination of the Spine and Extremities*. Norwalk, Connecticut: Appleton-Century-Crofts; 1976.
- [30] Thieme FP. *Lumbar Breakdown Caused By Erect Posture In Man*. Ann Arbor: University Of Michigan Press; 1959
- [31] Shiel W. Degenerative Disc Disease & Sciatica. Available at: http://www.medicinenet.com/degenerative_disc/article.htm. Accessed February 2, 2008
- [32] Laser Spine Institute, LLC. Upper (Cervical), Middle (Thoracic) and Lower (Lumbar) Back Pain. Available at: http://laserspinesite.com/back_problems/back_pain/. Accessed February 2, 2008
- [33] WebMD Medical Reference from Healthwise. Degenerative Disc Disease – Topic Overview. Available at: <http://www.webmd.com/back-pain/tc/degenerative-disc-disease-topic-overview> Accessed February 2, 2008
- [34] Iatridis JC, Setton LA, Weidenbaum M, Mow VC. The Viscoelastic Behavior of the Non-Degenerate Human Lumbar Nucleus Pulposus in Shear. *Journal of Biomechanics* 1997;30(10):1005-13.
- [35] Akeson WH, Woo SYL, Taylor TKF, Ghosh P, Bushell GR. Biomechanics and Biochemistry of the Intervertebral Disc. *Clin Orthop Rel Res* 1977;129:133-39.
- [36] Iatridis JC, Weidenbaum M, Setton LA, Mow VC. Is the Nucleus Pulposus a Solid or a Fluid? Mechanical Behaviors of the Nucleus Pulposus of the Human Intervertebral Disc. *Spine* 1996;21:1174-84.
- [37] Hedman TP, Kostuik JP, Fernie JR, Hellier WG. Design of an Intervertebral Disc Prosthesis. *Spine* 1991;16(6):S256-60.
- [38] Urban JPG, McMullin JF. Swelling Pressure of the Lumbar Intervertebral Discs: Influence of Age, Spinal Level, Composition and Degeneration. *Spine* 1988;13:179-87.
- [39] McNally DS, Adams MA. Internal Intervertebral Disc Mechanics as Revealed by Stress Profilometry. *Spine* 1992;17:66-73.
- [40] Weber H. Lumbar Disc Herniation: A Controlled Prospective Study with Ten Years of Observation. *Spine* 1993;8:131-40.
- [41] Goel VK, Goyal S, Clark C, Nishiyama K, Nye T. Kinematics of the Whole Lumbar Spine - Effect of Discectomy. *Spine* 1985;10:543-54.

- [42] Brinckmann P, Frobin W, Hierholzer E, Horst M. Deformation of the Vertebral End- Plate under Axial Loading of the Spine. *Spine* 1983;8:851.
- [43] Farfan HF, Cossette JW, Robertson GH, Wells RV, Kraus H. The Effect of Torsion on the Lumbar Intervertebral Joints: The Role of Torsion in the Production of Disc Degeneration. *J Bone Joint Surg* 1970; 52A:468-97.
- [44] Harris RI, Macnab I. Structural Changes in the Lumbar Intervertebral Discs. Their Relationship to Low Back Pain and Sciatica. *J Bone Joint Surg* 1954;36B:304-22.
- [45] Total lumbar disc replacement in athletes: clinical results, return to sport and athletic performance. *Eur Spine J* 2007;16:1001–1013
- [46] US National Prevalence and Correlates of Low Back and Neck Pain Among Adults. *Arthritis Rheum* Vol. 2007; 57(4): 656–665
- [47] Michael N et al. Low back pain. *Radiology* 2000; 217:321–330.
- [48] Battei MS, Videman T. Epidemiology of Disc Disease. In Wiesel S, Weinstein J, Herkowitz H, Dvorak J, Bell G eds. *The Lumbar Spine*. Philadelphia: W.B. Saunders Company, 1996:16-27.
- [49] Bogduk N, Twomey LT. *Clinical Anatomy of the Lumbar Spine*. Second ed. Melbourne: Churchill Livingstone, 1991.
- [50] White AA, Panjabi MM. *Clinical Biomechanics of the Spine*. II ed. Philadelphia: J.B. Lippincott Company, 1990.
- [51] Bell G. Developmental to Normal Adult Anatomy. In Wiesel S, Weinstein J, Herkowitz H, Dvorak J, Bell G eds. *The Lumbar Spine*. Philadelphia: W.B. Saunders Company, 1996:43-52.
- [52] The National Pain Foundation. Anatomy of the Spine. Available at: http://www.nationalpainfoundation.org/MyTreatment/articles/BackAndNeck_Part_2.asp. Accessed February 2, 2008
- [53] Elder S. *Biomechanics of Spine*. Starkville, MS: Biomechanics Lecture; 2006.
- [54] Shirazi A, Shrivastava SC, Ahmed SM. Stress Analysis of the Lumbar Disc-Body Unit in Compression. *Spine* 1984;9(2):120-34.
- [55] Lehman TR, Spratt KF, Tozzi JE, Weinstein JN, EL-Khoury GY. Long-Term Follow-up of Lower Lumbar Fusion Patients. *Spine* 1987;12:97-104.

- [56] Hellier WG, Hedman TP, Kostuik JP. Wear Studies for the Development of an Intervertebral Disc Prosthesis. *Spine* 1992;16:S256-S60.
- [57] Bao QB, Yuan HA. New Technologies in Spine: Nucleus Replacement. *Spine* 2002;27:1245-47.
- [58] Urban J. Disc Biochemistry in Relation to Function. In Wiesel S, Weinstein J, Herkowitz H, Dvorak J, Bell G eds. *The Lumbar Spine*. Philadelphia: W.B. Saunders Company, 1996:271-81.
- [59] Bendo J, Hale J, Levin D. Adjacent Segment Degeneration Following Spinal Fusion for Degenerative Disc Disease 2007;65(1):29
- [60] Boeree N. Degenerative disc disease: disc replacement. *Ann R Coll Surg Engl* [Serial Online] 2007; 89: 6–11. Available at: <http://www.pubmedcentral.nih.gov/picrender.fcgi?artid=1963555&blobtype=pdf> Accessed February 16, 2008
- [61] Buckwalter J, Do Intervertebral Discs Deserve Their Bad Reputation?. *Iowa Orthop J*. [Serial Online] 2005; 18: 1-11 Available at: <http://www.pubmedcentral.nih.gov/picrender.fcgi?artid=2378178&blobtype=pdf>
- [62] Ball J. New knowledge of intervertebral disc disease. *J. Clin. Path.* 31, Suppl. (Roy. Coll. Path.) [Serial Online] 12: 200-204. Available at: <http://www.pubmedcentral.nih.gov/picrender.fcgi?artid=1347139&blobtype=pdf>
- [63] Davis S, Edmondston J, Goh S, Price R, Song S, Tan C. Influence of age and gender on thoracic vertebral body shape and disc degeneration: an MR investigation of 169 cases. *J. Anat.* [Serial Online] 2000; 197: 647±657 Available at: <http://www.pubmedcentral.nih.gov/picrender.fcgi?artid=1468180&blobtype=pdf>
- [64] McCormack B, Weinstein P. Cervical Spondylosis: An Update. *West J Med* [Serial Online] 1996; 165:43-51 Available At: <http://www.pubmedcentral.nih.gov/picrender.fcgi?artid=1307540&blobtype=pdf>
- [65] Evaluating and Managing Acute Low Back Pain in the Primary Care Setting. *J Gen Intern Med*. [Serial Online] 2001 Feb;16(2):120-31. Available at: <http://www.pubmedcentral.nih.gov/picrender.fcgi?artid=1495170&blobtype=pdf> *J Gen Intern Med*.
- [66] Garg M, Kumar S. Interlaminar discectomy and selective foraminotomy in lumbar disc herniation. *J Orthop Surg* [Serial Online] Surgery 2001, 9(2): 15–18. Available at: <http://www.josonline.org/PDF/v9i2p15.pdf>

- [67] DePuy Spine. Charite Artificial Disc Web Site. Available at:
http://www.charitedisc.com/charitedev/domestic/patients/treatment_artificialdisc.asp
 Accessed February 26, 2008
- [68] Percy MJ: Stereo radiography of lumbar spine motion. Acta Orthop Scand (Suppl)212:1-14, 1985
- [69] Neurosurgical Center. The artificial lumbar disc. Web site. Available at:
http://www.neurochirurgie-zwolle.nl/ART_artificialdisc.html Accessed Jan1, 2008
- [70] Mayfield Clinic. FlexiCore™ Intervertebral Disc for the Treatment of Degenerative Disc Disease. Web site. Available at:
http://www.mayfieldclinic.com/CT_FlexiCore.htm Accessed April 2, 2008
- [71] Sukovich W. Progress, Challenges And Opportunities In Disc Space Preparation For Lumbar Interbody Fusion. Internet Journal of Spinal Surgery [Serial Online] Available at:
<http://www.ispub.com/ostia/index.php?xmlFilePath=journals/ijss/vol1n2/disc.xml>
- [72] Gilbert G . Lecture 2. Starkville, MS: Dynamics of Aging Lecture; 2007.
- [73] Bischoff U, Freeman M, Gregson P, Smith D, Tuke M. Wear Induced by Motion Between Bone and Titanium or Cobalt Chrome Alloys. J Bone Joint Surg. September 1994; 76-B:
- [74] Intervertebral Disc Arthroplasty Spine [Serial Online] 29(23):2779-2786 Available at: http://www.medscape.com/viewarticle/495415_3
- [75] Gibson N, Stamm H. The Use of Alloys in Prosthetic Devices. Medical device Manufacturing & Technology. Available at:
http://www.touchbriefings.com/pdf/753/mdev02_p_gibson.pdf